

Adaptations of the human eye to reduce the impact of chromatic aberrations on vision

Dissertation

zur Erlangung des Grades eines
Doktors der Naturwissenschaften

der Mathematisch-Naturwissenschaftlichen Fakultät

und

der Medizinischen Fakultät

der Eberhard-Karls-Universität Tübingen

vorgelegt

von

Yun Chen

aus Shanghai, China

July – 2015

Tag der mündlichen Prüfung: 30,Oct,2015

Dekan der Math.-Nat. Fakultät: Prof. Dr. W. Rosenstiel

Dekan der Medizinischen Fakultät: Prof. Dr. I. B. Autenrieth

1. Berichterstatter: Prof. Dr. Frank Schaeffel

2. Berichterstatter: Prof. Dr. Uwe Ilg

Prüfungskommission:

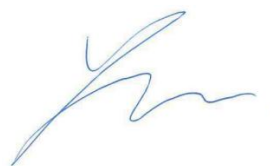
Prof. Dr. Frank Schaeffel

Prof. Dr. Dr. Uwe Ilg

Prof. Dr. Siegfried Wahl

Prof. Dr. Felix Wichmann

I hereby declare that I have produced the work entitled "**Adaptations of the human eye to reduce the impact of chromatic aberration on vision**", submitted for the award of a doctorate, on my own (without external help), have used only the sources and aids indicated and have marked passages included from other works, whether verbatim or in content, as such. I swear upon oath that these statements are true and that I have not concealed anything. I am aware that making a false declaration under oath is punishable by a term of imprisonment of up to three years or by a fine.



Tübingen,

.....

Date

Signature

To my parents

Contents

1. Acknowledgements	5
2. Abstract.....	6
3. Synopsis	8
3.1 The Eye: an optical instrument	10
3.2 Visual angle in the human eye	12
3.3 Optical models of the eye.....	12
3.4 Project 1: the effect of transverse chromatic aberration (TCA) on human visual perception	13
3.4.1 Historical review on the optical aberrations in eye.....	13
3.4.2 My PhD work on the effect of transverse chromatic aberration (TCA) on human visual perception (Paper 1).....	15
3.5 Project 2: the effect of longitudinal chromatic (LCA) on the S-cone distribution in the fovea	16
3.5.1 Historical review of S- (short wavelength) cone and its visual function	16
3.5.2 My PhD work on the relationship between foveal blue scotoma and the shape of foveal pit (Paper 2).....	18
3.6 Project 3: the potential of polychromatic eccentric photorefraction in measuring LCA in the human eye.....	19
3.6.1 Historical review of eccentric photorefraction	19
3.6.2 Historical review of white LEDs eccentric photorefraction.....	20
3.6.3 My PhD work on measuring LCA with white LEDs eccentric photorefraction (Manuscript 3)	21
3.7 Conclusions and outlook	22
3.8 References	23
4. List of publications.....	30
5. Descriptions of personal contributions.....	30
6. Appended/ Manuscripts	31

1. Acknowledgements

My PhD project has started at University of Tübingen, Germany and has been funded by OpAL - an Initial Training Network combining physics, optics and biology funded by the European Commission's Seventh Framework Program (FP7) under the Marie Curie Actions since 15th, Jan, 2012. During this period, I learnt a lot from my supervisor and colleagues and was supported and encouraged by them.

Foremost, I would like to express my gratitude to my thesis committee members, Prof. Dr. Frank Schaeffel, Prof. Dr. Felix Wichmann, and Prof. Dr. Uwe Ilg for their constant support, valuable advice and guidance.

I would like to thank my supervisor Prof. Dr. Frank Schaeffel. Throughout my project, he helped me not only on theoretical knowledge, but also on communication skills with other colleagues. There is no doubt that what he has done for me is more than a supervisor. His attitude toward the research will influence me in my future research. His timely concern of my project and useful suggestions are very important to me. Without his help, my project will not be accomplished successfully.

Many thanks to my other OpAL group members: Managing Coordinator Dr. Thomas Wheeler-schilling, project manager Dr. Michaela Bitzer, Prof. Dr. Pablo Artal, Dr. Peter Unsbo, Dr. Linda Lundstrom, Prof. Dr. Susana Marcos, Dr. Harilaos Ginis, Dr. Gregor Esser, Dr. Anne Seidemann, Dimitriou Christaras, Ebrahim Kamrani, Alexandros Pennos, Aiswaryah Radhakrishnan, Onurcan Sahin, Mengchan Sun, Abinaya Priya Venkataraman, Simon Winter, Ulrich Wildenmann. This three years with all of you were really a diamond in my life.

Also I received helpful support from my colleges in the lab: Dr. Marita Feldkaemper, MD. Weizhong Lan, Klaus Graef, Felix Maier, Marja-Liisa Franssila and other friends in our office. Without their assistance, I can not finish my project so smoothly.

Special thanks to my friends in Tübingen, MingYu Yang, BiWei Huang, LiJun Wang, XueJun Feng and other friends. I will never forget the life I spent in Tübingen with all of you.

Finally, I want to give my most precious appreciation to my beloved and respectable parents. For the last more than 30 years, your thoughtful support accompanied me wherever I was in Shanghai, Sweden, Nertherlands or Germany. During the last 6 years in Europe, I missed you all every minute.

*最后，要把我最珍贵的感谢送给我最亲爱的父母。在过去的 30 多年里，无论我在上海瑞典荷兰还是德国，感谢你们都无微不至地支持我，照顾我。在过去六年里的 1000 多个日日夜夜，我一直在遥远的欧洲思念着你们。
谨把这篇文献献给我至爱的父母。*

Thank you all,

Yun Chen

2. Abstract

Sharpness and contrast of the retinal image are affected by two types of optical aberrations, monochromatic and polychromatic. Monochromatic aberrations result from imperfections in the refracting surfaces, while polychromatic aberrations result from the dispersion of light in the ocular media. Wavelength-dependent differences in focal lengths are referred to as longitudinal chromatic aberration (LCA) while differences in image position and image magnification result from transverse chromatic aberration (TCA). The primary objective of my PhD work is to further clarify the relationship between two chromatic aberrations, longitudinal chromatic aberration (LCA) and transverse chromatic aberration (TCA), and visual perception. I have studied the morphological and optical adaptations of the visual system that were developed in the course of evolution to cope with chromatic aberrations. Generally, transverse chromatic aberration (TCA) has been less studied even though it causes more loss in retinal image contrast. While LCA is similar in different eyes, TCA shows large inter-individual variability. It is not known which ocular variables determine this variability. Therefore, in project 1 I have measured chromatic differences in perceived image magnification (determined by TCA) in different subjects with a newly established psychophysical procedure and found that a major part of the inter-individual variance in CDM (64%) was explained by lens thickness. Since lens thickness increase with age, also TCA will increase. **This study was published in the Journal of the Optical Society of America A, 2014.**

Due to longitudinal chromatic aberration (LCA), the focus of the image on the retina cannot be equally good at all wavelengths. Human eyes are about 2 D more myopic in blue light (450 nm) than in red (650 nm). For this reason, the retinal image in the fovea is typically in best focus for the mid- and long-wavelengths but severely out of focus for the blue (>1D). Probably for this reason, the short wavelength sensitive cones (the S-cones) are lacking from the foveal center, causing a “foveal blue scotoma”. I found that the foveal blue scotoma is highly variable among subjects but it is not known, why. Therefore, in project 2, I have studied the variables that might influence the appearance of the foveal blue scotoma: shape of the foveal pit and distribution of macular pigment. I found that the shape of the foveal pit is a strong predictor of the foveal blue scotoma - the steeper the foveal slopes, the larger the blue scotoma. Macular pigment distribution, on the other, gave rise to the percept of Maxwell’s spot, but was not correlated to the size of the blue scotoma. **This study was published in Vision Research, 2015.**

My third project deals with new technology to measure LCA. In our laboratory we use routinely eccentric infrared photorefractometry to measure refractive states in human and animal eye. The use

of infrared light has the advantage that the subject is not aware that is being measured and that pupils remain large which increases the signal-to-noise ratio. However eccentric photorefraction could also provide information on LCA if it is used in white light. The differences in refractions measured in the R, G and B channel of the video camera should provide LCA but this technique was never established even though it would be a great advance to obtain LCA from single pictures of the eye. Therefore, in project 3, I studied the potential of polychromatic eccentric photorefraction in measuring LCA. I found that the calibration of photorefraction in white light is much more variable in different subjects, than in infrared light. The major reason was the large individual variability in fundal reflectance in visible light and less variability in the near infrared. Fundal reflectance has a major effect on the brightness of the pupil during the measurements. Because the technique uses a brightness slope in the pupil, and determines the gradient of pixel values, the slope of pupil brightness depends on the absolute pixel brightness. This finding explains a lot of the variability of photorefraction and will be of interest to researchers using this technique. **The work was submitted to BOE in June 2015.**

3. Synopsis

There are many English versions of a Chinese saying that means “The eyes are the window of the mind”, “The heart's letter is read in the eyes”, or “Eyes are windows to the soul”. All these show how important the eye is in our daily life. Therefore, the human eye has been studied for several centuries. The theory that eyes emit light (emission theory of Plato, fourth century BC) rather than catching it lasted for many centuries. However, it was questioned over and over again by various scientists, including Aristotle and Euclid. Not until 1021, the Arabic physicist Ibn al-Haytham or Alhazen developed his intromission theory, along with optical considerations. He stated in his book that the eye captured the light since sunlight could hurt the eye. Besides of Alhazen, many other Arabic scientists were working in the visual optics field.

In Europe, since the 13th century, research on vision has become popular: many topics like the physiology of eyesight, anatomy of the eye, optics and vision were carried out. In the beginning of 17th century, the idea was common that an object was imaged on the anterior surface of the crystalline lens (CL) in the eye. However, Johannes Kepler applied Snell's law and reconstructed the optical paths of rays entering the eye. He demonstrated that an inverted image is projected on to the retina. Based on this discovery, many physical phenomena could now be explained, such as central visual acuity, visual field, dark adaptation, and errors of refractive state. In 1623, Benito Daza de Valdes wrote a book “Uso de los anteojos” (the use of Corrective Glasses), in which lenses were used to correct optical imperfections of vision. Nowadays, with the development of instruments to measure the optics of eyes in great detail, like wavefront sensors, many issues of the optical system of human eyes are much better understood [1]. However, there are also still interesting problems that wait to be solved. One of such problems is that how the retinal image and visual performance are affected by optical aberrations such as monochromatic and chromatic aberrations. There is already a large amount of work on the role of monochromatic aberrations in vision but chromatic aberrations are still not fully understood.

Hence, the primary objective of my PhD work is to further clarify the relationship between two chromatic aberrations, longitudinal chromatic aberration (LCA) and transverse chromatic aberration (TCA), and visual perception. Although the effect of LCA was widely studied not only in subjects but also in eye models, only little is known about the adaption of the visual system to chromatic aberrations. I have studied the morphological and optical adaptations of the visual system that were developed in the course of evolution to cope with chromatic aberrations. In third project, I have clarified how variations in fundal reflectance determined the inter-individual

variability of a common technique to measure the refractive state of eyes from a distance - eccentric photorefraction.

In **project 1**, I measured the chromatic difference in retinal image magnification (CDM) in a number of different human subjects. CDM is tightly related to TCA. I used a newly developed psychophysical procedure which turned out to be powerful. I found that a major part of the inter-individual variance in CDM (64%) is explained by the differences in the thickness of the crystalline lens in the eye. In addition, CDM increased 3.5% every year. This study was published in the Journal of the Optical Society of America A, 2014[2] (Paper 1).

In **project 2**, I studied the other type of chromatic aberration, longitudinal chromatic (LCA). Since the retinal image cannot be in focus at all wavelengths of the visible spectrum at one time, it seems as if the S-cones were removed from the foveal center in the course of evolution. This happened most likely to keep the sampling densities of the L- and M-cones as high as possible without wasting space for the S-cones. S-cones are exposed to a myopically defocused image due to the shorter focal length of cornea and lens in short wavelength light, as a result of dispersion. The lack of S-cones from the foveal center causes a “foveal blue scotoma” which can be visualized with a psychophysical trick. I found that the shape of foveal pit was found as a strong predictor of the shape and size of the foveal blue scotoma. The steeper the foveal slopes, the larger the blue scotoma. This study was published in Vision Research, 2015[3] (Paper 2).

In **project 3**, I studied a well-known problem of a widely used technique to measure the refractive state of the eye, eccentric photorefraction. This technique shows a high amount of variability among subjects but the optical features in the eye, responsible for this variability are not known. First, I found that the calibration of photorefraction in the white light was more variable in different subjects, than in infrared light. The major reason was the large individual variability in fundal reflectance in visible light, and less variability in the near infrared. Fundal reflectance has a major effect on the brightness of the pupil during the measurements. Because the technique uses a brightness slope in the pupil, and determines the gradient of pixel values, the slope of pupil brightness depends on the absolute pixel brightness - i.e. doubling the pixel brightness may change the measured slope and leads to an overestimation of the refractive error. This finding explains a lot of the variability of photorefraction and will be of interest to researchers using this technique. The work was submitted to BOE in June 2015.

Before starting to review my PhD work in detail, several general definitions of optical systems and human eye models will be described.

3.1 The Eye: an optical instrument

The eye, as a part of the visual system, is an optical instrument that also includes the light sensors, the photoreceptors in the retina and an image-forming optics, the cornea and the crystalline lens. A diagram of human eye is shown in Figure 1. The axial length of the human eye is around 24 mm, which requires an optical power of about 60 dioptres (D) to achieve emmetropia or “normal-sightedness”. The cornea, a transparent layer between air and the water-like media inside the eye, provides the largest fraction of refractive power, about 43D. Behind the cornea is the anterior chamber, filled with aqueous humor (a water-based salt solution), followed by the iris which forms an adjustable aperture and the crystalline lens (CL). The CL is biconvex. It is elastic and has an internal onion-shaped structure in which the refractive index increases smoothly from the periphery to the center [4] - the so called gradient refractive index (GRIN). The shape of the GRIN profiles varies with age since the refractive power of the CL has to be kept constant despite that the lens increases in thickness throughout life, with about doubling in thickness from school age to old age [5-7] (the “lens paradox”). The CL is an impressive optical element. In addition to correcting for spherical aberration due to its GRIN structure, it also allows for accommodation to maintain a clear image on the retina for different viewing distances. This process is controlled mostly unconsciously by the interaction of the elasticity of the CL and the ciliary muscle. In 1855, Helmholtz proposed that when the ciliary muscle, circularly arranged, is relaxed (viewing a far object), the lens zonules and suspensory ligaments attached to the choroid pull the lens flat. Accommodation is achieved by contracting the ciliary muscle which relaxes the zonular fibres and releases the tension of the lens so that it can follow its own elasticity and become more curved in shape (the “Helmholtz theory of accommodation”). The mechanisms of accommodation have been further studied after 1970. It is clear that accommodation is controlled mainly by defocus in the fovea [8-10], is also controlled by binocular disparity [11, 12], and to some extent by the spectral composition of light [13-17]. In the human eye, accommodation amplitude can amount to up to 22 D in young children but decreases with age. Beyond about 50 years, the CL is no longer elastic and even though the ciliary muscle is still functional, the CL does not longer change its shape when it constricts (presbyopia).

Due to accommodation by changing the surfaces curvatures and the GRIN structure, aberrations of the CL are variable. For instance, spherical aberration becomes variable. Jenkins [18] in 1963 indicated that there was no spherical aberration at all in the lens. In 1979, Millodot and Sivak found that spherical aberration in CL was positive, compensating negative spherical aberration from cornea [19]. Later, Sivak [20] stated that spherical aberration could be negative or positive,

depending on subjects. In 1993, Tomlinson and his colleagues stated that the spherical aberration was generally negative [21], in line with findings by Artal in 1998 [22]. In 2001, George Smith and his group found that spherical aberration of human eyes in vivo with relaxed lenses was negative [23].

The innermost layer in the globe is the retina - a protruded part of the diencephalon. The retina houses the photoreceptors, which are sensitive to light and provide conscious vision. In the past years, it was found that there are also intrinsically light sensitive ganglion cells (ipRGCs) on the vitreal side of the retina interestingly, which permit unconscious visual input and also drive the pupil. In vertebrate eyes, the retina is inverted, the photoreceptors pointing away from the light source, the pupil, and light has to pass through all retinal layers to reach them. There are two types of photoreceptors: rods and cones. Rods are in charge of night vision and provide no color, while cones work in the daytime and are responsible for color vision. The position and density of the different photoreceptors are variable in different locations of retina [24-29] (Figure 2). The perhaps most important structural specialization in the retina is the fovea. It is located in the center of the retina (slightly temporal of the intersection of the optical axis with the retina) and histologically recognized as a pit with tightly packed M- (middle wavelength) and L- (long wavelength) cones, providing maximal visual acuity [30-32]. Outside the fovea, rods become abundant and make up for about 95% of all photoreceptors [33]. Through ganglion cells, the photoreceptors transmit the neural signal to the brain [34, 35].

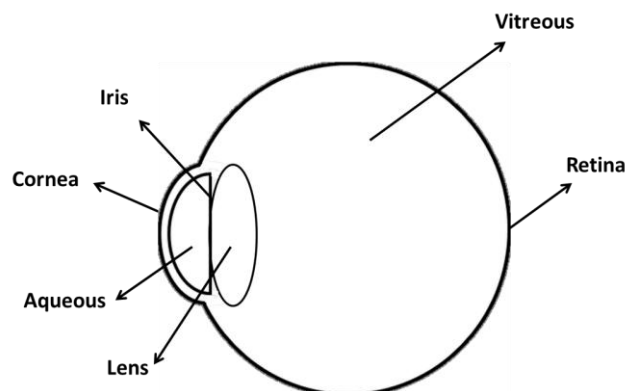


Figure 1. Eye Diagram

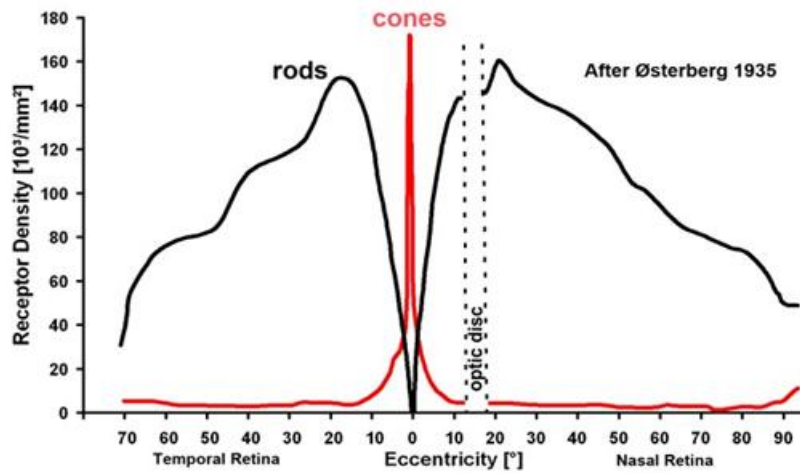


Figure 2. Topography of the distributions of rods and cones across the human retina [36].

3.2 Visual angle in the human eye

On average, one degree of visual angle is about 290 μm on the retina in the human eye. The calculation is:

$$\tan [1^\circ * (n_{\text{air}}/n_{\text{eye}})] = H/24,$$

$$\tan (1/1.416) = H/24,$$

So, $H = 290 \mu\text{m}$

However, because eye size varies among humans, it is more general to employ visual angles in degree rather than linear distances on the retina. Furthermore, several different axes and angles are important when referring to the location on retina, in combination with the visual angle.

3.3 Optical models of the eye

Cornea and lens represent the only two optical elements to focus light on the retina. In the 19th century, after Thomas Young made the first geometrical optical model of cornea and lens, the first physical eye model was built by Huygens [37]. This physical model eye was made of two hemispheres filled with water and a diaphragm (pupil aperture). Later, spherical surfaces were used to describe cornea and lens in the schematic eye models by Moser (1844) and Listing (1851). Based on Listing's eye model, Helmholtz modified the lens surface from one to two, one for cornea and two for the crystalline lens, so that there were three surfaces rather than two. In 1900, Tscherning described a new eye model which was the first with four surfaces. In the past century, with the development of measuring techniques to measure curvature and axial distances, popular eye models were proposed, like the Gullstrand eye model [38], the Le Grand eye model [39] and

the Emsley eye model [40]. These eye models were restricted to the description of the paraxial optics. They were useful in estimation of the cardinal planes and cardinal points of the eye, and for the design of new spectacles and power calculations for intraocular lenses (IOL). Nowadays, based on the improvement of the techniques for measuring lens surfaces and structures, a gradient refractive index lens was added to the schematic eyes [41-43]. However, calculation result with these models still could not match some of the optical features in the human eye, such as the peripheral refractive errors, and of longitudinal and transversal chromatic aberrations (LCA and TCA, respectively). In order to study chromatic aberration, some new models were published with onion shape lenses [44-46]. In a recent study, when simulating chromatic aberrations on the retina, the Liou and Brennan eye model [41] was established based on simulations with the commercially available lens design software "ZEMAX" (ZEMAX Development Corporation, 446 Bellevue, USA). In this model, the refraction of light was analyzed at different wavelengths, depending on biometry and curvatures, and based on the dispersion of the ocular media which made the simulations more realistic.

3.4 Project 1: the effect of transverse chromatic aberration (TCA) on human visual perception

3.4.1 Historical review on the optical aberrations in eye

Sharpness and contrast of the retinal image are affected by two types of optical aberrations: monochromatic and chromatic aberrations. Five primary or Seidel aberrations of monochromatic aberrations fall into two subgroupings: one group such as spherical aberration, coma and astigmatism, deteriorate the image, making it become progressively worse. The monochromatic aberrations in the other group deform the image, for example, field curvature and distortion. If the source is a broad spectral bandwidth, chromatic aberrations are far more significant.

Chromatic aberrations arise from the fact that refractive index (n) varies with frequencies of the wavelength (dispersion) and fall into two subgroups: longitudinal and transverse chromatic aberrations. Wavelength-dependent differences in optical power of the eye are referred to as longitudinal chromatic aberration (LCA). LCA has been extensively studied by measurements in subjects [47-52] and in eye models with ocular media of different refractive indexes [53]. LCA in the human eye shows a consistent difference in refractive state of about 2.5 D between the blue and red end of the visible spectrum, with more myopic refractions in the blue. Verified by both subjective and objective methods, it is true that LCA is quite stable among humans [48, 54]. In eye models, more efforts were made to model LCA. An equation was suggested by Thibos and

colleagues to model LCA in human eyes, in which they adapted coefficients of Cornu's hyperbolic formula to the human eye [44]. Later, a Cauchy dispersion equation was used which gave more chromatic differences in the long wavelength range [55].

Transverse chromatic aberration (TCA) is less well described although a study concluded that it caused more severe loss in retinal image contrast than spherical aberration or coma [56]. Hence, considerable efforts were made to understand the relation between TCA and optical parameters in the eye. Several studies agree that both perceived TCA and optical calculated TCA are highly variable among subjects and sometimes also clearly different from theoretical values [46, 53, 57-59]. Howland in 1976 measured TCA with an apparatus similar to Tscherning's aberroscope, and was the first one to report the high inter-individual variability in TCA [60]. Later, perceived TCA was measured psychophysically with a "two – color (red and blue) Vernier alignment method" by Ogbo and Bedell in 1987[61]. In 1989, Thibos and his colleagues used a similar approach but added a center pinhole aperture to measure the optical TCA [53]. Similar measurements were done by Simonet and Campbell in 1990 [59], as well as Rynders's group in 1995[45]. Variability of TCA among subjects was different in the two studies. The different position of the entrance pupil was thought to be a major reason for the different variability observed among studies. Calculations in reduced eye models appeared to support this assumption [62]. TCA was objectively measured using a spatially resolved refractometer by different groups [46, 57, 58]. In these studies, perceived and optical TCA were compared with each other and high variability of TCA was found not only between subjects but also between different eyes from same subject. Several ocular features were studied, such as tilt and optical surface misalignment between cornea and lens, variations in the distance of the fovea from the pupil axis (angle kappa) and corneal irregularities [57]. Among these factors, by comparing individual corneal topography data, corneal irregularities were assumed to be a major reason for the high inter-individual variability of TCA. However, the reason for the high variability of TCA was still not completely clear.

Similar to LCA, TCA was also theoretically studied by using schematic eye models. In the Thibos eye model, water was used with a fixed refractive index of 4/3[62]. However, since the natural crystalline lens is more dispersive than water and has a gradient index structure, the calculated transverse chromatic aberration was smaller than perceived one, especially in short wavelengths. Five years later, Thibos published a new reduced eye model, the "chromatic eye". The refractive index of this eye model was described more accurately in short wavelengths and the refracting surface of the cornea was changed to an aspherical shape that reduced spherical aberration [44]. However, the "chromatic eye" still appeared to be too simple for a complete description of the

real eye. Therefore, in 1997, Liou and Brennan developed a new eye model to simulate the visual performance under a wide range of conditions [41]. In Liou-Brennan eye model, a gradient index lens model [63] varying from 1.386 to 1.404 was used to simulate the natural lens with gradient refractive index. As a result, LCA could now be predicted within acceptable tolerances, but TCA was still different from the real eyes. With the improvement of TCA measuring approaches, it became clear that TCA is inherently variable among subjects [41, 44-46, 53, 57-59, 61, 62]. In 2000, Campbell calculated power changing between different optical surfaces under different wavelengths (400 nm – 800 nm) in four different Liou-Brennan eye models (4D hyperopic, -4D myopic, emmetropic, and 2.5D accommodating) [64]. He claimed that the anterior surface seemed to generate the major part of chromatic aberration. Since some differences persisted between the model eye and the human eye, in particular when the myopic eye was compared to the accommodating eye, it was concluded that power and thickness of lens must also be important parameters.

3.4.2 My PhD work on the effect of transverse chromatic aberration (TCA) on human visual perception (Paper 1)

In this project, I studied the magnitude and variability of transverse chromatic aberration (TCA) in the human eye, and identified the ocular parameters that might determine its magnitude. One aspect of TCA is the chromatic difference in lateral position on the image plane and the other is chromatic difference in magnification (CDM). There are four possible psychophysical methods for measuring CDM:

(1) CDM was measured from the physical tilt angle of the apparent fronto-parallel plane (AFPP) under dichoptic viewing conditions, in which the vision in one eye was limited to long-wavelength light (red) and the other was limited to short-wavelength light (blue) [65]. Initially, because of the CDM, the sizes of retinal images are different. During the experiment, the subjects had to move rods on the AFPP until they perceived the same retinal image sizes. The moved AFPP lateral tilt represented the magnitude of CDM.

(2) The “two color Vernier alignment method” [61]. In this method, the perceived lateral misalignment between a red and a blue bar was measured as an indicator of CDM. However, since the Vernier thresholds rapidly exceeds CDM in the periphery of the visual field, it is only valid in a close area around the fovea [53, 65].

(3) The artificial pinhole aperture. Compared to Method 2, the pinhole aperture of the Vernier alignment method was displaced at different vertical positions in front of the pupil. The other procedures were the same [53].

(4) A more direct technique is matching the size of two targets presented at different wavelengths, i.e. of red and blue color. However, the discrimination thresholds on size were assumed to be too high to resolve CDM [65]. Campbell had studied the discrimination thresholds of subjects between sinusoidal gratings of different spatial frequencies and found a difference in spatial frequencies detectable only when it exceeded 3–6% [66].

In my study, first I studied the possibility of using method (4). It was proved by a 2-AFC procedure that objects with well-defined contours (such as squares) can probably be matched by subjects in size with much better resolution, 0.68% [3]. Second, based on the 2-AFC experiment results, the chromatic differences in perceived image magnification (determined by TCA) in different subjects were measured with two similar newly established psychophysical procedures in Figure 1 and 2 in the my first published paper: 1) A red and a blue square were presented on a black screen and subjects were asked to match the size of the squares. 2) A filled red and blue square were presented flickering on top of each other at a frequency of 2 Hz. The perceived brightness and size were adjusted by subjects to minimize the impression of flicker. The size difference measured in two procedures was defined as CDM, which varied widely among subjects from 0.0% to 3.6% in my studies. In both two procedures, all the subjects reported the red squares to be larger than the blue squares. It was found that a major part of the inter-individual variance in CDM (64%) was explained by lens thickness, vertical lens tilt and lens decentration. Considering the age difference in subjects, CDM was found to increase by 3.5% per year, while lens thickness increased as well. As reported by other researchers, the GRIN profile of a lens changes with age [4-7], which might also contribute to the change in CDM. Therefore, a Liou-brennan eye model[41] with a GRIN CL [67] was built in Zemax to simulate CDM of two eyes from two different subjects with different ages (subject 1: 29 years, subject 2: 54 years; major difference was lens thickness). The results in simulations were in line with the results from experiments, CDM increases with age: Subject 2's eye (54 years old) has more CDM than subject 1's eye (29 years old).

3.5 Project 2: the effect of longitudinal chromatic (LCA) on the S-cone distribution in the fovea

3.5.1 Historical review of S- (short wavelength) cone and its visual function

Depends on major functional differences, there are two types of human photoreceptors: rods and cones. At very low light levels, i.e. during the night outside the range of street lamps, visual experience is based only on the rod signal (scotopic vision). As soon as colors become visible, we can be sure to approach the mesopic range with both rod and cone contributions, and with day

light, we see largely with cones (photopic vision; it is not so clear what rods are doing during photopic vision). In cones, there are three different types of cone cell, L- (long wavelength), M- (middle wavelength), S- (short wavelength) cones, distinguished by their absorption peaks at different wavelengths (Figure 3).

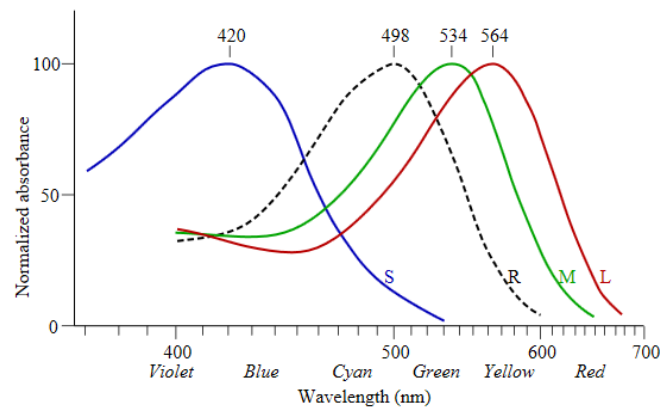


Figure 3. Normalized absorption curve of three human cones and rods (dashed) [68].

In 1894, a lecture at the Preussische Akademie der Wissenschaften was given by Arthur König at Berlin. In this lecture, he stated that the human fovea is “blue blind” and that human are “dichromatic” in the fovea (p. 591). He did some psychophysical studies in which subjects had to fixate a small monochromatic light spots, presented at different wavelengths. Subjects were found to have difficulties to distinguish between blue and green [69]. Later in 1999, Curcio’s group did histology in human retinal tissue to map out the foveal photoreceptor distribution. A tritanopic zone (about 20 arcmin in diameter) in the center of the fovea was found and also confirmed by psychophysical studies [70-72]. Even at the adjacent foveal slopes, the S-cone density was quite low [73]. The related visual consequence is a “foveal blue scotoma”. Since human visual system has the capability of neural “filling-in”, the foveal blue scotoma is normally not visible [72, 74-77]. During our normal visual experience, “neural filling-in” is a common but complex mechanism [74, 78-80]. It can be observed (1) when there is no or limited input in restricted regions of the visual field [81-84], (2) when it fails during steady fixation [85-87] during gaze contingent presentation [88-90], and (3) in some well-known illusions, like neon color spreading [91-94]. In spite of that, Magnussen and his colleagues worked on the visualization of blue scotoma for many years and published two methods [75, 76]. In their first method, a blue field, presented in Maxwellian view was sinusoidally modulated in luminance with a frequency of 1 – 2 Hz and presented to the subjects. The peak wavelength of the blue light was around 450 nm. Under this experimental condition, the blue scotoma was visualized as a small dark spot that moved with the subjects’ point of fixation. Apparently, the neural filling-in process is

compromized by the brightness modulation of the blue field. The visibility of blue scotoma rated by subjects at different wavelengths matched the spectral sensitivity of the S-cones. In the second method, the subjects saw their blue scotoma as a bright spot in a negative afterimage after adapted to a bright blue field. Subjects were asked to rate the visibility of the blue scotoma. The result of these ratings again matched the spectral sensitivity function of the S-cones. The diameter of subjective blue scotomas was about 24.8 to 44.3 arcmin consistent with the diameter of the S-cone free zone in the histological study described above [73].

3.5.2 My PhD work on the relationship between foveal blue scotoma and the shape of foveal pit (Paper 2)

The human fovea has the shape of a pit in which M- cones and L-cones are tightly packed. It permits maximal visual acuity because cones in the center of the fovea have their private lines to the visual cortex [95]. Recently, a negative correlation was found between the foveal diameter and the steepness of the foveal slopes [96]. In our studies [97], we used similar procedure/method as Magnussen and his colleagues[75]: A blue flicker field (frequency: 1 Hz) was shown on a computer screen. Subjects were asked to look at this blue field through a “blue” cut-off filter and draw their foveal blue scotoma on a transparent foil attached in front of the computer screen. Two shapes of blue scotoma were found in subjects: 1) a small spot; 2) a circular shape in the center, surrounded by star-shaped radial extension. It was found that the diameters of the blue scotomas in the left and right eyes of one subject were highly correlated: from 15.8 to 76.4 arcmin in the right eyes and 15.5 to 84.7 arcmin in the left eyes. The 2D-structures of the foveal pit were obtained from OCT images and also correlated to the blue scotoma diameters. Interestingly, the shape of the foveal pit highly varied among the human eyes and there was a significant correlation between the size of the foveal blue scotoma and the steepness of the foveal pit - the steeper the pit, the larger the blue scotoma.

The yellowish macular pigment that covers the foveal and parafoveal area consists of lutein and zeaxanthin and is embedded in the cone axons and the inner-plexiform layer in the central region. Its function is to protect the underlying photoreceptors from exposure to high energy short wavelength light [98-100] and prevent photo-oxidative damage [100-102]. The peak absorption of the macular pigment is close to the spectral sensitivity peak of the S-cones [103], around 460 nm [104]. In some studies [105, 106], it was found that the macular pigment distribution varies considerably among different subjects. Maxwell’s spot is assumed to be a consequence due to the preferential absorption of blue light in macular pigment. When looking at a bright white surface through a dichroic filter, Maxwell’s spot becomes visible as a brownish or reddish patch. It is

highly variable in shape and diameter among different subjects [107]. Rapid adaptation of macular photoreceptors caused Maxwell's spot to disappear soon [108]. Therefore, a dichroic filter was recommended not only by Maxwell himself to prevent retinal adaptation, but also many other scientists [107, 109, 110]. According to the absorption of the macular pigment, discussed here, we also compared "foveal" blue scotoma with macular pigment distribution and Maxwell's spot. Macular pigment distribution was measured by applying an image processing on fundus camera images in imageJ and correlated to blue scotoma diameters and Maxwell's spots diameters of every subject. The significant correlations were found between the macular pigment distribution and the diameters of Maxwell's spots but not between the macular pigment distribution and the diameters of blue scotoma. We also compared the appearance of Maxwell's spot with the perceived blue scotoma in the same eyes of the subject. It is found that the shapes, colors and visibilities varied. Therefore, we concluded that blue scotoma and Maxwell's spots were two different vision phenomenon: blue scotoma is a result of S- cones missing in the fovea, while the Maxwell's spot is a consequence of macular pigment absorption.

3.6 Project 3: the potential of polychromatic eccentric photorefraction in measuring LCA in the human eye

3.6.1 Historical review of eccentric photorefraction

Eccentric photorefraction, a technique that is widely used in animal models and humans, was invented by Schaeffel and Howland in 1987, and further developed by Schaeffel [111]. It is a brightness slope based technique, in which a few infrared LEDs, arrayed eccentrically to the optical axis of a camera lens, generated the steepness of the brightness slope in the pupil. In order to calibrate the photorefraction technique, the brightness slopes are determined by placing trial lenses of known power in front of the subjects' eye to induce defined refractive errors. On the other side, refractive errors of the eyes could be conducted by brightness slope multiplying with a "conversion factor". It is very powerful in measuring myopia, astigmatism and anisometropia of young children, as it is fast and easy to operate from a meter distance and binocular [112-115]. However, later Schaeffel's group [116] reported that this technique has difficulty in measuring infants and young children with hyperopia. The underestimate is due to no fogging procedure, which is employed to relax accommodation. Beside of this problem, there is another well-known difficulty: the conversion factor varies among subjects (variability is about 15%). Until now, no study revealed the optical reason. Some studies proposed several factors that

may have effect, such as ethnic background [117], contrast and luminance response of the video system, pupil size, reflectance properties of the fundus, wavefront aberrations of the measured eye, and arrangement and specification of the LEDs [118, 119]. In the other hand, lots of researchers also studied variability by optical calculation and simulation in the software. Kusel's group used ray-tracing techniques on Gaussian optics with 3 different light sources to study the changing of light crescent in the pupil with spherical aberration and astigmatism. The following types of light sources were studied: (1) a point source with a knife-edge aperture, (2) a long linear light source with knife-edge aperture, and (3) a point source with a circular camera aperture, as normally found in camera lenses [120]. In type (1) and (2), the calculations could be completed in closed form and the determined equations were permitted to derive sphere, cylinder and axis from crescent size and slope from minimally two pictures, taken with different orientations of the LED segments. However, for the light source (3), the mathematics became too complex, so there was no result. Later, Austin Roorda studied how the conversion factor ("gain" in his paper) changed with different light configuration: single point light source and extended light source by simulating the optical system of eccentric photorefraction system [121]. In his study, the effects of monochromatic aberrations, and the determined working range, dead zone and linearity of the photorefraction were also studied. It was found in his study that comparing to a point source, the intensity profile in the pupil produced by extended light source was more linear. He also found that the effects of asymmetric monochromatic aberrations were reduced by averaging refractions obtained with two eccentric light sources positioned at opposing positions. Pupil size was also reported to have an impact on the conversion factor in his study. In 2000, the reliability and accuracy of a commercially available eccentric infrared photorefractor (PowerRefractor) were studied by Choi, et al in both laboratories and a Kindergarten [112]. This PowerRefractor used 6 LED segments, which were arranged in opposing positions to the optical axis of the camera. Each segment consists of 9 IR LEDs. Through this design, in which three meridians could be refracted from two opposing positions, the effects of the asymmetrical aberrations were reduced and the linear range of refractor was extended from +4D to -6D, relative to infinity.

3.6.2 Historical review of white LEDs eccentric photorefraction

Hodgkinson, Chong and Molteno, in 1991, proposed a method based on the principle infrared eccentric photorefraction to determine longitudinal chromatic aberration (LCA) within a single video frame (one flash). In this method, broadband white light was used instead of infrared light and refractive errors could be simultaneously measured in the R, B, and G channels of the video

system [122]. However, a problem came with the reflectivity of the human fundus that the fundus reflectivity varies with wavelength and is very low in the short wavelength range [123]. In 2010, Schaeffel and Kaymak [124] used high power white LEDs (Conrad, Nichia white led NSPW500DS) to compensate for this problem. In this equipment, LEDs had an emission peak at 460 nm and a CCD RGB camera with a spectral sensitivity of the blue channel matching the emission peak of the LEDs. However, they didn't find the same LCA as in the literature [57] by measurements in human eyes. Then, with their white LEDs eccentric photorefraction, they measured two types of artificial eyes: one solid rubber ball eye that was made by Chris Kuether (ckuether@central.uh.edu) from Houston University and a second air filled eye model eye with a single +60 D glass lens and a grey cardboard as artificial retina. As a result, the proper amount of LCA was measured. Both model eyes had a single reflecting layer as "retina", so they believed that LCA might be disturbed by multi-layer reflection from different fundal layers in the real eye.

3.6.3 My PhD work on measuring LCA with white LEDs eccentric photorefraction (Manuscript 3)

In this project, I studied the well-known problem of high variability in the conversion factor among subjects, by analyzing the factors determining the calibration of eccentric photorefraction. The refractions in Red, Green, and Blue channels in Caucasian subjects were studied by the same device (CCD camera and white LEDs) as Schaeffel and Kaymak [124] in a dimly illuminated room with trial lenses (range +4D to -4D, 1D step). Pupil size was fixed by an artificial aperture of 5 mm which is similar to the natural pupil. The experiments were done in three different conditions: (1) in the fovea, (2) 10 degrees off-axis in the temporal retina, and (3) in the fovea after 10 minutes of previous exposure to bright light to alter the fundus reflectance. In addition, the non-linearity of the camera system was analyzed: a homogenous "white" surface was placed in front of the camera system. The luminance (relative brightness) was controlled by different combinations of five different aperture stops and two neutral density filters, ND4 and ND 11 (attenuating factor: 0.7 and 0.25) placed in front of the camera. The corresponding average pixel brightness in Red, Green and Blue channels on the photo was determined by a Matlab program, separately. It was found that in each channel the pixel to luminance function was non-linear and can be fitted by an x-order polynomial. As all the pixel grey levels in our measurement remained below 100, the camera response in this area could be thought as linear and the non-linearity could be ignored. After controlling for the possibility of the video systems non-linearity, the conversion factors in white LEDs eccentric photorefraction still varied among subjects, even more than that in infrared light. In condition 1, they varied from 3.8 to 13.8 in the fovea; in condition 2, from 2.3 to 8.0 in the

10 degrees off-axis in the temporal retina; in condition 3, from 7.6 to 16 in the fovea after 10 minutes of previous exposure to bright light. We found the conversion factors increasing with macular pigment optical density (MPOD), eye axial length and the history of exposure to brightness before. When we analyzed the changes of fundal reflectance in three different conditions, it was surprising to find that the fundal reflectance was reduced in condition 3 compared with condition 1, while the conversion factor was increased. It was obvious that all the factors we found here led to reduced pupil brightness. Therefore, we could make a conclusion that the factor affecting the pupil brightness also changed conversion factors. Our findings would be important for applications of eccentric photorefractive accommodation, different ethnic groups or subjects who have longer eye length such as high myopia: When pupil brightness is in low level, the conversion factors need to be adapted to the number which compensated the interference from low pupil brightness.

3.7 Conclusions and outlook

In my PhD work, I studied adaptations of the human visual system to the two types of chromatic aberration, LCA and TCA. A simple psychophysical procedure was applied on the measuring of the CDM (one of TCA) in the human vision. I found that the human crystalline lens plays a major role in the individual-variability of TCA. Lens thickness, tilt and decentration all affect TCA. I also studied the relationship between LCA and the “foveal blue scotoma”. A trick of the human eye seems to leave the S-cones out from the foveal center [125] because they would cover territory but cannot contribute to spatial resolution: The focal planes on the retina are different for light of different wavelengths due to longitudinal chromatic aberration (LCA). The retinal image for mid- and long-wavelengths is typically in best focus in the fovea but the image for short wavelength is severely myopically defocused. Finally, I discussed the problems in application of polychromatic eccentric photorefractive accommodation on measuring LCA in the human eye. It is found that some calibration problems in eccentric photorefractive accommodation, related to the low pupil brightness, could be solved easily by changing conversion factors to compensate the loss in slope of pupil brightness.

So far, my studies have been finished, however, there are still some problems left for further studies:

First, the simulated TCAs in model eye are smaller than measured value in human eye. Based on our results, an advanced human lens model with a more accurate GRIN profile is needed.

Second, due to lack of technique, it was difficult to correlate “foveal” blue scotoma size to the S-cone distribution in the fovea. Right now, several laboratories are developing adaptive optics photoreceptor imaging devices to be used *in vivo* to map out the foveal cone mosaics. The next step in the “foveal blue scotoma study” would be to directly compare the “foveal blue scotoma” with the extend of the S-cone free area in the foveal center.

Third, in eccentric photorefraction, it future work has to take into account that the calibration of eccentric photorefraction varies with pupil size, axial length, fundal reflectance and linearity of the camera luminance to pixel response function. However, all these variables are accessible and can be used to improve the reliability of eccentric photorefraction, also during dynamic “real-time measurements” where pupil size changes (i.e during accommodation).

3.8 References

1. Artal, P. and J. Taberero, *Optics of human eye: 400 years of exploration from Galileo’s time*. Applied optics, 2010. **49**(16): p. D123-D130.
2. Chen, Y. and F. Schaeffel, *Crystalline lens thickness determines the perceived chromatic difference in magnification*. Journal Optical Society of America A, 2014. **31**(3): p. 524-531.
3. Chen, Y., W. Lan, and F. Schaeffel, *Size of the foveal blue scotoma related to the shape of the foveal pit but not to macular pigment*. Vision Research, 2015. **106**: p. 81-9.
4. Kasthurirangan, S., et al., *In vivo study of changes in refractive index distribution in the human crystalline lens with age and accommodation*. Investigative Ophthalmology & Visual Science, 2008. **49**(6): p. 2531-40.
5. Jones, L.A., et al., *Comparison of ocular component growth curves among refractive error groups in children*. Investigative Ophthalmology & Visual Science, 2005. **46**(7): p. 2317-27.
6. de Castro, A., et al., *Age-dependent variation of the Gradient Index profile in human crystalline lenses*. Journal of Modern Optics, 2011. **58**(19-20): p. 1781-87.
7. Moffat, B.A., D.A. Atchison, and J.M. Pope, *Age-related changes in refractive index distribution and power of the human lens as measured by magnetic resonance micro-imaging in vitro*. Vision Research, 2002. **42**(13): p. 1683-93.
8. Kruger, P.B. and J. Pola, *Stimuli for accommodation: blur, chromatic aberration and size*. Vision Reseach, 1986. **26**(6): p. 957-71.
9. Phillips, S. and L. Stark, *Blur: a sufficient accommodative stimulus*. Documenta Ophthalmologica, 1977. **43**(1): p. 65-89.
10. Schaeffel, F. and C. Schmucker. *Spatial integration of peripheral defocus during emmetropization in chicks and during accommodation in humans*. in *ARVO Meeting Abstracts May*. 2006.
11. Schor, C., B. Bridgeman, and C.W. Tyler, *Spatial characteristics of static and dynamic stereoacuity in strabismus*. Investigative Ophthalmology & Visual Science, 1983. **24**(12): p. 1572-9.

12. Suryakumar, R., et al., *Vergence accommodation and monocular closed loop blur accommodation have similar dynamic characteristics*. Vision Research, 2007. **47**(3): p. 327-37.
13. Aggarwala, K.R., S. Nowbotsing, and P.B. Kruger, *Accommodation to monochromatic and white-light targets*. Investigative Ophthalmology & Visual Science, 1995. **36**(13): p. 2695-705.
14. Kroger, R.H. and S. Binder, *Use of paper selectively absorbing long wavelengths to reduce the impact of educational near work on human refractive development*. British Journal of Ophthalmology, 2000. **84**(8): p. 890-3.
15. Rucker, F.J. and P.B. Kruger, *Accommodation responses to stimuli in cone contrast space*. Vision Research, 2004. **44**(25): p. 2931-44.
16. Rucker, F.J. and P.B. Kruger, *The role of short-wavelength sensitive cones and chromatic aberration in the response to stationary and step accommodation stimuli*. Vision Research, 2004. **44**(2): p. 197-208.
17. Seidemann, A. and F. Schaeffel, *Effects of longitudinal chromatic aberration on accommodation and emmetropization*. Vision Research, 2002. **42**(21): p. 2409-17.
18. Jenkins, T., *Aberrations of the eye and their effects on vision. part 1*. The British journal of physiological optics, 1963. **20**: p. 59-91.
19. Millodot, M. and J. Sivak, *Contribution of the cornea and lens to the spherical aberration of the eye*. Vision Research, 1979. **19**(6): p. 685-7.
20. Sivak, J. and R. Kreuzer, *Spherical aberration of the crystalline lens*. Vision Research, 1983. **23**(1): p. 59-70.
21. Tomlinson, A., R.P. Hemenger, and R. Garriott, *Method for estimating the spheric aberration of the human crystalline lens in vivo*. Investigative Ophthalmology & Visual Science, 1993. **34**(3): p. 621-9.
22. Artal, P. and A. Guirao, *Contributions of the cornea and the lens to the aberrations of the human eye*. Optics Letters, 1998. **23**(21): p. 1713-5.
23. Smith, G., et al., *The spherical aberration of the crystalline lens of the human eye*. Vision Research, 2001. **41**(2): p. 235-243.
24. Wald, G., *AREA AND VISUAL THRESHOLD*. The Journal of General Physiology, 1938. **21**(3): p. 269-87.
25. Land, M.F. and A.W. Snyder, *Cone mosaic observed directly through natural pupil of live vertebrate*. Vision Research, 1985. **25**(10): p. 1519-23.
26. Ahnelt, P.K., H. Kolb, and R. Pflug, *Identification of a subtype of cone photoreceptor, likely to be blue sensitive, in the human retina*. Journal of Comparative Neurology, 1987. **255**(1): p. 18-34.
27. Coletta, N.J. and D.R. Williams, *Psychophysical estimate of extrafoveal cone spacing*. Journal of the Optical Society of America A, 1987. **4**(8): p. 1503-13.
28. Williams, D.R., *Topography of the foveal cone mosaic in the living human eye*. Vision Research, 1988. **28**(3): p. 433-54.
29. Williams, R.W., *The human retina has a cone-enriched rim*. Visual Neuroscience, 1991. **6**(4): p. 403-6.
30. Ahnelt, P.K., *The photoreceptor mosaic*. Eye (Lond), 1998. **12 (Pt 3b)**: p. 531-40.
31. Roorda, A. and D.R. Williams, *The arrangement of the three cone classes in the living human eye*. Nature, 1999. **397**(6719): p. 520-22.
32. Gowdy, P.D. and C.M. Cicerone, *The spatial arrangement of the L and M cones in the central fovea of the living human eye*. Vision Research, 1998. **38**(17): p. 2575-89.

33. Chui, T.Y.P., H. Song, and S.A. Burns, *Adaptive-optics imaging of human cone photoreceptor distribution*. Journal of the Optical Society of America. A, Optics, image science, and vision, 2008. **25**(12): p. 3021.
34. Siminoff, R., *Simulated bipolar cells in fovea of human retina. I. Computer simulation*. Biological Cybernetics, 1991. **64**(6): p. 497-504.
35. Siminoff, R., *Simulated bipolar cells in fovea of human retina. II. Spectral responses of bipolar cells*. Biological Cybernetics, 1991. **64**(6): p. 505-10.
36. Osterberg, G., *Topography of the layer of rods and cones in the human retina*. 1935: Nyt Nordisk Forlag.
37. Atchison, D.A., G. Smith, and G. Smith, *Optics of the human eye*. 2000.
38. Southall, J.P.C. and H. von Helmholtz, *Helmholtz's treatise on physiological optics*. 1925: Optical Society of America.
39. Le Grand, Y. and S.G. El Hage, *Physiological optics*. Springer Series in Optical Sciences, Berlin: Springer, 1980, 1980. **1**.
40. Emsley, H.H., *Visual optics*. 1948: Hatton Press.
41. Liou, H.-L. and N.A. Brennan, *Anatomically accurate, finite model eye for optical modeling*. Journal Optical Society of America A, 1997. **14**(8): p. 1684-95.
42. Goncharov, A.V. and C. Dainty, *Wide-field schematic eye models with gradient-index lens*. Journal Optical Society of America A, 2007. **24**(8): p. 2157-74.
43. Siedlecki, D., H. Kasprzak, and B.K. Pierscionek, *Schematic eye with a gradient-index lens and aspheric surfaces*. Optics Letters, 2004. **29**(11): p. 1197-99.
44. Thibos, L.N., et al., *The chromatic eye: a new reduced-eye model of ocular chromatic aberration in humans*. Applied Optics, 1992. **31**(19): p. 3594-3600.
45. Rynders, M., et al., *Statistical distribution of foveal transverse chromatic aberration, pupil centration, and angle ψ in a population of young adult eyes*. Journal Optical Society of America A, 1995. **12**(10): p. 2348-57.
46. Marcos, S., et al., *A new approach to the study of ocular chromatic aberrations*. Vision Research, 1999. **39**(26): p. 4309-23.
47. Bedford, R. and G. Wyszecski, *Axial chromatic aberration of the human eye*. Journal of the Optical Society of America, 1957. **47**(6): p. 564-65.
48. Charman, W. and J. Jennings, *Objective measurements of the longitudinal chromatic aberration of the human eye*. Vision Research, 1976. **16**(9): p. 999-1005.
49. Howarth, P.A. and A. Bradley, *The longitudinal chromatic aberration of the human eye, and its correction*. Vision Research, 1986. **26**(2): p. 361-66.
50. Rynders, M., R. Navarro, and M. Losada, *Objective measurement of the off-axis longitudinal chromatic aberration in the human eye*. Vision Research, 1998. **38**(4): p. 513-22.
51. Jenkins, T., *Aberrations of the eye and their effects on vision. II*. The British Journal of Physiological Optics, 1963. **20**: p. 161.
52. Wald, G. and D.R. Griffin, *The change in refractive power of the human eye in dim and bright light*. Journal of the Optical Society of America, 1947. **37**(5): p. 321-334.
53. Thibos, L., et al., *Theory and measurement of ocular chromatic aberration*. Vision Research, 1990. **30**(1): p. 33-49.
54. Manzanera, S., et al., *A wavelength tunable wavefront sensor for the human eye*. Optics Express, 2008. **16**(11): p. 7748-55.
55. Atchison, D.A. and G. Smith, *Chromatic dispersions of the ocular media of human eyes*. Journal Optical Society of America A, 2005. **22**(1): p. 29-37.
56. Van Meeteren, A. and C. Dunnewold, *Image quality of the human eye for eccentric entrance pupils*. Vision Research, 1983. **23**(5): p. 573-79.

57. Marcos, S., et al., *Investigating sources of variability of monochromatic and transverse chromatic aberrations across eyes*. Vision research, 2001. **41**(28): p. 3861-71.
58. He, J.C., et al., *Measurement of the wave-front aberration of the eye by a fast psychophysical procedure*. Journal Optical Society of America A, 1998. **15**(9): p. 2449-56.
59. Simonet, P. and M.C. Campbell, *The optical transverse chromatic aberration on the fovea of the human eye*. Vision Research, 1990. **30**(2): p. 187-206.
60. Howland, B. and H.C. Howland, *Subjective measurement of high-order aberrations of the eye*. Science, 1976. **193**(4253): p. 580-82.
61. Ogboso, Y.U. and H.E. Bedell, *Magnitude of lateral chromatic aberration across the retina of the human eye*. Journal Optical Society of America A, 1987. **4**(8): p. 1666-72.
62. Thibos, L., *Calculation of the influence of lateral chromatic aberration on image quality across the visual field*. Journal Optical Society of America A, 1987. **4**(8): p. 1673-80.
63. Ling, H., et al., *CCAT2, a novel noncoding RNA mapping to 8q24, underlies metastatic progression and chromosomal instability in colon cancer*. Genome research, 2013. **23**(9): p. 1446-1461.
64. Campbell, C.E., *Relative importance of sources of chromatic refractive error in the human eye*. Journal Optical Society of America A, 2010. **27**(4): p. 730-38.
65. Zhang, X., A. Bradley, and L.N. Thibos, *Experimental determination of the chromatic difference of magnification of the human eye and the location of the anterior nodal point*. Journal Optical Society of America A, 1993. **10**(2): p. 213-20.
66. Campbell, F.W., J. Nachmias, and J. Jukes, *Spatial-frequency discrimination in human vision*. Journal of the Optical Society of America, 1970. **60**(4): p. 555-59.
67. Jaeken, B., L. Lundström, and P. Artal, *Peripheral aberrations in the human eye for different wavelengths: off-axis chromatic aberration*. Journal of the Optical Society of America A, 2011. **28**(9): p. 1871-79.
68. Bowmaker, J.K. and H.J. Dartnall, *Visual pigments of rods and cones in a human retina*. The Journal of Physiology, 1980. **298**: p. 501-11.
69. König, A., *ber den menschlichen Sehpurpur und seine Bedeutung für das Sehen*. Sitzungsberichte der Preussischen Akademie der Wissenschaften, 1894. **30**.
70. Willmer, E. and W. Wright, *Colour sensitivity of the fovea centralis*. Nature, 1945. **156**(3952): p. 119-21.
71. Wald, G., *Blue-blindness in the normal fovea*. Journal of the Optical Society of America, 1967. **57**(11): p. 1289-1301.
72. Williams, D.R., D.I. MacLeod, and M.M. Hayhoe, *Punctate sensitivity of the blue-sensitive mechanism*. Vision Research, 1981. **21**(9): p. 1357-75.
73. Curcio, C.A., et al., *Distribution and morphology of human cone photoreceptors stained with anti - blue opsin*. Journal of Comparative Neurology, 1991. **312**(4): p. 610-624.
74. Gerrits, I.H. and A. Vendrik, *Simultaneous contrast, filling-in process and information processing in man's visual system*. Experimental Brain Research, 1970. **11**(4): p. 411-430.
75. Magnussen, S., et al., *Filling-in of the foveal blue scotoma*. Vision Research, 2001. **41**(23): p. 2961-67.
76. Magnussen, S., et al., *Unveiling the foveal blue scotoma through an afterimage*. Vision Research, 2004. **44**(4): p. 377-83.
77. Spillmann, L. and J.S. Werner, *Long-range interactions in visual perception*. Trends in neurosciences, 1996. **19**(10): p. 428-34.
78. Walls, G., *The filling-in process*. American journal of optometry and archives of American Academy of Optometry, 1954. **31**(7): p. 329.
79. Komatsu, H., I. Murakami, and M. Kinoshita, *Surface representation in the visual system*. Cognitive Brain Research, 1996. **5**(1): p. 97-104.

80. Pessoa, L., E. Thompson, and A. Noë, *Filling-in is for finding out*. Behavioral and Brain Sciences, 1998. **21**(06): p. 781-96.
81. Ramachandran, V.S. and R.L. Gregory, *Perceptual filling in of artificially induced scotomas in human vision*. Nature, 1991. **350**(6320): p. 699-702.
82. Gerrits, H. and G. Timmerman, *The filling-in process in patients with retinal scotomata*. Vision Research, 1969. **9**(3): p. 439-42.
83. Ramachandran, V.S., *An excellent introduction to the phenomenon of filling-in. Provides fascinating examples of perceptual filling-in at the blind spot*. Blind Spots Scientific American, 1992. **266**: p. 86–91.
84. Gassel, M.M. and D. Williams, *Visual function in patients with homonymous hemianopia. III. The completion phenomenon; insight and attitude to the defect; and visual functional efficiency*. Brain, 1963. **86**: p. 229-60.
85. Friedman, H.S., H. Zhou, and R. von der Heydt, *Color filling-in under steady fixation: behavioral demonstration in monkeys and humans*. Perception, 1999. **28**(11): p. 1383-95.
86. von der Heydt, R., Friedman, H. & Zhou, H. , *In Filling-in*. 2003, New York: Oxford Univ. Press.
87. Hamburger, K., et al., *Filling-in with colour: different modes of surface completion*. Vision Research, 2006. **46**(6-7): p. 1129-38.
88. Yarbus, A.L., *Eye Movements and Vision*. 1967, Plenum: New York.
89. Krauskopf, J., *Effect of retinal image stabilization on the appearance of heterochromatic targets*. Journal of the Optical Society of America, 1963. **53**: p. 741-4.
90. Gerrits, H.J., B. De Haan, and A.J. Vendrik, *Experiments with retinal stabilized images. Relations between the observations and neural data*. Vision Research, 1966. **6**(7): p. 427-40.
91. van Tuijl, H.F. and E.L. Leeuwenberg, *Neon color spreading and structural information measures*. Percept Psychophys, 1979. **25**(4): p. 269-84.
92. Redies, C. and L. Spillman, *The neon color effect in the Ehrenstein illusion*. Perception, 1982. **10**(6): p. 667-81.
93. Grossberg, S. and E. Mingolla, *Neural dynamics of form perception: boundary completion, illusory figures, and neon color spreading*. Psychological Review, 1985. **92**(2): p. 173-211.
94. Bressan, P., et al., *Neon color spreading: a review*. Perception, 1997. **26**(11): p. 1353-66.
95. Wässle, H. and B.B. Boycott, *Functional architecture of the mammalian retina*. Physiological reviews, 1991. **71**(2): p. 447-80.
96. Knighton, R.W. and G. Gregori, *The Shape of the Ganglion Cell plus Inner Plexiform Layers of the Normal Human Macula*. Investigative ophthalmology & visual science, 2012. **53**(11): p. 7412-20.
97. Chen, Y., W. Lan, and F. Schaeffel, *Size of the foveal blue scotoma related to the shape of the foveal pit but not to macular pigment*. Vision Research, 2015. **106**: p. 81-9.
98. Hammond, B.R., B.R. Wooten, and D.M. Snodderly, *Individual variations in the spatial profile of human macular pigment*. Journal Optical Society of America A, 1997. **14**(6): p. 1187-96.
99. Werner, J.S., S.K. Donnelly, and R. Kliegl, *Aging and human macular pigment density: appended with translations from the work of Max Schultze and Ewald Hering*. Vision Research, 1987. **27**(2): p. 257-68.
100. Werner, J.S., M.L. Bieber, and B.E. Scheffrin, *Senescence of foveal and parafoveal cone sensitivities and their relations to macular pigment density*. Journal Optical Society of America A, 2000. **17**(11): p. 1918-32.
101. Kirschfeld, K., *Carotenoid pigments: their possible role in protecting against photooxidation in eyes and photoreceptor cells*. Proceedings of the Royal Society of London. Series B. Biological Sciences, 1982. **216**(1202): p. 71-85.

102. Nussbaum, J.J., R.C. Pruett, and F.C. Delori, *Macular yellow pigment: the first 200 years*. Retina, 1981. **1**(4): p. 296-310.
103. Stockman, A. and L.T. Sharpe, *The spectral sensitivities of the middle-and long-wavelength-sensitive cones derived from measurements in observers of known genotype*. Vision Research, 2000. **40**(13): p. 1711-37.
104. Bone, R.A., J.T. Landrum, and A. Cains, *Optical density spectra of the macular pigment in vivo and in vitro*. Vision Research, 1992. **32**(1): p. 105-10.
105. Wooten, B.R. and B.R. Hammond, *Macular pigment: influences on visual acuity and visibility*. Progress in retinal and eye research, 2002. **21**(2): p. 225-40.
106. Wooten, B.R., et al., *A practical method for measuring macular pigment optical density*. Investigative Ophthalmology & Visual Science, 1999. **40**(11): p. 2481-89.
107. Isobe, K. and K. Motokawa, *Functional structure of the retinal fovea and Maxwell's spot*. Nature, 1955. **175**: p. 306-7.
108. Miles, W.R., *Comparison of functional and structural areas in human fovea. I. Method of entoptic plotting*. Journal of neurophysiology, 1954. **17**(1): p. 22-38.
109. Holm, E., *Das gelbe Maculapigment und seine optische Bedeutung*. Graefe's Archive for Clinical and Experimental Ophthalmology, 1922. **108**(1): p. 1-85.
110. Walls, G.L. and R.W. Mathews, *New means of studying color blindness and normal foveal color vision, with some results and their genetical implications*. Publications in psychology. University of California (1868-1952), 1952. **7**(1): p. 1.
111. Schaeffel, F., H. Wilhelm, and E. Zrenner, *Inter-individual variability in the dynamics of natural accommodation in humans: relation to age and refractive errors*. Journal of Physiology, 1993. **461**: p. 301-20.
112. Choi, M., et al., *Laboratory, clinical, and kindergarten test of a new eccentric infrared photorefractor (PowerRefractor)*. Optometry & Vision Science, 2000. **77**(10): p. 537-48.
113. Dahlmann-Noor, A.H., et al., *Vision screening in children by Plusoptix Vision Screener compared with gold-standard orthoptic assessment*. British Journal of Ophthalmology, 2009. **93**(3): p. 342-5.
114. Howland, H.C., *Photorefractive eyes: history and future prospects*. Optometry & Vision Science, 2009. **86**(6): p. 603-6.
115. Hunt, O.A., J.S. Wolffsohn, and B. Gilmartin, *Evaluation of the measurement of refractive error by the PowerRefractor: a remote, continuous and binocular measurement system of oculomotor function*. British Journal of Ophthalmology, 2003. **87**(12): p. 1504-8.
116. Schaeffel, F., U. Mathis, and G. Bruggemann, *Noncycloplegic photorefractive screening in pre-school children with the "PowerRefractor" in a pediatric practice*. Optometry & Vision Science, 2007. **84**(7): p. 630-9.
117. Sravani, N.G., V.K. Nilagiri, and S.R. Bharadwaj, *Photorefractive estimates of refractive power varies with the ethnic origin of human eyes*. Scientific Reports, 2015. **5**: p. 7976.
118. Blade, P.J. and T.R. Candy, *Validation of the PowerRefractor for measuring human infant refraction*. Optometry & Vision Science, 2006. **83**(6): p. 346-53.
119. Bharadwaj, S.R., et al., *Empirical variability in the calibration of slope-based eccentric photorefractive*. Journal Optical Society of America A, 2013. **30**(5): p. 923-931.
120. Kusel, R., et al., *Light-intensity distribution in eccentric photorefractive crescents*. Journal Optical Society of America A, 1998. **15**(6): p. 1500-1511.
121. Roorda, A., M.C. Campbell, and W.R. Bobier, *Slope-based eccentric photorefractive: theoretical analysis of different light source configurations and effects of ocular aberrations*. Journal Optical Society of America A, 1997. **14**(10): p. 2547-56.
122. Hodgkinson, I., K. Chong, and A. Molteno, *Characterization of the fundal reflectance of infants*. Optometry & Vision Science, 1991. **68**(7): p. 513-521.

123. Delori, F.C. and K.P. Pflibsen, *Spectral reflectance of the human ocular fundus*. Applied Optics, 1989. **28**(6): p. 1061-77.
124. Schaffel, F. and H. Kaymak, *New Techniques to Measure Lens Tilt, Decentration and Longitudinal Chromatic Aberration in Phakic and Pseudophakic Eyes*. Nova Acta Leopoldina NF, 2010. **111**(379): p. 127-136.
125. Rodieck, R.W., *The vertebrate retina: Principles of structure and function*. 1973, Oxford, England: W. H. Freeman.

4. List of publications

List of full papers by Yun Chen

1. Chen, Y. and F. Schaeffel, Crystalline lens thickness determines the perceived chromatic difference in magnification. *Journal Optical Society of America A*, 2014. 31(3): p. 524-531.
2. Chen, Y., W. Lan, and F. Schaeffel, Size of the foveal blue scotoma related to the shape of the foveal pit but not to macular pigment. *Vision Research*, 2015. 106: p. 81-9.
3. Chen, Y. and F. Schaeffel, Factors affecting the calibration of white light eccentric photorefraction. *Biomedical Optics Express*, June 2015 (under review)

5. Descriptions of personal contributions

In paper 1 and 3, some of the ideas for my experiments came, in part, from my supervisor (Prof. Frank Schaeffel) but I performed all the experiments, analyzed the data, studied the literature and wrote the drafts of manuscripts. I discussed the experimental results and revised the manuscript together with my supervisor until they were published.

In paper 2, M.D. W. Lan made inspection on all the fundus photos and confirmed all of them were health. Some of the experiments ideas came from my supervisor (Prof. Frank schaeffel). I performed all the experiments, analyzed the data, studied the literature and wrote the drafts of manuscripts. I discussed the experimental results and revised the manuscript together with my supervisor until they were published.

6. Appended/ Manuscripts

Crystalline lens thickness determines the perceived chromatic difference in magnification

Yun Chen and Frank Schaeffel*

Section of Neurobiology of the Eye, Ophthalmic Research Institute, Calwerstrasse 7/1, 72076 Tuebingen, Germany

*Corresponding author: frank.schaeffel@uni-tuebingen.de

Received October 21, 2013; accepted December 19, 2013;
posted January 13, 2014 (Doc. ID 199806); published February 13, 2014

Since the origin of the high interindividual variability of the chromatic difference in retinal image magnification (CDM) in the human eye is not well understood, optical parameters that might determine its magnitude were studied in 21 healthy subjects with ages ranging from 21 to 58 years. Two psychophysical procedures were used to quantify CDM. They produced highly correlated results. First, a red and a blue square, presented on a black screen, had to be matched in size by the subjects with their right eyes. Second, a filled red and blue square, flickering on top of each other at 2 Hz, had to be adjusted in perceived brightness and then in size to minimize the impression of flicker. CDM varied widely among subjects from 0.0% to 3.6%. Biometric ocular parameters were measured with low coherence interferometry and crystalline lens tilt and decentration with a custom-built Purkinjometer. Correlations were studied between CDM and corneal power, anterior chamber depth, lens thickness, lens tilt and lens decentration, and vitreous chamber depths. Lens thickness was found significantly correlated with CDM and accounted for 64% of its variance. Vertical lens tilt and decentration were also significantly correlated. It was also found that CDM increased by 3.5% per year, and part of this change can be attributed to the age-related increase in lens thickness. © 2014 Optical Society of America

OCIS codes: (330.0330) Vision, color, and visual optics; (330.4595) Optical effects on vision; (330.5370) Physiological optics; (330.1690) Color.
<http://dx.doi.org/10.1364/JOSAA.31.000524>

1. INTRODUCTION

Sharpness and contrast of the retinal image are affected by two types of optical aberrations: monochromatic and chromatic. Monochromatic aberrations result from imperfections in the refracting surfaces while chromatic aberrations result from dispersion of light in the ocular media [1] which makes the position of the focal plane and retinal image magnification dependent on wavelength [2].

Wavelength-dependent differences in optical power of the eye are referred to as longitudinal chromatic aberration (LCA). In the human eye, LCA amounts to about 2.5 D between the red and the blue ends of the visible spectrum, with more myopic refractions in the blue. Transverse chromatic aberration (TCA) has been less studied, but [3] described that it causes more loss in retinal image contrast than spherical aberration or coma. While LCA is similar among subjects because it is largely determined by the dispersion of water, almost all studies acknowledged that TCA is inherently variable not only among subjects [4–11] but sometimes also between the left and the right eyes [2,4–16].

One aspect of TCA is the chromatic difference in lateral image position, and the other is the chromatic difference in image magnification (CDM) [7,8,10,17]. The term TCA was used for slightly different phenomena in different studies. Conventionally, TCA occurs when light from an off-axis object enters in an oblique angle into the eye, as Ogboso and Bedell [8] measured it (the angle is then given from the achromatic axis of the eye). TCA will be larger the more oblique the incident angle becomes and should not depend on pupil size. This type of TCA also exists in the fovea as it is normally not coinciding

with the achromatic axis of the eye. However, in the study by Zhang *et al.* [18] the measurements were performed for on-axis objects, with a small displaced aperture in the plane of the pupil. As an effect of the LCA, this displaced aperture resulted in a shift in transverse displacement of the rays on the retina depending on wavelength. This type of induced TCA was also used as a method to measure the LCA of the eye.

Three different psychophysical procedures have been developed to study CDM. Zhang *et al.* [18] estimated CDM from the physical tilt angle of the apparent frontoparallel plane (AFPP) under dichoptic viewing conditions when vision in one eye was limited to long-wavelength light (red) and the other was limited to short-wavelength light (blue). Due to the CDM, the image sizes were different on the retina. The subjects were asked to move rods on the AFPP until the same sizes on the retina were perceived. The adjusted lateral tilt of the AFPP was a measure of the magnitude of CDM. In the second method, CDM was measured as the perceived vertical misalignment of a red and a blue bar, the “two color vernier alignment method” [8]. A shortcoming of this technique is that it can be used only near the fovea because vernier thresholds rapidly exceed CDM in the periphery of the visual field [10,18]. The third method is the combination of the two color vernier alignment method with an artificial pinhole aperture which is displaced at different lateral positions in front of the pupil [10]. While all techniques described above measure CDM indirectly, a fourth technique would be more direct: matching the size of two targets that are presented at short and long wavelengths, respectively. However, until now, no study has been published that used this approach because size

discrimination thresholds were assumed to be too high to resolve CDM [18]. The authors of [18] perhaps based their conclusion in part on an article by Campbell *et al.* [19], who had looked at the ability of subjects to discriminate between sinusoidal gratings of different spatial frequencies. Campbell *et al.* [19] found that a difference in spatial frequency needs to exceed 3%–6% to become detectable. In contrast, objects with well-defined contours (such as squares) can probably be matched in size with much better resolution. An advantage of a size-matching procedure is that it can be done on a computer screen with software that allows adjusting the size of objects presented at different colors and sizes in fine steps. Therefore, we tested this approach. First, we measured the size-discrimination thresholds in our subjects for achromatic stimuli and found that they were sufficiently low to resolve the expected differences in size due to CDM. Second, the psychophysically determined CDM in each subject was correlated with optical and biometric variables in the eye, measured by low coherence interferometry and by a custom-built Purkinjmeter.

2. METHODS

A. Subjects

Twenty-one subjects, with an average age of 34.0 ± 13.8 years (range 21–58 years; 13 female and 8 male) and normal color vision, were recruited for the experiments. Nine subjects were myopic (average spherical equivalent \pm SD: OD: -4.4 ± 1.6 D; OS: -3.6 ± 1.3 D) and three were hyperopic (OD: $+1.8 \pm 0.6$ D; OS: $+1.8 \pm 0.6$ D). Refractions of the left and right eyes were highly correlated among the subjects (refraction left eyes = $0.841 \times$ refraction right eyes $+0.11$, $R = 0.99$); and the mean absolute difference between both eyes of the nine myopic subjects was 0.7 ± 0.6 D). Six of the myopic subjects wore spectacles, and three wore contact lenses, also during the experiments. The hyperopic subjects did not wear any corrections. To evaluate the impact of optical corrections on the measurements, CDM was correlated with the spherical refractive errors of the subjects. The study adhered to the tenets of the declaration of Helsinki and was approved by the local University Ethics Commission.

B. Psychophysical Measurements

A blue open square and a red open square with line width of 10 pixels were generated by software written in Microsoft Visual C++ 6.0. They were presented side by side on a black screen (experiment 1, Fig. 1), or they alternately covered each other at a frequency of 2 Hz (experiment 2, Fig. 2). Peak wavelengths of the squares, also used in a later simulation of CDM in ZEMAX, were at about 432 and 590 nm, respectively. According to the subjects' reports, similar brightness was perceived for the red and the blue squares when the RGB coordinates were 0, 0, 255 (blue) and 200, 0, 0 (red). Both squares had the same side length of 34.9 mm, equivalent to 3.32 deg in the visual field at a viewing distance of 60 cm. A chin rest was used to minimize head movements. Subjects were tested with their right eyes; the left was covered. The test procedures were as follows.

1. Experiment 1

To verify that the subjects were able to discriminate the small differences in size between the red and blue squares,

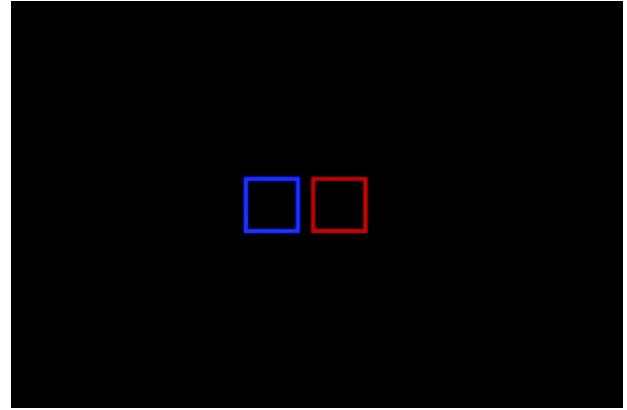


Fig. 1. Blue and red open squares, presented on a black background. For most subjects, the blue square appeared smaller than the red, despite that they had the same size.

psychometric functions were measured in 11 of the subjects using a two-alternative forced choice (2-AFC) procedure. Two gray squares were presented on the monitor at the same places as the red and blue squares shown in Fig. 1. The sizes difference of the two squares was randomly varied by the software from 0% to 6.4% (diameter $+0$, $+1$, $+2$, $+3$, $+4$, $+6$, $+8$ pixels), and subjects had to decide which of the two squares was larger. The procedure was repeated 10 times for each subject.

2. Experiment 2

Subjects adjusted the size of the blue square to match the size of the red square, using the left and right arrow keys of the keyboard. One step was equivalent to 0.294 mm (one pixel) on the LCD screen (EIZO FlexScan S1921, 19 in.), equivalent to 1.6 arcmin of visual angle at a distance of 60 cm. The size of the red square was fixed, but the initial size of the blue square was randomly varied by the software. Experiments were done with brighter red [RGB (255, 0, 0)] versus darker blue [RGB (0, 0, 200)] and with darker red [RGB (200, 0, 0)] versus brighter blue [RGB (0, 0, 255)]. The average of four repeated measurements provided the perceived size difference between the red

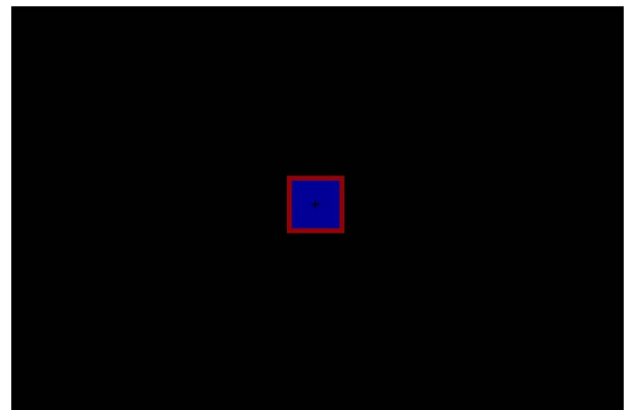


Fig. 2. Stimulus to minimize the perceived brightness differences between red and blue and to quantify perceived differences in size of the filled red and blue squares. The filled squares were presented on top of each other in an alternating fashion, being replaced at 2 Hz. The black cross in the center provides a fixation point. Both brightness and size could be adjusted by the subjects until luminance flicker was minimized and until the perceived sizes were matched.

and the blue squares for each subject, together with their standard deviations (SDs).

3. Experiment 3

A second paradigm was employed to measure CDM. A filled blue and a red square were alternatingly presented on top of each other (Fig. 2) with a flicker frequency of 2 Hz. The subjects had to adjust two variables. In the first step, they had to match the brightness of the blue and the red by minimizing perceived brightness differences. On average this condition was met when the blue square was set to RGB (0, 0, 255) and the red to (0, 0, 200). In the second step, they had to minimize the perceived size differences between both squares. As in experiment 1, the size of the red square was fixed at 34.9 mm (visual angle 3.2 deg). A black cross was presented in the center of the squares to lock fixation. As in experiment 1, the procedure was repeated four times, and averages and SDs were calculated.

4. Experiment 4

CDM was compared also in both eyes of five randomly selected subjects. As before, averages and SDs from four repetitions were determined.

C. Optical and Biometrical Measurements in the Eyes

All subjects were measured with a commercially available low-coherence interferometer, the Haag–Streit Lenstar LS 900 (HAAG–STREIT AG, Bern, Switzerland). The instrument provides central corneal thickness, corneal curvature (both flattest and steepest meridians along with the angle of the astigmatism, and the refractive powers in the two principal meridians), anterior chamber depth, lens thickness, and vitreous chamber depth. Pupils did not need to be dilated for the measurements.

D. Kappa Angle, Lens Tilt, and Decentration Measurement

A custom-built semi-automated device [20] was used to record Kappa angle, lens tilt, and lens decentration in 15 subjects who were selected based on availability from the full sample of 21 subjects. The positions of three Purkinje images (P1, P3, and P4) in the pupil were recorded for three different gaze positions. The software determined horizontal and vertical Kappa angle, horizontal and vertical lens tilt, and horizontal and vertical lens decentration. Pupils did not need to be dilated for the measurements.

E. Statistics

Paired *t*-tests were performed in Microsoft Excel (Asknet AG, Germany) to determine the significance of the differences between experiments. Linear regression analysis was used to determine correlations between psychophysical results and optical or biometrical measurements in the eyes. SPSS (version 16.0, SPSS, Chicago, Illinois) was used to build a multiple regression model for multivariable analysis. Using the “simultaneous” method, all the variables are set up together to determine which variable has the strongest impact on the dependent variable, that is, which provides the most accurate prediction of CDM. Since all variables such as lens thickness, lens tilt, lens decentration, and age may contribute to CDM, their relative impact on CDM is ranked. The four

variables (x_{i1} : lens thickness, x_{i2} : lens tilt, x_{i3} : lens decentration, x_{i4} : age, y : CDM) are assumed to satisfy the linear model: $y = b_0 + b_1x_{i1} + b_2x_{i2} + b_3x_{i3} + b_4x_{i4} + u_i$ while $i = 1, 2, 3, 4$, where u_i are values of an unobserved error term; u_i and b_i the unknown parameter constants. b_i are called standard regression coefficients. The variable which had strongest impact on the dependent variable (CDM) was identified.

3. RESULTS

A. Experiment 1—Detection Thresholds for Size Differences of the Two Squares: Psychometric Function

Using a 2-AFC procedure, 11 subjects had to indicate which of two gray squares was larger (no chromatic cues). The percentage of correct responses was plotted as a function of size differences of the gray squares (Fig. 3). The psychometric function shows that size differences of 0.68% could be correctly discriminated in 75% of the cases.

B. Experiment 2—Perceived Differences in Magnification between the Blue and Red Squares

None of the subjects had reversed CDM (which would show up as a negative value in the percentage magnification difference shown in Fig. 4). All subjects judged the blue squares to be smaller than the red (Fig. 1), although the variability among subjects was large. Three perceived only a tiny magnification difference of 0.2%, while others saw differences of up to 3.2%. The average magnification difference between the red and blue squares were $1.2\% \pm 0.7\%$ when the red square was presented at RGB (200, 0, 0) and the blue RGB (0, 0, 255), and $1.1\% \pm 0.7\%$ when the red was presented at RGB (255, 0, 0) and the blue at RGB (0, 0, 200), suggesting that the perceived differences in size were not due to brightness differences. Figure 4 shows that the perceived magnification differences in the two conditions were highly correlated ($R = 0.814$; $df = 20$, $p < 0.01$). There were also no statistically significant differences between the two data sets (paired *t*-test, $p = 0.18$), suggesting that we really measured the effects of CDM.

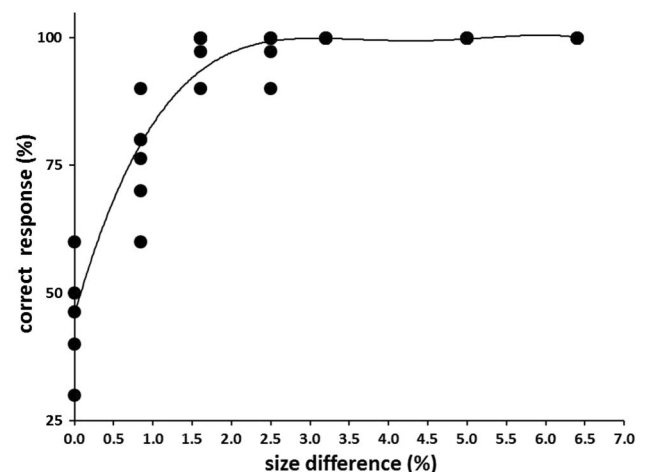


Fig. 3. Psychometric function showing the percentage of correct responses of 11 subjects judging the size differences between two gray squares. Data are from 11 subjects, but fewer data points may be visible because they may be superimposed.

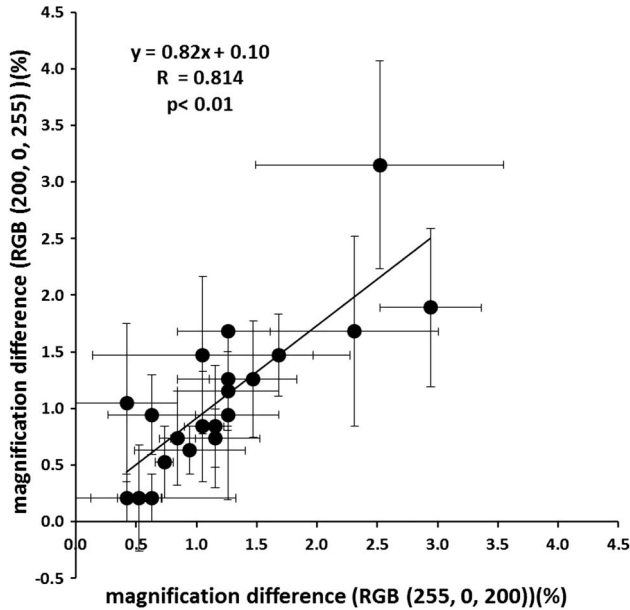


Fig. 4. Perceived differences in the size of the red and blue squares, measured in percent, when the red square was brighter (abscissa; red pixel value 255, blue 200) or the blue square was brighter (ordinate; red 200, blue 255). The perceived differences in size were highly correlated. Data points represent the means and their SDs from four repetitions.

C. Experiment 3—Perceived Differences in CDM as Measured with the Second Paradigm

In this second test, three subjects perceived negative magnifications; that is, the blue filled square appeared larger to them than the red even though they were same size. CDM as measured in experiment 2 was plotted results from experiment 3 (Fig. 5). Two subjects perceived exactly the same size differences in both experiments, so that their data points are on top of each other. The results of experiments 2 and 3 were highly correlated ($R = 0.622$, $df = 20$, $P < 0.01$).

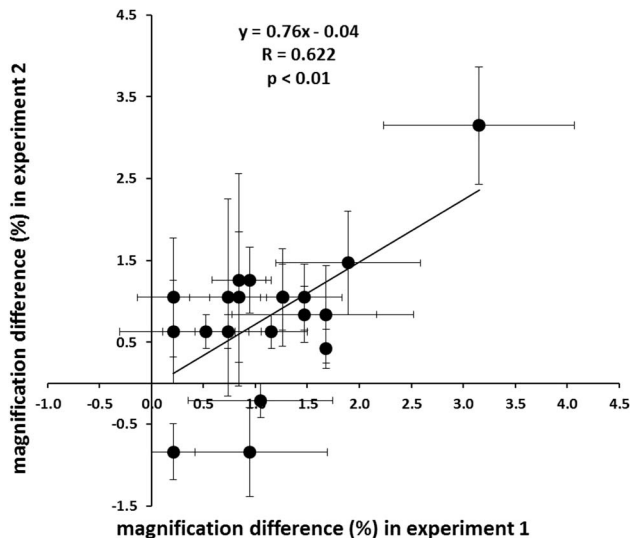


Fig. 5. Correlations of the magnification differences in the red and the blue as measured in experiments 2 and 3.

D. Experiment 4—Correlations of CDM in Both Eyes

Five subjects were randomly selected to repeat experiment 2 also with their left eyes. CDM was found to be highly correlated between both eyes even though the number of subjects was small ($R = 0.975$, $df = 4$, $P < 0.01$). That CDM is correlated in both eyes of a subject matches similar measurements by [21], who found that monochromatic aberrations display mirror symmetry in both eyes.

E. Measurements of the Optical Parameters in the Eyes of the Subjects with Low-coherence Interferometry

Biometrical and optical variables in the eyes of the 21 subjects, as well as their ages, are shown in Table 1. Dimensions of ocular structures, as well as corneal radius of curvature, were provided by the Lenstar LS-900. Effective corneal power was determined from the averages of corneal curvatures in the two principle meridians, using an effective refractive index of 1.332 [22,23].

F. Measurements of Kappa Angle, Lens Tilt, and Decentration in the Eyes of the Subjects

In 15 subjects, kappa, lens tilt angles, and lens decentration were measured with a custom-built Purkinjmeter [20]. Results are shown in Table 2. The sign conventions used by the Purkinjmeter were as follows: In the horizontal direction, positive kappa indicates that the fovea is located in the temporal retina, relative to the intersection of the pupillary axis with the retina, and negative kappa indicates nasal retina location. A positive lens tilt angle indicates that the optical axis of the lens is tilted toward the nasal side, relative to the fixation axis, and negative value indicates temporal tilt of the lens optical axis. A positive value in horizontal lens decentration indicates nasal decentration, and a negative one indicates temporal decentration. In the vertical direction, a negative vertical kappa indicates that the fovea is above the intersection of the pupil axis with the retina, and a positive value indicates it is below the intersection of the pupil axis with the retina. A negative value indicates that the top of the lens is tilted toward the image space, and a positive one indicates tilt away from the image space. In lens decentration, a positive value indicates lens superior decentration, and a negative indicates lens inferior decentration.

In the horizontal direction, kappa ranged from -1.4 deg to $+6.3$ deg, and one subject had a negative horizontal kappa angle. Horizontal lens tilt angles varied from negative (-4.6 deg) to positive ($+4.2$ deg). Horizontal lens decentration varied from -0.3 to $+0.2$ mm. In the vertical direction, three subjects had a negative kappa (-2.6 , -0.6 , and -1.5 deg) while the remaining ones had positive kappas. Vertical lens tilts ranged from -5.5 to $+6.1$ deg. The lenses of all subjects were decentered in the superior direction, relative to pupil center, by 0.29 mm on average.

G. Correlations of CDM with Optical and Biometrical Data of the Eyes

No significant correlations were found between CDM and corneal thickness, anterior chamber depth, corneal power, vitreous chamber depth, axial length, kappa angle (horizontal or vertical), and horizontal lens tilt and decentration (regression analyses not shown). However, the thickness of the crystalline lens was highly correlated to CDM (Fig. 6A; $R = 0.708$,

Table 1. Biometric and Optical Data of the Right Eyes of the Subjects

Subject Number	Age	Corneal Thickness (μm)	Lens Thickness (mm)	Corneal Radius, Flat Meridian	Corneal Radius, Steep Meridian	Anterior Chamber Depth (mm)	Refraction Error (Right Eye, Spectacle) (D)	Axial Length (mm)	Effective Corneal Power (D)	Perceived CDM (%)
1	29	543	4.12	7.79	7.55	2.61	-4.75	24.92	49.02	1.68
2	22	558	3.55	7.87	7.7	2.86	0	23.43	48.29	1.26
3	29	450	3.68	7.53	7.19	3.28	-2.5	24.05	51.08	0.42
4	58	525	4.29	7.5	7.41	2.69	2.5	23.12	50.43	2.94
5	54	549	4.43	8.07	7.98	2.87	0	24.93	46.85	2.52
6	26	583	3.56	8.13	8.11	3.05	-7.5	26.97	40.32	1.05
7	52	537	4.57	7.91	7.82	2.32	1.5	23.14	47.8	1.26
8	24	518	3.45	7.71	7.42	3.49	0	25.76	49.7	1.26
9	30	558	3.81	7.95	7.74	2.4	0	23.62	47.93	0.63
10	48	577	5.11	8.02	7.84	2.27	1.5	23.18	47.41	2.31
11	24	536	3.6	8.06	7.82	2.96	-2.25	26.16	47.36	1.26
12	23	540	3.56	8.05	7.82	3.28	-4	26.89	47.39	0.95
13	58	595	4.24	7.61	7.44	2.71	-4	24.65	49.97	1.47
14	24	502	3.59	7.77	7.56	2.63	-5	24.66	49.05	0.42
15	23	509	3.41	7.7	7.56	3.31	-5.75	25.72	49.28	0.63
16	21	580	3.31	7.93	7.72	3.17	-3.5	25.25	48.05	0.53
17	28	539	4.15	7.19	6.98	2.44	0	20.6	53.07	1.16
18	27	535	3.56	7.97	7.8	3.12	0	23.52	47.69	0.84
19	21	576	3.46	8.11	8.02	3.13	0	24.55	46.62	0.74
20	48	450	3.92	7.29	7.16	2.97	0	24.06	52.04	1.16
21	45	566	4.18	7.92	7.66	2.39	0	23.55	48.27	1.05

Table 2. Kappa, Lens Tilt, and Decentration in 15 Young Subjects^a

	Kappa Horizontal (degree)	Kappa Vertical (degree)	Lens Tilt Horizontal (degree)	Lens tilt Vertical (degree)	Decentration Horizontal (mm)	Decentration Vertical (mm)
1	2.0	2.5	-1.8	-5.5	-0.1	0.6
2	3.7	0.9	1.4	0.4	0.1	0.4
3	0.5	3.1	-2.9	-3.5	-0.1	0.1
4	3.6	2.8	4.2	-3.9	0.1	0.2
5	2.5	-2.6	2.9	6.1	-0.1	0.3
6	3.1	0.9	1.2	0.6	-0.1	0.3
7	1.3	0.5	-1.6	1.4	-0.1	0.1
8	0.1	-0.6	-3.0	2.6	-0.2	0.3
9	1.4	0.2	-3.2	-1.7	-0.1	0.2
10	4.3	3.2	0.6	-3.9	-0.1	0.3
11	1.0	2.9	-1.3	-3.5	-0.1	0.5
12	4.5	-1.5	3.7	2.2	0.2	0.1
13	2.0	0.1	-3.3	2.6	-0.1	0.3
14	-1.4	2.8	-4.6	-4.7	0.1	0.3
15	6.3	1.8	0.9	-2.6	-0.3	0.5

^aFor sign conventions, see text.

$df = 20$, $p < 0.01$). Significant correlations were also found between vertical lens tilt and CDM (Fig. 6B; $R = 0.525$, $df = 14$, $p < 0.05$), and between vertical lens decentration and CDM (Fig. 6C; $R = -0.571$, $df = 14$, $p < 0.05$). In conclusion, CDM increases with lens thickness and lens vertical decentration and decreases with lens vertical tilt.

We also analyzed the correlation of CDM versus age. On average, CDM increased by 3.5% per year of age (Fig. 6D: $\text{CDM} = \text{lens thickness} * 0.035 + 0.03$, $R = 0.696$, $p < 0.01$).

H. SPSS Model: Multiple Regression Analysis

It was found that CDM increases with lens thickness and vertical decentration, and decreases with vertical lens tilt. To evaluate the relative importance of these variables, a multiple

regression analysis was performed using SPSS. An enter model with one dependent variable, CDM, and three independent variables, lens thickness, lens vertical tilt, and lens vertical decentration, was analyzed. The highest impact variable was lens thickness ($\beta = 0.609$, $p < 0.01$). The finding was significant (ANOVA: $F = 9.3$, $df = 14$; $p < 0.01$) and accounted for about 63.7% of the variance of CDM (adjusted $R = 0.798$).

4. DISCUSSION

A. Comparisons of Our Measurements of CDM to the Literature Data

Our data are similar to the ones in the literature as long as we restrict the analysis to younger eyes. Hartridge [24] calculated

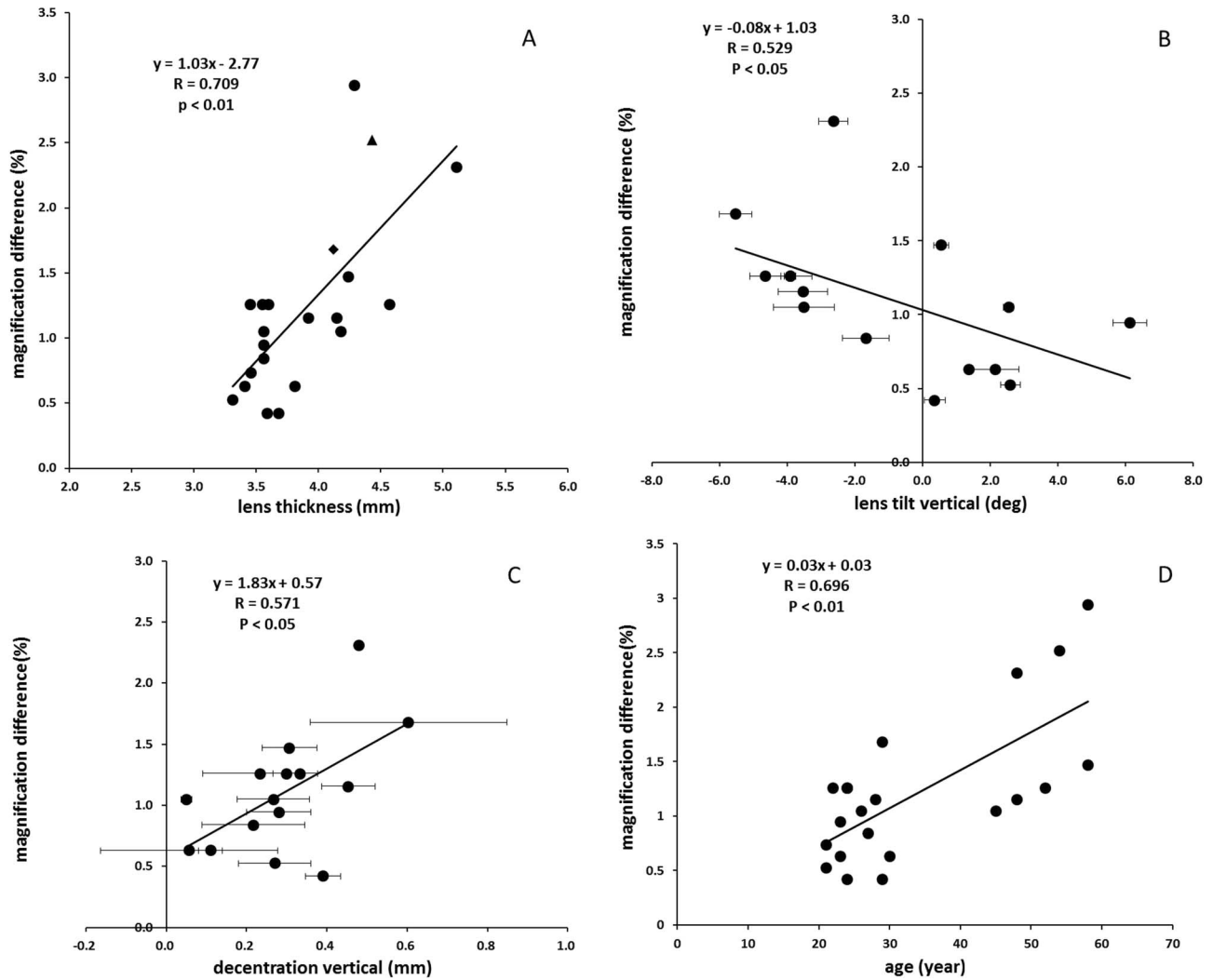


Fig. 6. Correlations of CDM with optical and biometrical data in the eye. A, Crystalline lens thickness. Filled diamonds (subject 1) and filled triangles (subject 2) denote the two subjects with similar axial lengths whose CDM was later simulated with the Liou-Brennan eye model (see Section 4). B, Vertical lens tilt. C, Vertical lens decentration. D, Age. Error bars denote SD.

that CDM can vary between 0.45% and 3.0%. Later, Thibos *et al.* [10] found that CDM varied from -0.36 to $+1.67$ arcmin in the fovea in six subjects (equivalent to about 0.6% to 2.8%), using the two-color vernier alignment task and an artificial pinhole pupil. However, the subjects in the study by Rynders *et al.* [2] were younger (19–36 years) than ours (22–58 years), and if we limit our analysis to subjects under 30 years of age, CDM was also less than 1 min of arc.

Also, schematic eye models were used to estimate foveal CDM. Zhang *et al.* [18] arrived at a theoretical value of less than 1%, but the age factor was not considered. CDM was also calculated from the chromatic difference in refraction [17] using the distance between the entrance pupil and the nodal point of the eye. The calculated CDM was only 0.37% between 400 and 700 nm and did not match the experimental data. It was proposed that this discrepancy can be attributed to the variability of the posterior nodal point positions in the different eyes [18]. Zhang *et al.* [17] developed a formula to estimate $CDM = \Delta R_x \cdot EN$, where ΔR_x is the chromatic difference of focus (LCA measured in object space) and EN is the distance between the entrance pupil and the nodal point of the eye. According to the modeling, EN changes from 3.91 mm at 20 years to 4.35 mm at 60 years, an 11% increase. As ΔR_x

does not seem to change with age, this is an estimate of increase in CDM with age. Our psychophysical data suggest that CDM is more than doubled between 20 years and 60 years.

B. Changes in Lens Thickness with Age

Changes in lens thickness with age have been studied, for instance, by Scheimpflug photography, magnetic resonance imaging (MRI), optical coherence tomography (OCT), or A-scan ultrasonography [25–31]. All authors report that the lens thickness increases with age, with an annual rate ranging from 19 to 26 μm . Our measurements with the Lenstar LS 900 in 51 subjects (including also the subjects of this study) were in line with these findings (average increase in lens thickness per year: 24 μm , regression plot not shown).

C. Optical Factors to Determine the Increase in CDM with Age

Vertebrate lenses consist of several onion-shaped layers with increasing refractive index from the periphery to the center [32]. In some studies [29,33,34] the shape of the gradient refractive index (GRIN) profile was found to vary with age. These profiles are necessary to solve the lens paradox, the fact that lens power remains almost constant during aging

despite the fact that lens thickness increases. MRI studies in the lens [32] show that the central plateau region maintains a constant refractive index with age while its size increases but that the peripheral refractive index gradient becomes steeper in older lenses. It is likely that, in addition to lens thickness, the change in gradient index profile may contribute to the increase in CDM. Until now, no accurate GRIN lens model has been published for the human eye, but it is known that there is considerable interindividual variability.

D. Lack of a Correlation of CDM with Horizontal Kappa

It was surprising that no correlation with the kappa angle was found, especially since variations in CDM are thought to be caused by TCA. The argument here is that since LCA is very similar between eyes, it would probably have given the same CDM for all subjects. A possible explanation could be that the younger subjects might have changed their accommodative state slightly when viewing the red and blue squares in experiment 2 and perhaps even experiment 3. Since the lens becomes thicker during accommodation it could have more LCA, resulting in more CDM. This possible explanation was further analyzed. During accommodation, lens thickness increases by about 0.064 mm/D [24]. This is a small effect. Even if the subjects would accommodate 10 D, the lens would have increased in thickness by only about 0.64 mm, 16.5% of the average total lens thickness in our subjects (3.88 mm). Therefore, a related effect on CDM should be small compared to the age-related increase in lens thickness from 3.21 to 5.11 mm. Another possible explanation why there is no significant correlation between CDM and horizontal kappa in experiment 2 is that the subjects scanned the red and blue squares continuously with their fovea, taking averages of their size with different eye positions.

E. Could the Measurements of CDM Be Confounded by the Power of the Spectacle Corrections?

It is well known that retinal image magnification is changed by spectacle correction. To evaluate the potential impact of this factor, CDM was correlated with the refractive errors of the subjects (Fig. 7A, all subjects; Fig. 7B, only the subjects wearing spectacles). There was no correlation detectable of CDM

and refractive errors ($R = 0.033$, $df = 20$, $p \gg 0.05$). To further analyze the potential impact of refractive errors, CDM was plotted against lens thickness only for the emmetropic subjects. The statistical significance of the correlation between CDM and lens thickness declined from $p < 0.01$ to $p < 0.05$ due to the smaller sample size, but the regression equations remained very similar (all subjects: $\text{CDM} [\%] = \text{lens thickness} * 1.03 - 2.78$, $R = 0.708$, $p < 0.01$; only subjects with no refractive error: $\text{CDM} [\%] = \text{lens thickness} * 0.92 - 2.28$, $R = 0.633$, $p < 0.05$). Therefore, the basic finding that CDM is correlated with lens thickness stands up even when refractive errors were corrected with spectacles or contact lenses.

F. Simulations of CDM with the Liou–Brennan Eye Model

We tested the performance of the Liou–Brennan eye model [14] using ZEMAX (ZEMAX Development Corporation, Bellevue, USA) but with a new crystalline lens as described by [35], who also simulated chromatic aberration. The optical parameters of the two eyes used in our simulation are shown in Table 1 (subject 1, 29 years old, and subject 2, 54 years old; denoted as filled diamonds and filled triangles, respectively, in Fig. 6A). The tested wavelengths were 432 and 590 nm. Both subjects had similar axial lengths. The major difference was lens thickness. In the image plane, subject 1 had also less CDM (0.38%) than subject 2 (0.58%), similar to data calculated by Bennett and Rabbetts [36] and Zhang *et al.* [17]. The calculated differences in TCA were small compared to the ones that were actually measured in our psychophysical experiment (1.68% for the young subject and 2.52% for the older one). Possible explanations for the discrepancy between optical calculations and psychophysical measurements are the changes in the gradient index profile in the lens that occur with age.

G. Why Do We Not See Our CDM?

One of the puzzles in vision is that we do not see our CDM. At least three subjects in our study had a difference in image magnification in the red and the blue of about 3%, which should give rise to considerable color fringes at all edges that are tangential to the optical axis of the eye. A possible mechanism could be that the visual cortex scales image

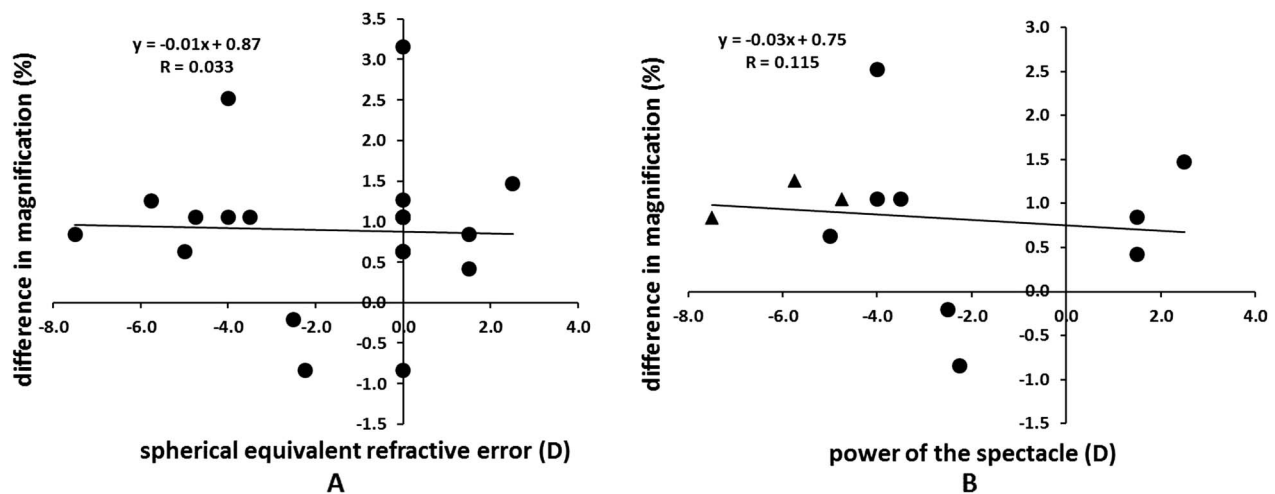


Fig. 7. Effects of spectacle corrections on the perceived magnification difference of the red and the blue squares. A, All subjects; B, only subjects wearing spectacles (filled circles) or contact lenses (filled triangles). Spectacle lens power was not an important factor to determine CDM. Data are from right eyes.

magnification in the cortical topographic maps according to wavelengths. For instance, if the blue image would be represented 3% larger than the red, color fringes would be removed in the neural representation. Interestingly, no electrophysiological recordings from cortical neurons are available with stimuli at different wavelengths to support or refute this hypothesis. Since CDM becomes more severe at older age, the wavelength-dependent scaling of the topographic maps would have to change with increase in age.

5. CONCLUSION

CDMs were psychophysically measured and ranged from 0.0% to 3.6% in our subjects. For the first time, we employed an object-size matching technique to measure CDM after we had found that subjects could discriminate 0.68% of a size difference in 75% of the cases. Size-discrimination thresholds were therefore low enough to resolve a significant part of the differences in CDM. Our major finding was that about 64% of the interindividual variance of CDM was explained by the variability in crystalline lens thickness.

ACKNOWLEDGMENTS

This work was supported by OpAL, an Initial Training Network funded by the European Commission under the Seventh Framework Programme (PITN-GA-2010-264605).

REFERENCES

1. D. A. Atchison and G. Smith, "Chromatic dispersions of the ocular media of human eyes," *J. Opt. Soc. Am. A* **22**, 29–37 (2005).
2. M. Rynders, B. Lidkea, W. Chisholm, and L. N. Thibos, "Statistical distribution of foveal transverse chromatic aberration, pupil centration, and angle psi in a population of young adult eyes," *J. Opt. Soc. Am. A* **12**, 2348–2357 (1995).
3. A. van Meeteren and C. J. Dunnwald, "Image quality of the human eye for eccentric entrance pupils," *Vis. Res.* **23**, 573–579 (1983).
4. J. C. He, S. Marcos, R. H. Webb, and S. A. Burns, "Measurement of the wave-front aberration of the eye by a fast psychophysical procedure," *J. Opt. Soc. Am. A* **15**, 2449–2456 (1998).
5. B. Howland and H. C. Howland, "Subjective measurement of high-order aberrations of the eye," *Science* **193**, 580–582 (1976).
6. S. Marcos, S. A. Burns, E. Moreno-Barriusop, and R. Navarro, "A new approach to the study of ocular chromatic aberrations," *Vis. Res.* **39**, 4309–4323 (1999).
7. S. Marcos, S. A. Burns, P. M. Prieto, R. Navarro, and B. Baraibar, "Investigating sources of variability of monochromatic and transverse chromatic aberrations across eyes," *Vis. Res.* **41**, 3861–3871 (2001).
8. Y. U. Ogboso and H. E. Bedell, "Magnitude of lateral chromatic aberration across the retina of the human eye," *J. Opt. Soc. Am. A* **4**, 1666–1672 (1987).
9. P. Simonet and M. C. Campbell, "The optical transverse chromatic aberration on the fovea of the human eye," *Vis. Res.* **30**, 187–206 (1990).
10. L. N. Thibos, A. Bradley, D. L. Still, X. Zhang, and P. A. Howarth, "Theory and measurement of ocular chromatic aberration," *Vis. Res.* **30**, 33–49 (1990).
11. L. N. Thibos, M. Ye, X. Zhang, and A. Bradley, "The chromatic eye: a new reduced-eye model of ocular chromatic aberration in humans," *Appl. Opt.* **31**, 3594–3600 (1992).
12. R. E. Bedford and G. Wyszecski, "Axial chromatic aberration of the human eye," *J. Opt. Soc. Am.* **47**, 564–565 (1957).
13. A. Ivanoff, *Les aberrations de l'œil* (Éditions de la Revue d'optique théorique et instrumentale, 1953).
14. H. L. Liou and N. A. Brennan, "Anatomically accurate, finite model eye for optical modeling," *J. Opt. Soc. Am. A* **14**, 1684–1695 (1997).
15. L. N. Thibos, "Calculation of the influence of lateral chromatic aberration on image quality across the visual field," *J. Opt. Soc. Am. A* **4**, 1673–1680 (1987).
16. G. Wald and D. R. Griffin, "The change in refractive power of the human eye in dim and bright light," *J. Opt. Soc. Am.* **37**, 321–336 (1947).
17. X. X. Zhang, L. N. Thibos, and A. Bradley, "Relation between the chromatic difference of refraction and the chromatic difference of magnification for the reduced eye," *Optom. Vis. Sci.* **68**, 456–458 (1991).
18. X. Zhang, A. Bradley, and L. N. Thibos, "Experimental determination of the chromatic difference of magnification of the human eye and the location of the anterior nodal point," *J. Opt. Soc. Am. A* **10**, 213–220 (1993).
19. F. W. Campbell, J. Nachmias, and J. Jukes, "Spatial-frequency discrimination in human vision," *J. Opt. Soc. Am.* **60**, 555–559 (1970).
20. F. Schaeffel, "Binocular lens tilt and decentration measurements in healthy subjects with phakic eyes," *Investig. Ophthalmol. Vis. Sci.* **49**, 2216–2222 (2008).
21. J. F. Castejon-Mochon, N. Lopez-Gil, A. Benito, and P. Artal, "Ocular wave-front aberration statistics in a normal young population," *Vis. Res.* **42**, 1611–1617 (2002).
22. H. Littmann, "Grundlegende Betrachtungen zur Ophthalmometrie," *Albrecht v. Graefes Arch. Ophthalmol.* **151**, 249–274 (1951).
23. F. Schaeffel and H. C. Howland, "Mathematical model of emmetropization in the chicken," *J. Opt. Soc. Am. A* **5**, 2080–2086 (1988).
24. H. Hartridge, "The visual perception of fine detail," *Philos. Trans. R. Soc. Lond.* **232**, 519–671 (1947).
25. K. Richdale, L. T. Sinnott, M. A. Bullimore, P. A. Wassenaar, P. Schmalbrock, C. Y. Kao, S. Patz, D. O. Mutti, A. Glasser, and K. Zadnik, "Quantification of age-related and per diopter accommodative changes of the lens and ciliary muscle in the emmetropic human eye," *Investig. Ophthalmol. Vis. Sci.* **54**, 1095–1105 (2013).
26. J. J. Rozema, D. A. Atchison, S. Kasthurirangan, J. M. Pope, and M. J. Tassignon, "Methods to estimate the size and shape of the unaccommodated crystalline lens in vivo," *Investig. Ophthalmol. Vis. Sci.* **53**, 2533–2540 (2012).
27. K. Richdale, M. A. Bullimore, and K. Zadnik, "Lens thickness with age and accommodation by optical coherence tomography," *Ophthalm. Physiol. Opt.* **28**, 441–447 (2008).
28. R. Navarro, F. Palos, and L. Gonzalez, "Adaptive model of the gradient index of the human lens. I. formulation and model of aging ex vivo lenses," *J. Opt. Soc. Am. A* **24**, 2175–2185 (2007).
29. L. A. Jones, G. L. Mitchell, D. O. Mutti, J. R. Hayes, M. L. Moeschberger, and K. Zadnik, "Comparison of ocular component growth curves among refractive error groups in children," *Investig. Ophthalmol. Vis. Sci.* **46**, 2317–2327 (2005).
30. M. Dubbelman, G. L. Van der Heijden, and H. A. Weeber, "The thickness of the aging human lens obtained from corrected Scheimpflug images," *Optom. Vis. Sci.* **78**, 411–416 (2001).
31. S. A. Strenk, J. L. Semmlow, L. M. Strenk, P. Munoz, J. Gronlund-Jacob, and J. K. DeMarco, "Age-related changes in human ciliary muscle and lens: a magnetic resonance imaging study," *Investig. Ophthalmol. Vis. Sci.* **40**, 1162–1169 (1999).
32. S. Kasthurirangan, E. L. Markwell, D. A. Atchison, and J. M. Pope, "In vivo study of changes in refractive index distribution in the human crystalline lens with age and accommodation," *Investig. Ophthalmol. Vis. Sci.* **49**, 2531–2540 (2008).
33. A. de Castro, D. Siedlecki, D. Borja, S. Uhlhorn, J.-M. Parel, F. Manns, and S. Marcos, "Age-dependent variation of the gradient index profile in human crystalline lenses," *J. Mod. Opt.* **58**, 1781–1787 (2011).
34. B. A. Moffat, D. A. Atchison, and J. M. Pope, "Age-related changes in refractive index distribution and power of the human lens as measured by magnetic resonance micro-imaging in vitro," *Vis. Res.* **42**, 1683–1693 (2002).
35. B. Jaeken, L. Lundstrom, and P. Artal, "Peripheral aberrations in the human eye for different wavelengths: off-axis chromatic aberration," *J. Opt. Soc. Am. A* **28**, 1871–1879 (2011).
36. A. G. Bennett and R. B. Rabbetts, *Clinical Visual Optics*, 2nd ed. (Butterworths, 1984).



Size of the foveal blue scotoma related to the shape of the foveal pit but not to macular pigment



Yun Chen^a, Weizhong Lan^{a,b}, Frank Schaeffel^{a,*}

^a Section of Neurobiology of the Eye, Ophthalmic Research Institute, 72076 Tuebingen, Germany

^b State Key Laboratory of Ophthalmology, Zhongshan Ophthalmic Center, 510060 Guangzhou, China

ARTICLE INFO

Article history:

Received 15 April 2014

Received in revised form 15 September 2014

Available online 15 November 2014

Keywords:

S-cones

Fovea

Scotoma

Maxwell's spot

Macular pigment

ABSTRACT

When the eye is covered with a filter that transmits light below 480 nm and a blue field is observed on a computer screen that is modulated in brightness at about 1 Hz, the fovea is perceived as small irregular dark spot. It was proposed that the “foveal blue scotoma” results from the lack of S-cones in the foveal center. The foveal blue scotoma is highly variable among subjects. Possible factors responsible for the variability include differences in S-cone distribution, in foveal shape, and in macular pigment distribution. Nine young adult subjects were instructed to draw their foveal blue scotomas on a clear foil that was attached in front of the computer screen. The geometry of their foveal pit was measured in OCT images in two dimensions. Macular pigment distribution was measured in fundus camera images. Finally, blue scotomas were compared with Maxwell's spot which was visualized with a dichroic filter and is commonly assumed to reflect the macular pigment distribution. The diameters of the foveal blue scotomas varied from 15.8 to 76.4 arcmin in the right eyes and 15.5 to 84.7 arcmin in the left and were highly correlated in both eyes. It was found that the steeper the foveal slopes and the narrower the foveal pit, the larger the foveal blue scotoma. There was no correlation between foveal blue scotoma and macular pigment distribution or Maxwell's spot. The results are therefore in line with the assumption that the foveal blue scotoma is a consequence of the lack of S-cones in the foveal center. Unlike the foveal blue scotoma, Maxwell's spot is based on macular pigment as previously proposed.

© 2014 Elsevier Ltd. All rights reserved.

1. Introduction

In 1894, Arthur König presented a lecture to the “Preussische Akademie der Wissenschaften” at Berlin, in which he claimed that the human fovea is “blue blind” and that subjects are “dichromatic” in the fovea (p. 591). His conclusion was based on psychophysical studies in which subjects had to fixate small monochromatic light spots presented at different wavelengths. He found that subjects had difficulties to distinguish between “blue” and “green” (König, 1894). Later, histological (Willmer & Wright, 1945) and psychophysical studies (Wald, 1967) confirmed that there is a tritanopic zone of about 20 arcmin in diameter in the center of the fovea (Williams, MacLeod, & Hayhoe, 1981). More recently, Curcio et al. (1991) mapped the foveal photoreceptors and found that a 20–25 arcmin S-cone free zone exists in the human foveola with sparsely and irregularly distributed S-cones in the adjacent foveal slopes. Under normal viewing conditions, the foveal blue scotoma is not visible because of the neural process of filling-in (Gerrits &

Vendrik, 1970; Magnussen et al., 2001, 2004; Spillmann & Werner, 1996; Williams, MacLeod, & Hayhoe, 1981). However, Magnussen et al. (2001, 2004) described two procedures to make the blue scotoma visible. In the first study (Magnussen et al., 2001), subjects were presented with a blue field in Maxwellian view with a peak wavelength around 450 nm that was sinusoidally modulated in luminance at a frequency of 1–2 Hz. In this case, subjects could see their blue scotomas as a small dark spot that moved with their point of fixation. Apparently, the process of filling-in was compromised by the brightness modulation of the blue field. When subjects were asked to rate the visibility of the blue scotoma at different wavelengths, their ratings matched about the spectral sensitivity of the S-cones. In their second approach, Magnussen et al. (2004) showed that the foveal blue scotoma becomes visible as a bright spot in a negative afterimage when subjects were adapted to a bright blue field. Again, the subjects' rating as to how clearly they could see the blue scotomas varied with the peak wavelength of the adapting field and followed the spectral sensitivity function of the S-cones. The diameters of the perceived blue scotomas ranged from 24.8 to 44.3 arcmin, similar to the diameter of the S-cone free zone that was histologically identified in the foveal center by (Curcio et al., 1991).

* Corresponding author. Fax: +49 7071 295196.

E-mail address: frank.schaeffel@uni-tuebingen.de (F. Schaeffel).

The primate fovea is histologically recognized as a pit with tightly packed M- and L-cones, providing maximal visual acuity. In this area, one single cone (M- or L-) is connected to 3–4 bipolar cells and 3 ganglion cells. This ratio decreases to one ganglion cell per cone at an eccentricity of 15–20 deg (3–4 mm). In peripheral retina there are more cones than ganglion cells. The ganglion cell density changes by a factor of 1000–4000 between peripheral and central retina (Wässle & Boycott, 1991; Wässle et al., 1990). Excluding S-cones from the foveal center appears to be an elegant trick to cope with chromatic defocus that results from longitudinal chromatic aberration of the optics of the eye (Rodieck, 1973). Shapes of foveas can be divided into two extremes: ‘convexiculate’ and ‘concavicate’ (Polyak, 1951). Since the retinal tissue has a substantially higher refractive index than the vitreous (1.38 vs 1.335), the vitreo-retinal interface acts as a refracting surface. In a convexiculate fovea, the interface acts as a magnifying glass to the image projected on the photoreceptors on the back of the retina. This design is found in reptiles, birds and some fishes. Harkness and Bennet-Clark (1978) have simulated the optical effects of the deep convexiculate fovea and found that the perceived image distortions vary with the focus of the eye and could therefore be used as “focus indicator”. On the other hand, in a concavicate fovea the image is minified because a flatter fovea is combined with a photoreceptor layer that is bulged out towards the center of the fovea pit, generating the effects of a concave lens. This case is mostly found in primates (Harkness & Bennet-Clark, 1978) but it is not clear what the advantage might be of minifying the projected image. The minification effect appears very small (<1%, see Section 4).

Interestingly, the shape of the foveal pit in human subjects is highly variable (see, for instance, OCT data in the current study) but probably not random since a negative correlation was found between the steepness of the foveal slopes and foveal diameter (Knighton & Gregori, 2012).

In the central region of the human retina, a yellowish macular pigment, consisting of lutein and zeaxanthin, is embedded in the cone axons and in the inner-plexiform layer. It acts as a screening pigment for the underlying photoreceptors (Hammond, Wooten, & Snodderly, 1997; Werner, Bieber, & Scheffrin, 2000; Werner, Donnelly, & Kliegl, 1987) and is assumed to protect photoreceptors from photo-oxidative damage by short wavelength light (Kirschfeld, 1982; Nussbaum, Pruett, & Delori, 1981; Werner, Bieber, & Scheffrin, 2000). The peak absorption of the macular pigment is around 460 nm (Bone, Landrum, & Cains, 1992), close to the spectral sensitivity peak of the S-cones (Stockman & Sharpe, 2000). The distribution of macular pigment varies considerably among subjects (Wooten & Hammond, 2002; Wooten et al., 1999). It is assumed that the percept of Maxwell’s spot is related to the macular pigment distribution.

Since foveal shape, foveal blue scotomas, and macular pigment distribution are all highly variable among subjects, it is interesting to study how they are related. Furthermore, there is recently increasing interest in this question (i.e. the ongoing MacTel project <https://web.emmes.com/study/mactel/>). To further elucidate the relationship between macular pigment distribution and foveal blue scotoma, we also explored how they are related to the appearance of Maxwell’s spot.

2. Methods

2.1. Subjects

Nine subjects (5 female and 4 male) with an average age of 29.6 ± 7.7 years (ranging from 22 to 49 years) and normal color vision were recruited for the experiments. The Chinese subjects

(1, 3, 5, 8) had undergone color vision testing with the Ishihara pseudo-isochromatic color plates prior to their enrollment at their home universities. The remaining German subjects were tested at school and had no known color vision deficiencies. The study adhered to Code of Ethics of the World Medical Association (Declaration of Helsinki) and was approved by the local University Ethics Commission.

2.2. Psychophysical experiments

2.2.1. Measurement of the foveal blue scotomas

A blue field (size 900×900 pixel), sinusoidally modulated in luminance at a frequency of 1 Hz between RGB (0, 0, 255) and RGB (0, 0, 0), was presented on a thin film transistor (TFT) display (screen refresh rate 60 Hz, EIZO FlexScan S1921, 19 in.). Maximal pixel radiance of the “B” channel (RGB (0, 0, 255)), as measured by a photometer (Minolta LS100), was 10.70 cd/m^2 . Since the “blue” gun of computer screen contains energy also in the middle wavelength range, M- and L-cones were also stimulated by the B gun. To preferentially stimulate the S-cones, a filter excluding light above 500 nm was needed. We used the bandpass glass filter BG25 (Schott, Germany) with a peak transmission at about 400 nm and a FWHM of about 50 nm. Subjects viewed the modulated “blue” field on the screen in a dark room from a distance of 74 cm. The blue field had a diameter of 26.4×26.4 cm on the screen which converts into a visual angle of 20.2 deg. Assuming a retinal image magnification for the human eye of $290 \mu\text{m/deg}$ (Gullstrand, 1909), the linear size of the retinal image was about $5850 \mu\text{m}$.

Subjects were instructed to draw their foveal blue scotomas, one eye after the other, with a marker pen on a transparent plastic sheet that was attached in front of the screen. The procedure was repeated four times. The four drawings were averaged pixel by pixel using “ImageJ” (<http://rsb.info.nih.gov/ij/>). Image J offers an “image calculator” function which calculates the arithmetic mean of each pixel gray value from two or more images. The resulting “average” of several drawings made it more easy to measure the diameters of the foveal blue scotomas, or of Maxwell’s spots, and also increased the confidence in the measurements.

2.2.2. Visualization and measurement of Maxwell’s spot

Maxwell’s spot was visualized as described by Isobe and Motokawa (1955). A bright white field was generated by aiming a video projector (Sharpe XG-NV21SE) at a white paper that was attached to the wall. Subjects were instructed to look into the bright white field through a dichroic filter in front of one eye, the other eye was covered (KIF 483, Schott, Germany; light transmission below 480 nm and above 610 nm, with prominent attenuation between 500 and 600 nm). Typically, Maxwell’s spot becomes visible as a brownish or reddish spot on bright white background with variable shapes and diameters among different subjects, as shown in Fig. 6. Transmission of the dichroic filter also at longer wavelengths is necessary and was already recommended by Maxwell himself to counteract retinal adaptation. When subjects look into white light without a filter, Maxwell’s spot disappears almost immediately due to rapid adaptation of macular photoreceptors (Miles, 1954). In order to maintain visibility of Maxwell’s spot, a dichromatic filter was also used by Holm (1922), Walls and Mathews (1952), and Isobe and Motokawa (1955). As in the previous experiments where the blue scotoma was measured, the distance between the subject and the wall was 74 cm. The instructions to the subjects were to draw the pattern that they saw directly on the paper. It was mentioned to them that, while the blue scotoma appears as a dark gray or black spot, Maxwell’s spot looks reddish or brownish.

2.3. Optical Coherence Tomography (OCT)

Foveal shape was measured in the horizontal and vertical direction by a high-resolution OCT (Spectralis HRA + OCT, Heidelberg Engineering, Heidelberg, Germany) in the 9 subjects (18 eyes). 512 A-scans were performed in each B-scan with a scan length of 20 deg in terms of visual angle (linear distance on the retina approximately 6 mm). The minimal foveal thickness (MFT) was assumed to define the center of the fovea. It was automatically determined by built-in software of the instrument. Differences in retinal thickness (ΔRT) were determined between the center of the fovea and at four parafoveal positions (0.4 and 0.8 mm away from the central fovea on either side) using ImageJ. ΔRT s were plotted against the dimensions of the drawn foveal blue scotomas. The diameter of the floor of the central fovea was also measured, defined as the area where retinal thickness remained at a minimum. While different OCT devices may select different boundaries for measuring retinal thickness (Giani et al., 2010), we were interested in inter-individual differences. Such differences would show up no matter which boundary is used, as long as the device and the criteria are always the same.

2.4. Fundus photography and measurement of the macular pigment distributions

Distributions of the macular pigment were analyzed in fundus pictures in each eye of the nine subjects, obtained by a Non-Mydriatic Retinal Camera (Nonmyd WX3D, Kowa, Germany). The fundus pictures were taken in the University Eye Hospital Tuebingen and the responsible ophthalmologist confirmed that no pathological features were apparent. For analysis, the RGB fundus pictures were separated into their 3 RGB channels, again using “ImageJ”. Since the macular pigment has a peak absorption around 460 (Bone, Landrum, & Cains, 1992), the analysis was done in the image generated by the blue channel of the RGB format. “ImageJ” provides a function to measure the number of pixel that are above an adjustable threshold. A square of 4×4 deg (244×244 pixels) was adjusted to cover the macular area (gray box in Fig. 1A). The threshold was adjusted to 50% of the average brightness of the pixels in the square. Supra-threshold pixels were marked in gray (Fig. 1B) and the horizontal diameter of the marked area was measured in pixels. Conversion into visual angle was simple since one pixel in the fundus image was equivalent to about one arcmin. Our procedure produced diameters of the pigmented areas (Table 3; average diameter 2.36 deg, radius 1.18 deg) that are comparable to those in the literature. Hammond, Wooten, and Snodderly

(1997) described a mean radius of the distribution at half maximum in macular pigment optical density (MPOD) of 1.03 deg, Makridaki et al. (2009) 1.30 deg and Smith et al. (2004) 1.03 deg, similar to the data in the current study (1.18 deg). Furthermore, the macular pigment densities were quantitatively analyzed using their pixel brightness profiles (Fig. 1C), with the profiles again provided by ImageJ.

2.5. Statistical analysis

Linear regression and correlation analysis was performed in Microsoft Excel (Asknet AG, Germany). Significance was assumed at $p < 0.05$.

3. Results

3.1. Shapes and diameters of the perceived blue scotomas

The shapes of the perceived foveal blue scotomas, as determined from the drawings of the subjects, are shown in Fig. 2. Reproducibility was high which can be seen when the individual drawings are compared to the averages of four repetitions. Two types of blue scotomas were observed, a small spot (type 1: subjects 2, 4, 5, and 9) and a circular shape in the center, surrounded by star-shaped radial extensions (type 2: subjects 1, 3, 6, 7 and 8).

Horizontal and vertical diameters of the perceived blue scotomas are listed in Table 1. In the right eyes, visual angles ranged from 15.75 to 76.35 arcmin (3.4 to 16.4 mm on the computer screen at 74 cm distance). In left eyes, they ranged from 15.50 to 84.72 arcmin.

Significant correlations were found between both eyes, both in the horizontal and vertical diameters of blue scotomas (Fig. 3, horizontal $R = 0.969$, $df = 8$, $p < 0.01$; vertical $R = 0.976$, $df = 9$, $p < 0.01$).

3.2. Optical Coherence Tomography (OCT) of the foveal region

The minimum values for the foveal thickness (MFT, the location of the central fovea) and dimensions of the bottom diameter of the foveal pit for each subject are listed in Table 2. The average MFT was 0.253 ± 0.023 mm in the right eyes, and 0.257 ± 0.039 mm in the left. The diameter of the floor of the foveal pit in the right eyes was on average 0.12 ± 0.04 mm (24.8 arcmin) wide, and 0.15 ± 0.05 mm (31.0 arcmin) in the left eye (Table 2).

To quantify the slopes of the foveal pit, two lateral positions from the foveal center were chosen, ± 0.4 mm, and ± 0.8 mm. The difference of retinal thickness (ΔRT) between the central fovea

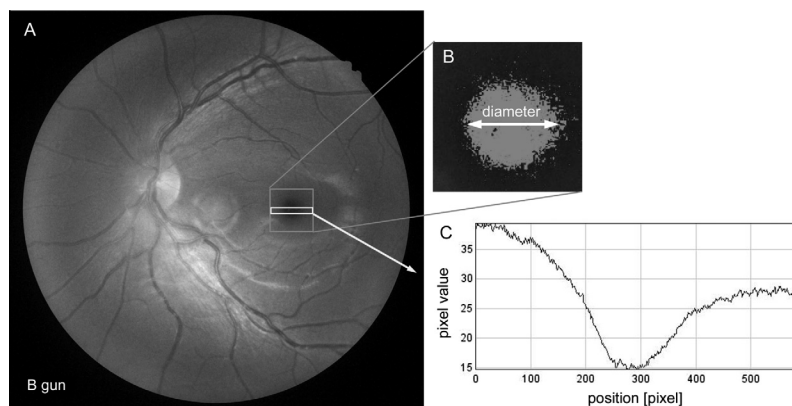


Fig. 1. (A) Fundus picture generated from the B gun of the RGB format. The gray box denotes a square of 244×244 pixel in which pixels were thresholded and extracted as shown in (B) to measure the diameter of the macular pigment distribution (white arrow). In (C), the pixel brightness profile is shown as extracted from the pixels in the white rectangle, denoting the macular pigment optical density (MPOD). One pixel is equivalent to about 1 min of arc.

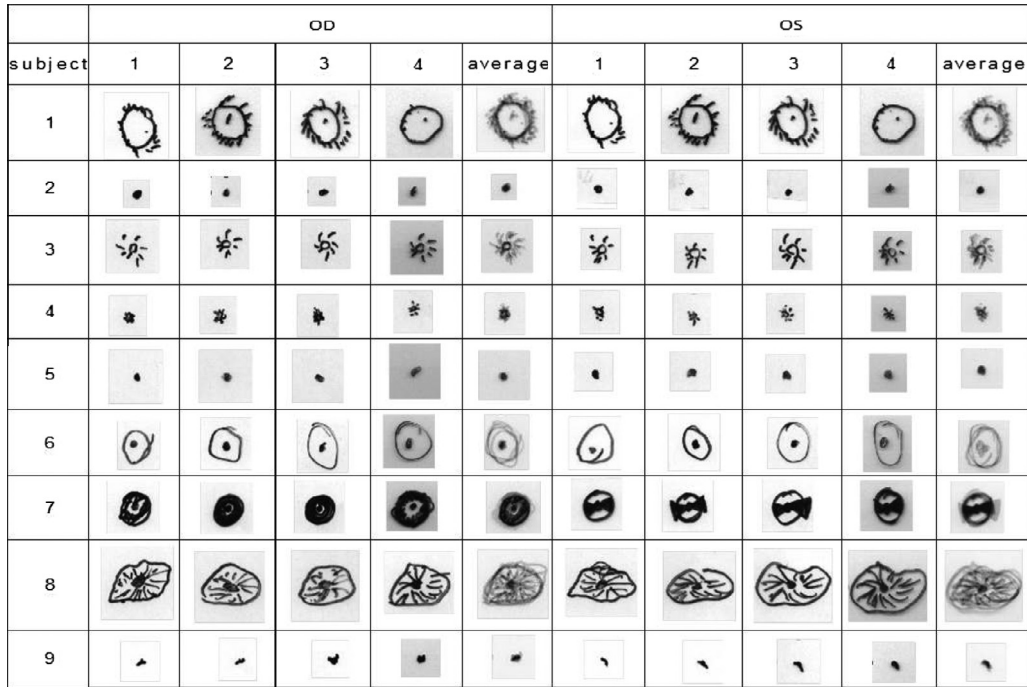


Fig. 2. Original drawings by the subjects of their blue scotomas. Four repetitions are shown, followed by their averages, as determined by “ImageJ”.

Table 1

Diameters of the perceived foveal blue scotomas in nine subjects, as determined from averages of four drawings prepared by each subject.

Subject	Right eyes (OD)		Left eyes (OS)	
	Vertical visual angle (arcmin)	Horizontal visual angle (arcmin)	Vertical visual angle (arcmin)	Horizontal visual angle (arcmin)
1	77.9	76.4	89.7	84.7
2	16.4	16.3	13.7	15.8
3	50.8	49.4	50.2	45.2
4	24.3	21.7	25.0	25.1
5	14.9	15.8	17.5	17.0
6	71.5	65.0	74.0	64.5
7	61.8	63.2	57.6	60.8
8	48.5	67.1	36.9	60.8
9	17.1	20.3	16.4	15.5

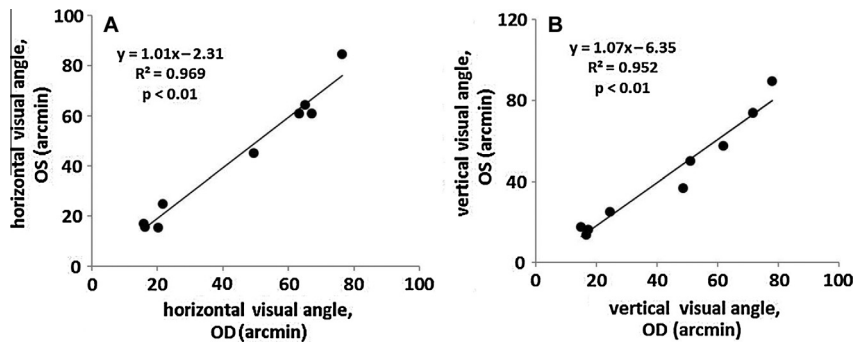


Fig. 3. Correlations of the diameters of the perceived blue scotomas between the left and right eyes of the nine subjects, both in horizontal (A) and vertical directions (B). OS = left eyes, OD = right eyes.

and four parafoveal positions was measured by “ImageJ” in pixels as shown in Fig. 4. One pixel was equivalent to 1.90 μm. Significant correlations were found between ΔRT values on both sides of the foveal center (OD: 0.4 mm vs -0.4 mm: $R = 0.64$, $df = 8$, $p < 0.05$; 0.8 mm vs -0.8 mm: $R = 0.922$, $df = 8$, $p < 0.01$; 1.2 mm vs -1.2 mm: $R = 0.963$, $df = 8$, $p < 0.01$. OS: $R = 0.814$, 0.919 , 0.965 for each pair, $df = 8$, $p < 0.01$).

3.3. Correlations of the diameters of the foveal blue scotomas and foveal geometry

Significant correlations were found between the diameters of the foveal blue scotomas and the increase in retinal thickness at ±0.4 mm and ±0.8 mm from the foveal center (R ranging from 0.634 to 0.723 in the right eyes, $p < 0.05$ in all cases, $df = 8$, shown

Table 2

Minimum foveal thickness (MFT, the minimum thickness of the retina in the center of the fovea) and diameter of the floor of the foveal pitas measured by built-in software of the “Heidelberg Eye Explorer”. OS = left eyes, OD = right eyes.

Subject	MFT (mm)		Diameter of the floor of foveal pit (arcmin)	
	OD	OS	OD	OS
1	0.272	0.246	11.57	26.62
2	0.263	0.207	27.78	28.93
3	0.272	0.266	12.73	40.51
4	0.250	0.250	32.41	35.88
5	0.281	0.344	32.41	40.51
6	0.225	0.241	28.93	27.78
7	0.231	0.220	24.30	25.46
8	0.218	0.260	20.83	13.89
9	0.269	0.275	26.62	43.98

in Fig. 5, and *R* ranging from 0.651 to 0.741, in the left; plot of left eye data not shown). The correlations were always positive indicating that the steeper the foveal slope, the larger the foveal blue scotoma. Similarly, the diameters of the foveal blue scotomas were correlated to the diameters of foveal pit (OD: *R* = −0.656, *df* = 8, *p* < 0.05; OS: *R* = −0.645, *df* = 8, *p* < 0.05; shown in Fig. 5). The negative correlations indicate that a wide foveal pit was associated with a small foveal blue scotoma while a narrow foveal pit was associated with a large blue scotoma. We also analyzed the relationship between the steepness of the foveal slopes (from 0 to 0.4 mm and from 0 to 0.8 mm) and the horizontal diameters of the foveal blue scotoma. Correlations were similarly significant (*p* < 0.05).

At 1.2 mm distance from the foveal center, no significant correlations were found between the increase in retinal thickness and the blue scotoma. In several subjects, ±1.2 mm was already outside the foveal pit.

3.4. Macular pigment distributions and perceived blue scotomas

The horizontal diameters of the macular pigment distributions are shown in Table 3. Repeatability of measurement was tested by correlating the data gathered by two independent observers (observer 1 vs observer 2: OD: *R* = 0.913, *df* = 8, *p* < 0.01; OS: *R* = 0.823, *df* = 8, *p* < 0.01). The average horizontal diameters of the macular pigment distributions were 0.69 ± 0.19 mm (2.37 deg) in the right eyes and 0.68 ± 0.18 mm (2.34 deg) in left (note that the 50% criterion for detection of the borders of the pigmentation may underestimate the total width of the distributions). With this criterion, subject 1 had the smallest pigmented area (horizontal diameter right eye, 0.32 mm; left eye 0.29 mm) and subject 8 the largest (right eye 0.96 mm, left eye 0.95 mm). The diameters of the macular pigment distributions were highly correlated in left and right eyes (*R* = 0.929, *p* < 0.01). However, no correlation was found between the extension of the pigmented area and the diameters of the perceived foveal blue scotomas (*R* < 0.179 in all cases, *df* = 8, n.s.).

3.5. Possible contributions of the macular pigment to the foveal blue scotoma

Above, the margins of the area covered with macular pigment were defined by a 50% brightness criterion for the pixels in the “blue” channel in the RGB images of the fundus. However, a 50% threshold criterion does not provide the full information about the macular pigment distribution. Therefore, we plotted the density of the macular pigment, as inferred from the pixel values in the “blue” channel in the horizontal meridian and compared it to the diameters of the foveal blue scotomas (Fig. 6). It is obvious that the angular diameters of the blue scotomas were smaller than of the macular pigment distributions in most subjects. Magnussen et al. (2004) also compared the size of the blue scotomas with Haidinger’s brushes, an entoptic phenomenon that occurs due to the dichroic properties of macular pigment. They also concluded that macular pigment is unlikely to contribute to the foveal blue scotoma. It was previously found that the slope of the foveal pit is unrelated to the macular pigment distribution (Westrup et al., 2014).

Diameters of the Maxwell’s spots as perceived by the 8 subjects are shown in Table 4.

3.6. Foveal blue scotoma and Maxwell’s spot

Maxwell’s spot is described in the literature as “a darker ring or shell-burst” (Miles, 1954), “a spot rounded by a clear ring and a halo” (Isobe & Motokawa, 1955), or as a “dark diffuse spot”, a “dark spot with star”, a “dark ring with no central dark spot” or a “dark ring with central dark spot”. In our study, 8 of the 9 subjects were available and were instructed to look at bright white field through the dichroic filter. Subjects were asked to draw their perceived Maxwell’s spot (Fig. 5). One subject (subject 4) could not see Maxwell’s spot at all, subjects 2 and 5 saw it only with one eye. The drawings of the remaining subjects had little similarity with their drawings of the blue scotomas: (1) Maxwell’s spot was always larger (average: 105 ± 35 arcmin) than the blue scotomas, (2) Maxwell’s spot was more blurry and weaker, and (3) Maxwell’s spot appeared as a reddish or brownish spot. When left and right eyes were treated as independent samples, the diameters of the perceived Maxwell’s spot were correlated to the diameters of the macular pigment distributions (Fig. 7, *R* = 0.563, *df* = 11, *p* < 0.05). Therefore, we concur with Delori et al. (2006) who state that “Maxwell’s spot matched the measured macular pigment distributions”.

4. Discussion

We found that the diameters of the foveal blue scotomas were highly variable among subjects but closely correlated in both eyes. We also found that the diameter of the foveal blue scotomas were related to the steepness of the foveal slope – the steeper the

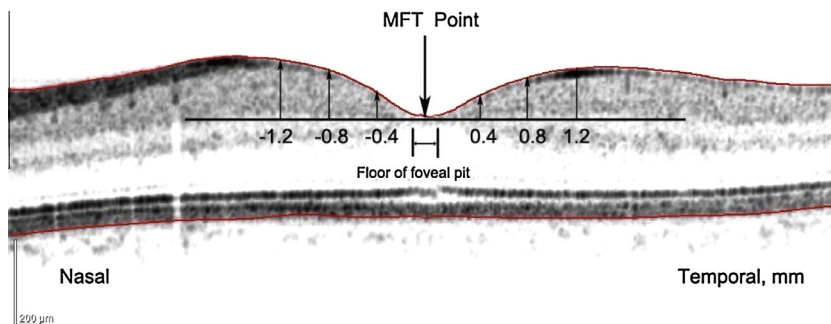


Fig. 4. OCT scan of the foveal area as provided by the “Heidelberg Eye Explorer”, indicating the foveal center (MFT). Vertical black lines indicate the six eccentricities where retinal thickness was determined and correlated to the diameters of the perceived blue scotomas.

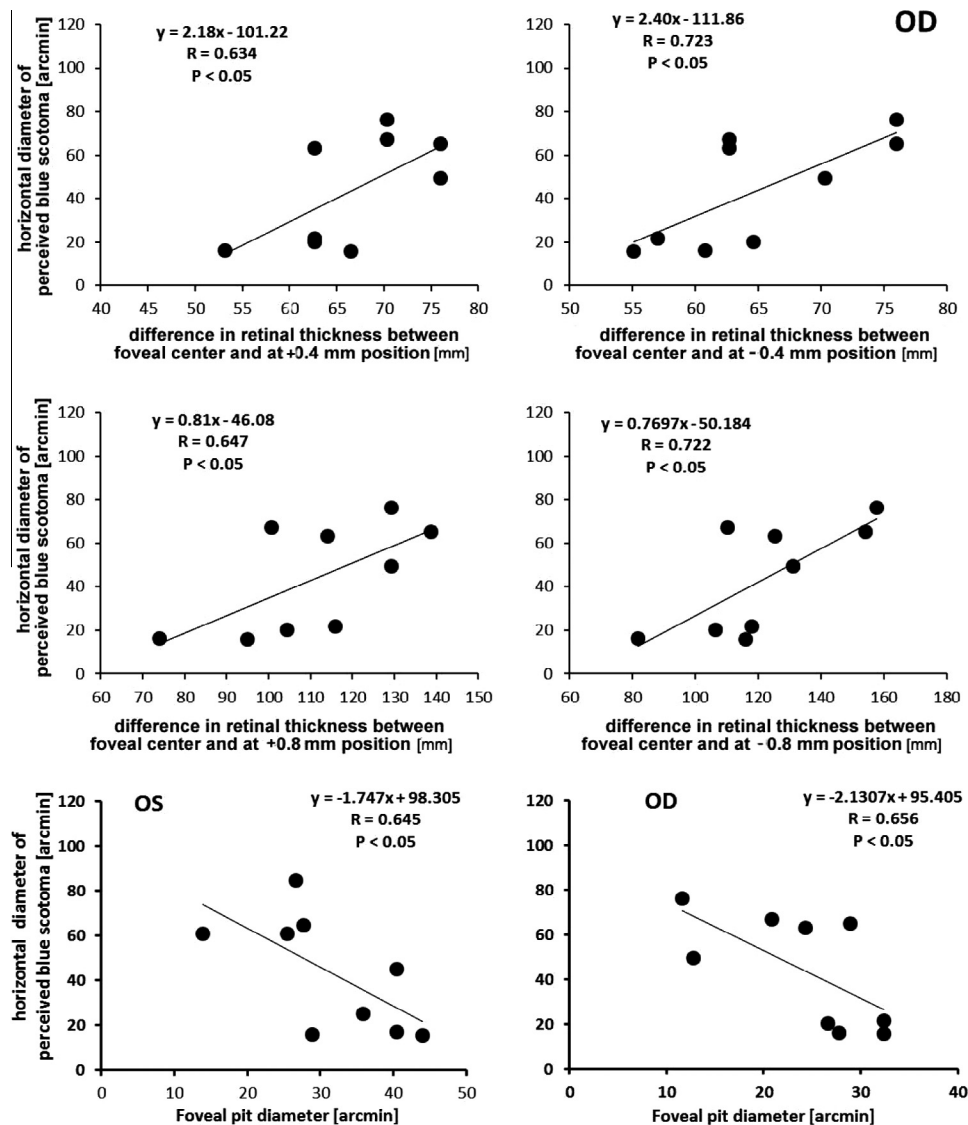


Fig. 5. Horizontal diameters of the perceived foveal blue scotomas plotted against the increase in retinal thickness from the foveal center in the right eyes (OD) of the nine subjects (top four figures). In the lowest two figures, the horizontal diameters of the perceived foveal blue scotomas are plotted against the diameters of the floor of the foveal pit. OS = left eyes, OD = right eyes.

Table 3

Horizontal diameters of the macular pigment distributions in the nine subjects, using a criterion of a drop in brightness below 50% in the RGB blue channel, provided in mm and arcmin. The diameters of the macular pigment distributions were highly correlated in left and right eyes ($R = 0.929$, $p < 0.001$). OS = left eyes, OD = right eyes.

Subject	OD		OS	
	Diameter of pigmented areas (mm)	Diameter of pigmented areas (arcmin)	Diameter of pigmented areas (mm)	Diameter of pigmented areas (arcmin)
1	0.32	65.5	0.29	59.5
2	0.50	103.2	0.65	134.9
3	0.86	178.6	0.79	162.7
4	0.78	160.7	0.75	154.8
5	0.64	131.9	0.61	127.0
6	0.64	131.9	0.67	138.9
7	0.77	158.7	0.81	166.7
8	0.96	198.4	0.95	196.4
9	0.72	147.8	0.63	130.9

increase in retinal thickness from the foveal center to the foveal rim, the larger the blue scotoma. These findings indicate that the

blue cone distributions in the fovea interact with the shape of the fovea although it is not known how and at which time during development this happens. We also found that the macular pigment distributions were highly correlated in both eyes but cannot account for the inter-individual differences in the size of the foveal blue scotomas.

4.1. Appearance and diameters of the S-cone free zone as described in the literature

The drawings of the blue scotomas as perceived by our subjects match descriptions in the literature: “the scotoma appears as a small, colorless dark spot with irregular, ragged borders in central vision” (Magnussen et al., 2001). They also match the patterns of the S-cone free zone described by Curcio and colleagues, and Williams and colleagues (Curcio et al., 1991; Williams, MacLeod, & Hayhoe, 1981). Also the diameters are in close agreement with the literature. The S-cone free zone was described as “about 20–25 arcmin wide, surrounded by an irregular pattern of S-cones at the foveal rim” (Curcio et al., 1991), 24–32 arcmin (Magnussen

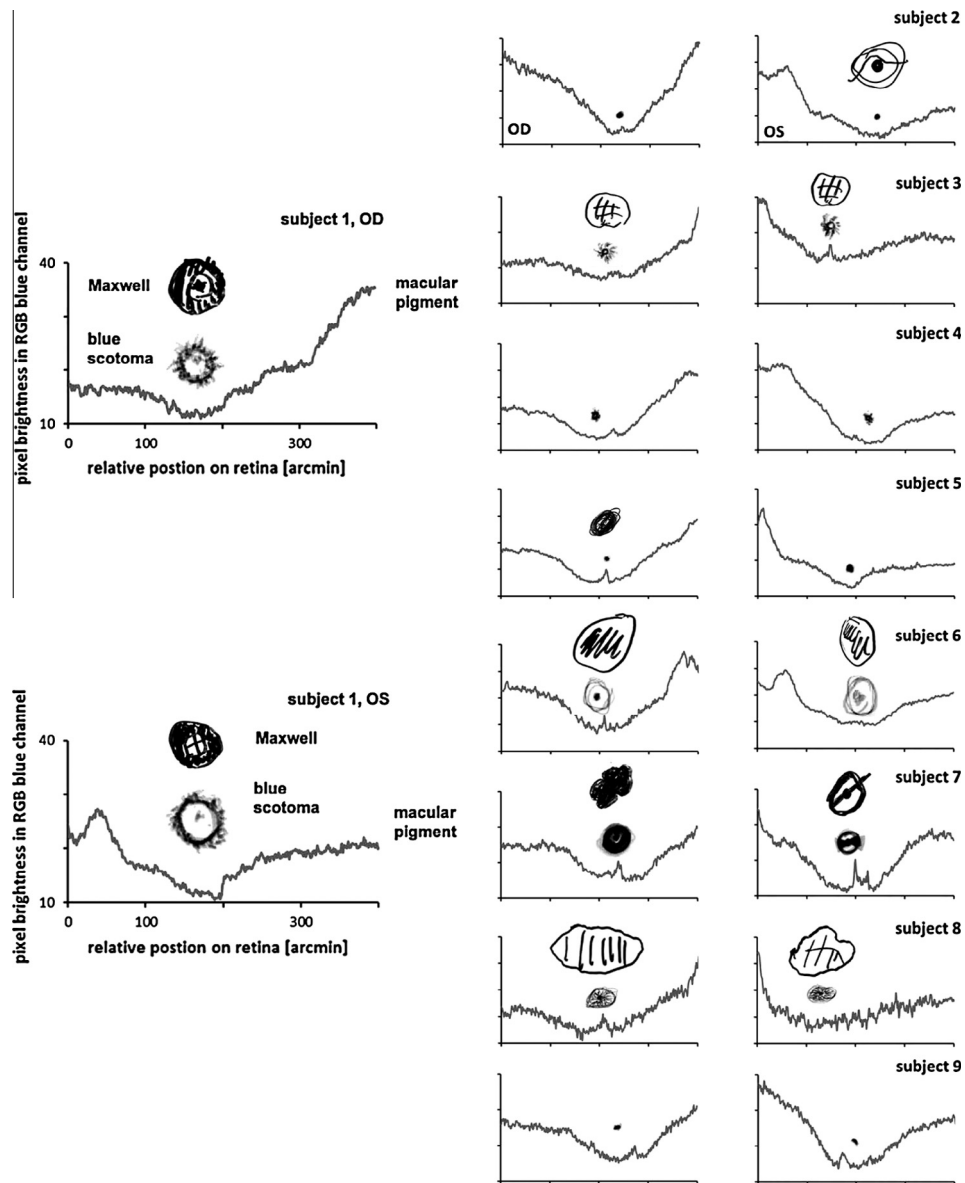


Fig. 6. Macular pigment density profiles in the horizontal meridian, as measured in 9 subjects. Drawings of the Maxwell's spot and foveal blue scotomas are also shown, adjusted to the same angular magnification (1 pixel on the fundus = 1 arcmin). Subject 9 was no longer available for the measurements of Maxwell's spot. Subject 4 could not see Maxwell's spot at all. Subject 2 and subject 5 saw it only in one eye. Note the large differences in perceived size between foveal blue scotoma and Maxwell's spot in subjects 2, 3, 5, 7 and 8. OS = left eyes, OD = right eyes.

Table 4
Horizontal diameters of Maxwell's spots as measured in visual angles (arcmin). OS = left eyes, OD = right eyes.

	OD	OS
1	67.2	80.7
2	No	130.6
3	95.7	102.8
4	Not seen	Not seen
5	65.1	Not seen
6	132.3	73.5
7	92.0	95.2
8	191.9	134.8

et al., 2001), or 24.8–44.3 arcmin (Magnussen et al., 2004). In our study, the drawings showed that the central scotomas were sometimes surrounded by an irregular circle. In these cases, the total diameters of area of the blue scotomas were larger than previously described. The dimensions of central spot still matched the

literature data (Magnussen et al., 2001, 2004). The linear diameter of the human fovea was described as 600–750 μm (2.0–2.5 degree of visual angle; Yuodelis & Hendrickson, 1986). The foveal avascular zone diameter (FAZ) in recent studies ranges from 0.20 to 1.08 mm (Dubis et al., 2012). Obviously, the S-cone free zone covers only a small proportion of the center of the foveal pit.

4.2. Relations of foveal shape and blue scotomas to gender and age

Delori et al. (2006) found that women have broader macular pigment distributions than men. They also found that “the radius of curvature of the concave inner limiting membrane surface is . . . larger in women than in men (1185 and 744 μm, respectively), which is consistent with a flatter foveal floor and/or broader foveal depression”. In our study, we did not see a correlation of foveal shape or diameter of the blue scotomas with gender

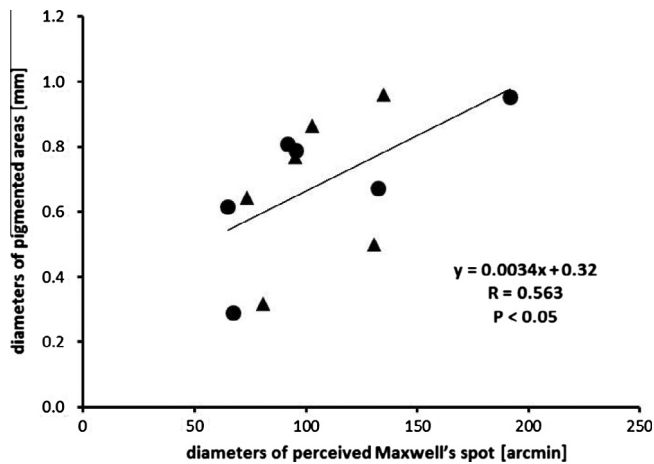


Fig. 7. Correlation between Maxwell's spot and diameter of macular pigment distributions. Triangles represent data from left eyes and circles from right eyes.

(5 male and 4 females were tested). It is possible that more than 9 subjects are necessary to confirm such a relationship.

Recently, it was reported that the area covered with macular pigment increases with age (Baptista & Nascimento, 2014). If macular pigment played a role in the percept of the foveal blue scotoma, there should have been a change with age. However, no significant correlation with age was found in our sample, may be, because their ages were too similar and the sample size too small ($R < 0.225$, $df = 8$, $p > 0.05$ in either eye).

4.3. Current conventions in the evaluation of the morphology of the fovea

The group of Joe Carroll (Dubis et al., 2012; Wagner-Schuman et al., 2011) used the change of the foveal slope to define the central fovea, the foveal pit depth and the foveal rim. In our measurements, we basically used the same measurement parameters:

- (1) We defined the center of the fovea as the area where the retina was thinnest. In the slope method, the center was defined as the area where the slope was zero (Dubis et al., 2012) or its value switched from negative to positive (Wagner-Schuman et al., 2011).
- (2) While we did not measure foveal depth as “the axial distance between a plane connecting the foveal rims and bottom of the foveal pit”, the differences in retinal thickness (ΔRT) in the six positions evaluated in our study were measured in a similar way. We used the transversal distance between the bottom of the foveal pit and four parafoveal positions.
- (3) While these data are not shown in the manuscript, we used the similar way to locate the foveal rim. On either side of foveal center, the foveal rim was located as the position where the retina reached the first peak thickness which is equivalent to the position where the slope is zero. A difference is the foveal profile was measured at 5 different angular positions, 30 deg away from each other, while we measured only in the horizontal meridian (Dubis et al., 2012; Wagner-Schuman et al., 2011) while we measured only in the horizontal and vertical meridians.

Our measurement results were similar to the ones by Wagner-Schuman et al. (2011) and Dubis et al. (2012). We also found that, at 0.8 mm distance from the foveal center, ΔRT values are significantly correlated in both eyes ($R = 0.9621$ and 0.8854 , $df = 8$,

$p < 0.01$). Center foveal thickness was 0.20–0.32 mm in their study, and 0.22–0.34 mm in ours. The slopes of the foveal pit were also significantly correlated between both eyes in their study, as well as in ours. We also did not find any gender bias, similar to Wagner-Schuman et al. (2011). We did not show data on the foveal rim diameters in our manuscript but these data were similar to the ones by Wagner-Schuman et al. (2011) (1.5–2.5 mm vs 1.74–2.76 mm in our study). Two other variables (central retina thickness in two eyes, gender bias in retinal thickness in the central fovea) did not produce any significant correlations in our study although they were in the same absolute range, probably because our sample size was much smaller ($n = 9$ subject, 18 eyes, versus $n = 90$ subject, 180 eyes). We did not analyze other parameters like foveal pit diameter, foveal pit volume and foveal pit area.

4.4. Comparison to other studies on the diameters of the macular pigment distributions

Westrup et al. (2014) also studied the relationship between foveal geometry and macular pigment distribution. They found that interocular correlations for several measures of retinal thickness (RT) and RT layers were high. RT was inversely related to MPOD at 1 and 2 deg from the foveal center, but not to central MPOD. The radius of the pigmented areas came out similar (their half-width 1.19 deg vs 1.18 deg in our study). A difference was that they used the green channel image whereas we used the blue channel image.

4.5. Relationship between the blue scotoma and the geometry of the foveal pit

In the current study, 5 subjects reported extra star-shaped radial extensions outside the central dark spot had larger blue scotomas. These subjects also had steeper foveal slopes and smaller foveal pit diameters, as can be seen in Fig. 4. Apparently, the anatomical structure of the foveal pit interacts with the foveal blue scotoma and determines whether star-shaped radial extensions are seen. There are at least two mechanisms that could explain these findings: (1) flatter foveas should have less minification effect as they act as a negative lens which could cause smaller blue scotomas and (2) S-cones embedded in the foveal slopes could be more tilted with respect to the incoming rays which could reduce their sensitivity due to their Stiles–Crawford effect (Burns et al., 1997a, 1997b; Stiles & Crawford, 1933). However, both hypotheses suffer from shortcomings: (1) The estimated magnification effects of the foveal pit are very small and cannot account for the magnitude of the differences that were observed among the subjects. The estimated change in retinal image magnification, derived from the approximate radius of the fovea (about 4.3 mm, calculated from foveal width of 2 mm and a depth of 0.12 mm) and the refractive indices of vitreous and retina ($n = 1.335$ and $n = 1.380$) were only about 0.22%. (2) While the perceived blue scotomas were often wider than the diameters of the foveal floor (foveal floor widths ranging from 19.7 to 26.9 arcmin (Table 2), blue scotomas ranging from 15.5 to 84.7 arcmin (Table 1)), it is highly unlikely that the S-cones located in the foveal slopes would have been so misaligned that they were almost not stimulated. Therefore, none of these explanations is convincing and further studies are required to uncover the underlying mechanisms.

Acknowledgments

This study was supported by OpAL (Optical and Adaptational Limits of Vision); OpAL is an Initial Training Network funded by the European Commission under the Seventh Framework Program (PITN-GA-2010-264605). We are grateful to Dr. Susanna Schweyer,

University Eye Hospital Tübingen, for her help with the OCT measurements.

References

- Baptista, A. M., & Nascimento, S. (2014). Changes in spatial extent and peak double optical density of human macular pigment with age. *Journal of the Optical Society of America A*, 31(4), A87–A92.
- Bone, R. A., Landrum, J. T., & Cains, A. (1992). Optical density spectra of the macular pigment in vivo and in vitro. *Vision Research*, 32(1), 105–110.
- Burns, S., He, J., Delori, F., & Marcos, S. (1997a). Do the cones see light scattered from the deep retinal layers? *Vision Science and Its Applications*, 1, 94–97.
- Burns, S. A., Wu, S., He, J. C., & Elsner, A. E. (1997b). Variations in photoreceptor directionality across the central retina. *Journal of the Optical Society of America A*, 14(9), 2033–2040.
- Burcio, C. A., Allen, K. A., Sloan, K. R., Lerea, C. L., Hurley, J. B., Klock, I. B., et al. (1991). Distribution and morphology of human cone photoreceptors stained with anti-blue opsin. *Journal of Comparative Neurology*, 312(4), 610–624.
- Delori, F. C., Goger, D. G., Keilhauer, C., Salvetti, P., & Staurenghi, G. (2006). Bimodal spatial distribution of macular pigment: Evidence of a gender relationship. *Journal of the Optical Society of America A*, 23(3), 521–538.
- Dubis, A. M., Hansen, B. R., Cooper, R. F., Beringer, J., Dubra, A., & Carroll, J. (2012). Relationship between the foveal avascular zone and foveal pit morphology. *Investigative Ophthalmology & Visual Science*, 53(3), 1628–1636.
- Gerrits, I. H., & Vendrik, A. (1970). Simultaneous contrast, filling-in process and information processing in man's visual system. *Experimental Brain Research*, 11(4), 411–430.
- Giani, A., Cigada, M., Choudhry, N., Deiro, A. P., Oldani, M., Pellegrini, M., et al. (2010). Reproducibility of retinal thickness measurements on normal and pathologic eyes by different optical coherence tomography instruments. *American Journal of Ophthalmology*, 150(6), 815–824. e811.
- Gullstrand, A. (1909). *Appendix to Helmholtz's Physiologische Optik*.
- Hammond, B. R., Wooten, B. R., & Snodderly, D. M. (1997). Individual variations in the spatial profile of human macular pigment. *Journal of the Optical Society of America A*, 14(6), 1187–1196.
- Harkness, L., & Bennet-Clark, H. (1978). The deep fovea as a focus indicator. *Nature*, 272, 814–816.
- Holm, E. (1922). Das gelbe Maculapigment und seine optische Bedeutung. *Graefes Archives for Clinical and Experimental Ophthalmology*, 108(1), 1–85.
- Isobe, K., & Motokawa, K. (1955). Functional structure of the retinal fovea and Maxwell's spot. *Nature*, 175, 306–307.
- Kirschfeld, K. (1982). Carotenoid pigments: Their possible role in protecting against photooxidation in eyes and photoreceptor cells. *Proceedings of the Royal Society of London, Series B: Biological Sciences*, 216(1202), 71–85.
- Knighton, R. W., & Gregori, G. (2012). The shape of the ganglion cell plus inner plexiform layers of the normal human macula. *Investigative Ophthalmology & Visual Science*, 53(11), 7412–7420.
- König, A. (1894). Über den menschlichen Sehpurpur und seine Bedeutung für das Sehen. *Sitzungsberichte der Preussischen Akademie der Wissenschaften*, 30.
- Magnussen, S., Spillmann, L., Sturzel, F., & Werner, J. S. (2001). Filling-in of the foveal blue scotoma. *Vision Research*, 41(23), 2961–2967.
- Magnussen, S., Spillmann, L., Sturzel, F., & Werner, J. S. (2004). Unveiling the foveal blue scotoma through an afterimage. *Vision Research*, 44(4), 377–383.
- Makridaki, M., Hendrikse, F., Carden, D., van der Veen, R. L., Berendschot, T. T., & Murray, I. J. (2009). Correspondence between retinal reflectometry and a flicker-based technique in the measurement of macular pigment spatial profiles. *Journal of Biomedical Optics*, 14(6), 064046.
- Miles, W. R. (1954). Comparison of functional and structural areas in human fovea. I. Method of entoptic plotting. *Journal of Neurophysiology*, 17(1), 22–38.
- Nussbaum, J. J., Pruett, R. C., & Delori, F. C. (1981). Macular yellow pigment: The first 200 years. *Retina*, 1(4), 296–310.
- Polyak, S. (1951). *The retina*. University of Chicago Press.
- Rodieck, R. W. (1973). *The vertebrate retina: Principles of structure and function*. Oxford, England: W.H. Freeman.
- Smith, R. T., Nagasaki, T., Sparrow, J. R., Barbazetto, I., Koniarek, J. P., & Bickmann, L. J. (2004). Photographic patterns in macular images: Representation by a mathematical model. *Journal of Biomedical Optics*, 9(1), 162–172.
- Spillmann, L., & Werner, J. S. (1996). Long-range interactions in visual perception. *Trends in Neurosciences*, 19(10), 428–434.
- Stiles, W., & Crawford, B. (1933). The luminous efficiency of rays entering the eye pupil at different points. *Proceedings of the Royal Society of London, Series B*, 112(778), 428–450.
- Stockman, A., & Sharpe, L. T. (2000). The spectral sensitivities of the middle-and long-wavelength-sensitive cones derived from measurements in observers of known genotype. *Vision Research*, 40(13), 1711–1737.
- Wagner-Schuman, M., Dubis, A. M., Nordgren, R. N., Lei, Y., Odell, D., Chiao, H., et al. (2011). Race- and sex-related differences in retinal thickness and foveal pit morphology. *Investigative Ophthalmology & Visual Science*, 52(1), 625–634.
- Wald, G. (1967). Blue-blindness in the normal fovea. *Journal of the Optical Society of America*, 57(11), 1289–1301.
- Walls, G. L., & Mathews, R. W. (1952). New means of studying color blindness and normal foveal color vision, with some results and their genetical implications. *Publications in Psychology. University of California (1868–1952)*, 7(1), 1.
- Wässle, H., & Boycott, B. B. (1991). Functional architecture of the mammalian retina. *Physiological Reviews*, 71(2), 447–480.
- Wässle, H., Grünert, U., Röhrenbeck, J., & Boycott, B. B. (1990). Retinal ganglion cell density and cortical magnification factor in the primate. *Vision Research*, 30(11), 1897–1911.
- Werner, J. S., Bieber, M. L., & Scheffrin, B. E. (2000). Senescence of foveal and parafoveal cone sensitivities and their relations to macular pigment density. *Journal of the Optical Society of America A*, 17(11), 1918–1932.
- Werner, J. S., Donnelly, S. K., & Kliegl, R. (1987). Aging and human macular pigment density: Appended with translations from the work of Max Schultze and Ewald Hering. *Vision Research*, 27(2), 257–268.
- Westrup, V. K. M., Dietzel, M., Pauleikhoff, D., & Hense, H. W. (2014). The association of retinal structure and macular pigment distribution. *Investigative Ophthalmology & Visual Science*, 55(2), 1169–1175.
- Williams, D. R., MacLeod, D. I., & Hayhoe, M. M. (1981). Punctate sensitivity of the blue-sensitive mechanism. *Vision Research*, 21(9), 1357–1375.
- Willmer, E., & Wright, W. (1945). Colour sensitivity of the fovea centralis. *Nature*, 156(3952), 119–121.
- Wooten, B. R., & Hammond, B. R. (2002). Macular pigment: Influences on visual acuity and visibility. *Progress in Retinal and Eye Research*, 21(2), 225–240.
- Wooten, B. R., Hammond, B. R., Land, R. I., & Snodderly, D. M. (1999). A practical method for measuring macular pigment optical density. *Investigative Ophthalmology & Visual Science*, 40(11), 2481–2489.
- Yuodelis, C., & Hendrickson, A. (1986). A qualitative and quantitative analysis of the human fovea during development. *Vision Research*, 26(6), 847–855.

Factors affecting the calibration of white light eccentric photorefraction

Yun Chen and Frank Schaeffel*

*Section of Neurobiology of the Eye, Ophthalmic Research Institute, University of Tuebingen, Calwerstrasse 7/1,
72076 Tuebingen, Germany*

**frank.schaeffel@uni-tuebingen.de*

Abstract: Eccentric photorefraction is a convenient technique to measure refractive state of the eyes from a distance of a meter or more but its reliability is limited by the fact its calibration is variable among subjects. To calibrate, trial lenses are held in front of the eye and the brightness slope in the pupil is measured. Thereafter, a brightness slope can be assigned to a refractive error by multiplication with a constant, the “conversion factor”. It is unclear why conversion factors vary among subjects. In the current study, we determined conversion factors in white light in 12 eyes of 8 subjects, using an artificial pupil aperture of 5 mm. A RGB CCD camera was used and it was verified that it operated in its linear range when automatic gain controls were switched off. Calibration was done separately for the R, G, and B channel of the camera. Correlations of the conversion factors to the following ocular variables were analyzed (1) fundal reflectance at different retinal locations, or after exposing the subjects to bright light for 10 minutes to reduce fundal reflectivity, (2) macular pigment optical density, (3) axial length, (4) higher order ocular aberrations. It was found that all factors that reduced the overall brightness of the pupil increased the conversion factors, and vice versa. The relationship may have a simple explanation. If the pupil becomes brighter because it dilates, all pixel grey levels increase proportionally by a constant factor. Therefore, the slope of the linear regression through the pixel values in the pupil increases by the same factor. Accordingly, conversion factors need to be reduced to measure the same refractive state. The result has important implications: (1) when accommodation is measured and the pupil constricts, a correction to the conversion factor needs to be made for the drop in pupil brightness, or accommodation will be severely underestimated, (2) measurements in different ethnic groups with different fundal reflectivity become incorrect unless the conversion factor is normalized to respective pupil brightness, (3) calibration in subjects with axial anisometropia results in different conversion factors for both eyes.

©2015 Optical Society of America

OCIS codes: (000.1430) Biology and medicine; (170.4460) Ophthalmic optics and devices

References and links

1. F. Schaeffel, H. Wilhelm, and E. Zrenner, "Inter-individual variability in the dynamics of natural accommodation in humans: relation to age and refractive errors." *Journal of Physiology*, 461, 301-20 (1993).
2. F. Schaeffel, U. Mathis, and G. Bruggemann, "Noncycloplegic photorefractive screening in pre-school children with the "PowerRefractor" in a pediatric practice." *Optometry & Vision Science*, 84(7), 630-9 (2007).
3. M. Choi, S. Weiss, F. Schaeffel, A. Seidemann, H. C. Howland, B. Wilhelm, and H. Wilhelm, "Laboratory, clinical, and kindergarten test of a new eccentric infrared photorefractor (PowerRefractor)." *Optometry & Vision Science*, 77(10), 537-48 (2000).
4. A. H. Dahlmann-Noor, K. Vrotsou, V. Kostakis, J. Brown, J. Heath, A. Iron, S. McGill, and A. J. Vivian, "Vision screening in children by Plusoptix Vision Screener compared with gold-standard orthoptic assessment." *British Journal of Ophthalmology*, 93(3), 342-5 (2009).

5. H. C. Howland, "Photorefracton of eyes: history and future prospects." *Optometry & Vision Science*, 86(6), 603-6 (2009).
 6. O. A. Hunt, J. S. Wolffsohn, and B. Gilmartin, "Evaluation of the measurement of refractive error by the PowerRefractor: a remote, continuous and binocular measurement system of oculomotor function." *British Journal of Ophthalmology*, 87(12), 1504-8 (2003).
 7. A. Seidemann and F. Schaeffel, "An evaluation of the lag of accommodation using photorefracton." *Vision Research*, 43(4), 419-430 (2003).
 8. N. G. Sravani, V. K. Nilagiri, and S. R. Bharadwaj, "Photorefracton estimates of refractive power varies with the ethnic origin of human eyes." *Scientific Reports*, 5, 7976 (2015).
 9. P. J. Blade and T. R. Candy, "Validation of the PowerRefractor for measuring human infant refracton." *Optometry & Vision Science*, 83(6), 346-53 (2006).
 10. S. R. Bharadwaj, N. G. Sravani, J.-A. Little, A. Narasaiah, V. Wong, R. Woodburn, and T. R. Candy, "Empirical variability in the calibration of slope-based eccentric photorefracton." *Journal Optical Society of America A*, 30(5), 923-931 (2013).
 11. R. Kusel, U. Oechsner, W. Wesemann, S. Russlies, E. M. Irmer, and B. Rassow, "Light-intensity distribution in eccentric photorefracton crescents." *Journal Optical Society of America A*, 15(6), 1500-1511 (1998).
 12. A. Roorda, M. C. Campbell, and W. R. Bobier, "Slope-based eccentric photorefracton: theoretical analysis of different light source configurations and effects of ocular aberrations." *Journal Optical Society of America A*, 14(10), 2547-2556 (1997).
 13. I. Hodgkinson, K. Chong, and A. Molteno, "Characterization of the fundal reflectance of infants." *Optometry & Vision Science*, 68(7), 513-521 (1991).
 14. F. C. Delori and K. P. Pflibsen, "Spectral reflectance of the human ocular fundus." *Applied Optics*, 28(6), 1061-1077 (1989).
 15. F. Schaeffel and H. Kaymak, "New Techniques to Measure Lens Tilt, Decentration and Longitudinal Chromatic Aberration in Phakic and Pseudophakic Eyes." *Nova Acta Leopoldina NF*, 111(379), 127-136 (2010).
 16. S. Marcos, S. A. Burns, P. M. Prieto, R. Navarro, and B. Baraibar, "Investigating sources of variability of monochromatic and transverse chromatic aberrations across eyes." *Vision research*, 41(28), 3861-3871 (2001).
 17. R. A. Bone and J. T. Landrum, "Heterochromatic flicker photometry." *Archives of Biochemistry and Biophysics* 430(2), 137-42 (2004).
 18. N. A. McBrien and D. W. Adams, "A longitudinal investigation of adult-onset and adult-progression of myopia in an occupational group. Refractive and biometric findings." *Investigative Ophthalmology & Visual Science*, 38(2), 321-33 (1997).
 19. C. Wildsoet and J. Wallman, "Choroidal and scleral mechanisms of compensation for spectacle lenses in chicks." *Vision Research*, 35(9), 1175-94 (1995).
 20. F. Schaeffel, A. Glasser, and H. C. Howland, "Accommodation, refractive error and eye growth in chickens." *Vision Research*, 28(5), 639-57 (1988).
 21. J. B. Orr, D. Seidel, M. Day, and L. S. Gray, "Is Pupil Diameter Influenced by Refractive Error?" *Optometry & Vision Science* [Epub ahead of print] (2015).
 22. K. Kirschfeld, "Carotenoid pigments: their possible role in protecting against photooxidation in eyes and photoreceptor cells." *Proceedings of the Royal Society of London. Series B. Biological Sciences*, 216(1202), 71-85 (1982).
 23. J. J. Nussbaum, R. C. Pruett, and F. C. Delori, "Macular yellow pigment: the first 200 years." *Retina*, 1(4), 296-310 (1981).
 24. J. S. Werner, M. L. Bieber, and B. E. Scheffrin, "Senescence of foveal and parafoveal cone sensitivities and their relations to macular pigment density." *Journal Optical Society of America A*, 17(11), 1918-1932 (2000).
 25. R. A. Bone, J. T. Landrum, and A. Cains, "Optical density spectra of the macular pigment in vivo and in vitro." *Vision Research*, 32(1), 105-110 (1992).
-

1. Introduction

Eccentric photorefracton is a popular technique to measure refractive errors in animal models and humans. For these measurements, the steepness of the brightness slope in the pupil, usually generated by a few infrared LEDs that are eccentrically positioned relative to the optical axis of a camera lens, is quantified by linear regression analysis [1]. To calibrate the technique, trial lenses of known power are placed in front of the eye to induce defined refractive errors and the brightness slopes in the pupil are recorded for each lens. Conversely, refractive errors of the eyes, relative to the position of the camera, can be inferred by simple multiplication of the brightness slope with a "conversion factor" that was obtained by the calibration. The technique is powerful in detecting myopia, astigmatism and anisometropia but may be limited to detect hyperopia in infants and young children without cycloplegia since no fogging procedure is employed to relax accommodation [2] - a general problem,

however, in open field refractors. Nevertheless, since it is fast, operates from a distance and is binocular, it has been widely used for screening studies in young children [3-6]. Choi et al. studied the reliability and accuracy of a commercially available eccentric infrared photorefractor, the PowerRefractor, in laboratory tests and in a Kindergarten [3]. The PowerRefractor uses 6 LED segments, consisting of 9 IR LEDs each which are arranged in opposing positions to the optical axis of the camera so that three meridians could be refracted from two opposing positions. The design was chosen to reduce the effects of the asymmetrical aberrations and to extend the linear range of refractor from +4D to -6D, relative to infinity.

It is well known that conversion factors vary among subjects (variability up to about 15 percent, [1]) but, up to now, no consistent optical reason was identified [7]. Several factors contribute to the variability, including ethnic background [8], contrast and luminance response of the video system, pupil size, reflectance properties of the fundus, wavefront aberrations of the measured eye, and arrangement and type of the LEDs [9, 10]. Accordingly, to improve the reliability of the photorefraction, individual calibrations may become necessary which eliminates a major advantage of the technique, namely that it is fast and easy to perform.

The problem was previously tackled using ray tracing based on Gaussian optics. Kusel and colleagues calculated how the light crescent in the pupil varies with spherical aberration and astigmatism for different light source configurations. The following configurations were studied (1) a point source with a knife-edge aperture, (2) a long linear light source with knife-edge aperture, and (3) a point source with a circular camera aperture, as normally found in camera lenses [11]. In configuration (1) and (2), the calculations could be completed in closed form but in configuration (3), the mathematics became too complex. The equations determined in configuration (1) and (2) permitted to derive sphere, cylinder and axis from crescent size and slope from minimally two pictures, taken with different orientations of the LED segments. Later, Austin Roorda simulated the optics of eccentric photorefractive system and studied how the conversion factor (“gain” in his paper) varied with different light configurations (single point light source and extended light source). He also studied the effects of mono-chromatic aberrations, and determined the working range, dead zone and linearity of the photorefractive system [12]. He found that intensity profile in the pupil was more linear when extended light sources were used rather than a point source. He also described that averaging refractions obtained with two eccentric light sources positioned at opposing positions reduces the effects of asymmetric monochromatic aberrations. Furthermore, he recognized that the conversion factor changes with pupil size.

If broadband white light is used instead of infrared light, refractive errors can be simultaneously measured in the R, B, and G channel of the video system. Schaeffel and Kaymak [15] tried to determine longitudinal chromatic aberration (LCA) from a single video frame, as initially proposed by Hodgkinson, Chong and Moltano already in 1991 [13]. A problem is that the reflectivity of the human fundus varies with wavelength; it is very low in the short wavelength range [14]. In order to compensate for this problem, Schaeffel and Kaymak [15] used high power white LEDs with an emission peak at 460 nm and a CCD RGB camera in which the spectral sensitivity of the blue channel matched the emission peak of the LEDs. Unexpectedly, measurements in human eyes showed scarcely any LCA, even though the literature provides abundant data as to how large it is [16]. Since an appropriate amount of LCA was measured with the white light photorefractor in two types of artificial eyes (one solid rubber ball eye that was made by Chris Kuether (ckuether@central.uh.edu) from Houston University and a second air filled eye model eye with a single +60 D glass lens and a grey cardboard as artificial retina. Since both eyes had a single reflecting layer as “retina”, it was concluded that multi-layer reflection from the fundal layers in the real eye may hide the effects of LCA. If red light is reflected from deeper layers than blue, it could compensate for the effects of LCA such that no LCA is detected with eccentric photorefractive system.

To shed more light on factors that determine the calibration of eccentric photorefractive system, we used the same CCD RGB camera as Schaeffel and Kaymak, as well as the same white LEDs

[15] and studied the refractions in R, G, and B in Caucasian subjects. Conversion factors were individually determined with trial lenses, ranging from +4D to -4D in 1D steps. After controlling for non-linearities of the camera, the effects of fundal reflectivity, macular pigment density, ocular biometry, as well as higher order aberrations on the conversion factors were analyzed.

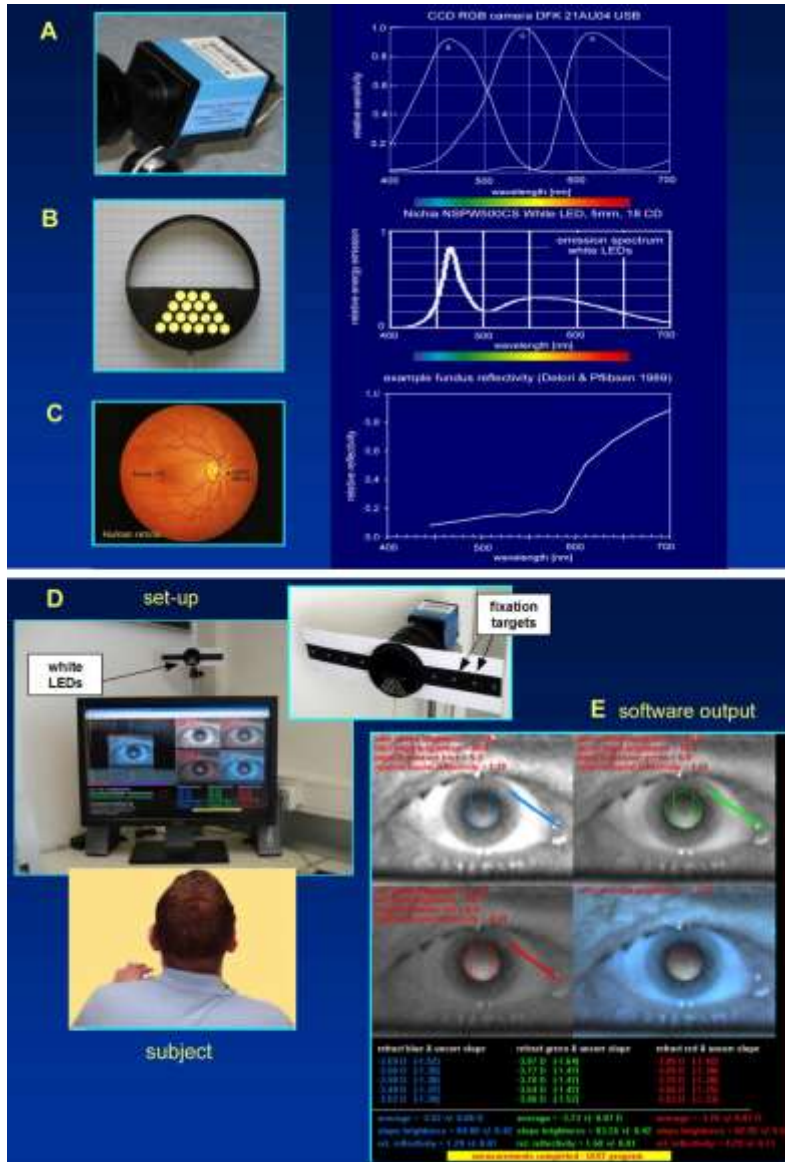
2. Methods

3.1 Subjects

Twelve eyes of 8 young Caucasian subjects with an average age of 31.2 ± 8.6 years (ranging from 25–47 years) and no known ocular pathologies other than small refractive errors were studied. The study adhered to the tenets of the declaration of Helsinki and was approved by the local University Ethics Commission.

3.2 Experimental set-up

Sixteen high power white LEDs (Nichia NSPW500CS, 5 mm; Conrad Electronics, Germany) were positioned under the knife edge of the eccentric photorefractor (Figure 1B) which was attached to an RGB CCD camera (DFK21 AU04, The ImagingSource, Bremen, Germany; Figure 1A). Since fundal reflectance is poor in the short wavelengths range (Figure 1C), it was helpful that the LEDs had an emission peak at 460 nm which matched the sensitivity peak of the blue channel of the camera. Software was developed under Visual C++ 6.0 to flash the white light LEDs through the USB port of the laptop with a USB to serial converter cable (# 33304, www.inline-info.com) and record a video frame during the flash. Subjects were measured refracted at one meter distance from the camera (Figure 1D). The slope of the brightness profiles in the vertical pupil meridian in the R, G, B channel was automatically determined by custom-developed software written in C++ (Figure 1E).



Average pixel brightness in video frames grabbed for different combinations of aperture sizes and neutral density filters are shown in Table 1.

F (aperture size)	filter	relative luminance
4	no	16
5.6	no	8
8	no	4
11	no	2
16	no	1
16	NG11	0.75
11	NG4	0.6
16	NG4	0.3

Table 1. Used combinations of aperture sizes and neutral density filters to achieve different luminances.

The average pixel brightness in each picture was determined with “Image J” (<http://rsb.info.nih.gov/ij/>), separately for R, G, and B channels. Over the the full dynamic range of the camera, with pixel values ranging from 0 to 255, the pixel to luminance function was non-linear and was fit by a x-order polynomial (Figure 2A). Since the pixel grey levels always remained below 100 during the measurements (illustrated by “collected luminance data” in Figure 2B), the non-linear part of the curve was ignored and the camera response curve could be considered linear over the range in which the calibrations took place.

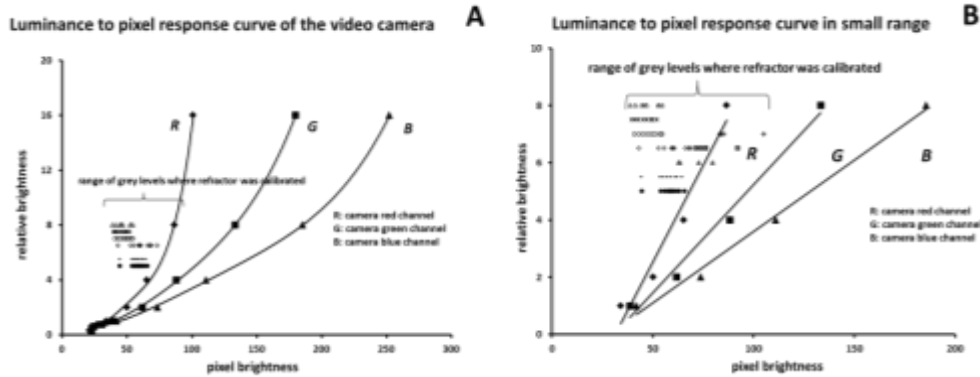


Figure 2. (A) Luminance to pixel conversion of the video camera, up to the highest pixel values (255) in the case of the R channel. It can be seen that pixel grey levels grew non-linearly with luminance. Symbols denote the average pupil pixel grey levels during the calibration of photorefraction in the subjects’ eyes. (B) In the range in which the calibration of the photorefraction was performed (see data points denoted “collected luminance data”) the luminance to pixel conversion function could be considered linear.

3.4 Measurement of conversion factors

Twelve young were asked to monocularly fixate a target close to the camera at one meter distance in a dimly illuminated room. Trial lenses (range +4D to -4D, in steps of 1D) were held in front of their eye as described in [15]. Conversion factors were simultaneously determined in R, G and B by analyzing the brightness slopes in the pupils, separately for each channel. Pupil size was fixed to 5 mm by using an artificial aperture, centered in the natural pupil. Conversion factors were determined (1) in the fovea, (2) 10 degrees off-axis in the temporal retina, and (3) in the fovea after 10 minutes of previous exposure to bright light, to alter fundal reflectance. Trial lens powers were were plotted against the slopes of the

brightness profiles in the pupil and a linear regression was fit to the data as previously described [1]. The slope of the linear regression of lens power versus brightness slope in the pupil was the “conversion factor”, as previously described [1].

3.5 Macular pigment optical density (MPOD) measurements

Macular pigment optical density (MPOD) was psychophysically measured with the MPOD Tinsley device (Tinsley Precision Instruments, UK). The procedures are as follows. Using heterochromatic flicker photometry (HFP)[17], the subjective-equal-luminance point of two flicking light of different wavelengths was determined at two retinal positions, in the fovea and 8 degrees off where macular pigment is known to be reduced or absent. The two wavelengths were 460 (blue) and 540 nm (green). While the brightness of the green light was fixed, the subject could adjust the blue to match its brightness. In the fovea, the blue light appears dimmer than that in the 8 degree position due to macular pigment absorption. A series of different intensity ratios of the blue and green lights were presented to subjects at different flicker frequency. Matches were repeated 5 times both in the central fovea and at 8 degrees off. MPOD was expressed as logarithm of ($I_{\text{center}}/I_{8\text{degrees}}$). Subjects had to look at the flickering stimulus through the eyepiece of the instrument in a dark room.

3.6 Higher order aberrations and biometrical measurements in the eyes

Monocular ocular aberrations (spherical aberration, astigmatism, coma, defocus), were measured by the Hartman-Shack sensor-based WASCA wavefront Analyzer (Carl Zeiss Meditec AG, Germany). Ocular biometry was done with a commercially available low-coherence interferometer, the Lenstar LS 900 (HAAG–STREIT AG, Bern, Switzerland). The instrument provided central corneal thickness, corneal radius of curvature, anterior chamber depth, lens thickness, vitreous chamber depth and axial length. No pupil dilatation was necessary for these measurements.

3.7 Statistics

Linear regression analysis was used to determine correlations between psychophysical results and optical or biometrical measurements. A multiple regression model for multivariate analysis was built using SPSS (version 16.0, SPSS, Chicago, IL). Using the “simultaneous” method, all tested variables (MOPD and axial length) were set up together to determine which had the strongest impact on the dependent variable, the conversion factor. Their relative importance was ranked. The three variables (x_{i1} : MPOD, x_{i2} Spherical aberration, x_{i3} : axial length; y : conversion factor in the blue channel, for example) were assumed to satisfy the linear model: $y = b_0 + b_1x_{i1} + b_2x_{i2} + b_3x_{i3} + u_i$ while $i = 1, 2, 3, 4$, where u_i were values of an unobserved error term and b_i unknown parameter constants. B_i were the standard regression coefficients.

3. Results

3.1 Measurement of conversion factors in different retinal location, and after previous exposure to bright light

Conversion factors were found highly variable among subjects, clearly more variable than what is typically found for infrared light. They ranged from 3.8 to 13.8 for measurements in the fovea (condition 1), from 2.3 to 8.0 if measurements took place 10 degrees off-axis in the temporal retina (condition 2), and from 7.6 to 16.0 in the fovea after 10 minutes of previous exposure to bright light (condition 3). Average values and standard deviations of the conversion factors in the 12 subjects for conditions 1-3 are shown in the last two lines in Table 2. It is obvious that they decreased in temporal retina (condition 2) and increased after exposure to bright light (condition 3), compared to conversion factors measured in the fovea (condition 1).

Eye	Condition (1)			Condition (2)			Condition (3)		
	red	green	blue	red	green	blue	red	green	blue
1	6.06	6.55	7.35	4.16	4.45	4.69			
2	5.5	4.91	5.21	3.43	3.33	3.33	8.51	7.64	8.38
3	10.18	9.58	11.64	4.71	4.22	4.99			
4	10.42	10.43	13.85	7.52	8	6.74	13.53	13.59	18.15
5	6.56	6.28	7.56	2.86	2.7	2.61	9.46	8.93	10.1
6	4.79	4.25	4.6	2.77	2.26	2			
7	9.24	8.2	8.46	4.95	4.57	4.64			
8	6.67	6.01	7.03	3.86	3.4	3.32	15.97	14.04	14.03
9	4.47	3.81	3.93	2.98	2.43	2.37			
10	5.07	4.59	5.13	3.65	3.08	2.82	13.02	10.44	11.12
11	7.52	7.01	8.13	4.32	3.96	4.01	5.91	5.51	6.37
12	6.6	5.72	6.37	5.01	4.18	4.06			
average	6.9	6.4	7.4	4.2	3.9	3.8	11.1	10	11.4
SD	2	2.08	2.9	1.3	1.5	1.3	3.7	3.4	4.2

Table 2. Conversion factors as determined in subjects 1-12. Note that pupil size was normalized to 5 mm by using an artificial pupil aperture.

It is interesting that the conversion factors determined in the fovea and in the temporal retina were correlated in each individual eye as shown in Figure 3 (Red: R = 0.804; Green: R = 0.829; Blue: R = 0.889; df = 11, all p < 0.001).

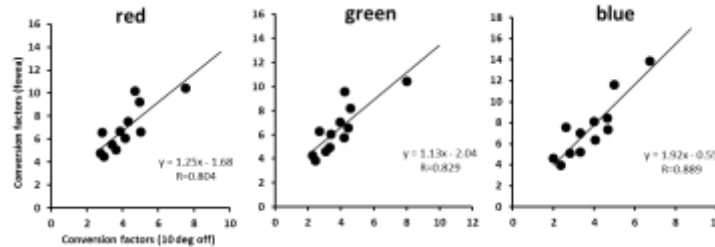


Figure 3. Correlations of the conversion factors determined at two different fundal positions in the same eyes (fovea and 10 degrees in the temporal retina), for the R, G, and B channel.

3.2 Macular pigment optical density (MPOD) and its effect on the conversion factors

Averages of three repeated measurements of MPOD and their standard deviations are shown in Table 3. Subject 3 had the largest MPOD, 0.97, and subject 6 eye had the smallest one, 0.29. Measurements of MPOD appeared reliable since the the standard deviations were small compared to the values, and most subject differed from each other with high significance.

subject	1	2	3	4	5	6	7	8	9	10	11	12
MPOD	0.51	0.47	0.97	0.8	0.43	0.29	0.62	0.55	0.52	0.6	0.3	0.36
SD	0.13	0.02	0	0	0.06	0.03	0.03	0	0.03	0	0	0

Table 3. Average values of MPOD and standard deviations from three repeated measurements in 12 subjects.

When MPOD was correlated to the conversion factors determined in the fovea, significant correlations were found in the R, G and B channel (Figure 4, Blue: R = 0.689; Green: R = 0.689; Red: R = 0.685; df = 11, p < 0.001 in all cases). No significant correlation was found 10 degrees off-axis in the temporal retina which is not surprising since MPOD declines with the distance from the fovea. It was surprising, however, that a correlation was also found in the red channel (Figure 4, right), even though the absorption of macular pigment is known to be low in the red end of the visible spectrum.

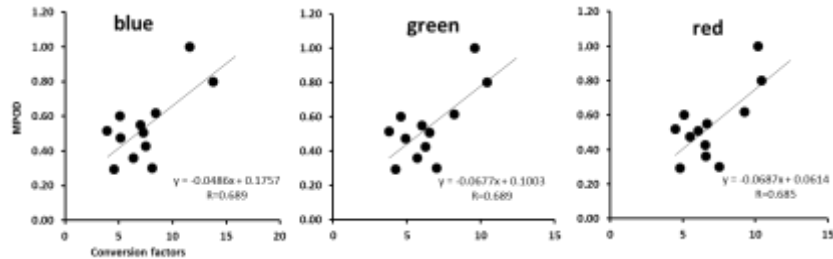


Figure 4. Conversion factors, determined in the fovea, are significantly correlated to foveal MPOD.

3.3 Effects of higher order aberrations and ocular biometry on conversion factors

Two clearly significant correlations (p < 0.01 in all cases) were found: (1) conversion factor to foveal refractive error, and (2) conversion factor to axial length (Figure 5). No significant correlations were found to higher order ocular aberrations (spherical aberration or coma).

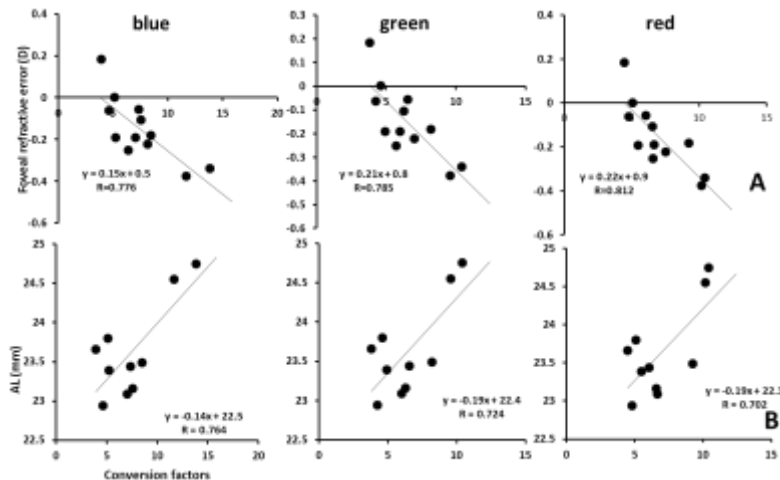


Figure 5. Correlations of the conversion factors with (A) foveal refractive error and (C) axial length of the eyes (all correlations p < 0.01).

3.4 Changes of the conversion factor after the subject were exposed to bright light

Since the conversion factors were larger in the fovea than at 10 deg in the temporal retina, where the density of macular pigment is low, we tested changes in fundal reflectance may also change the conversion factors. Subjects were calibrated with lenses and the conversion factors determined. They were then asked to go outside into the bright sunlight for 10 minutes. After their return, they were calibrated again. It was found that fundal reflectance was reduced after exposure to bright light (Figure 6A). At the same time, the conversion factors became larger.

Figure 6B shows linear regressions through the conversion factors determined for different pupil brightness values, generated by variations in fundal reflectance. Interestingly, the changes in conversion factor due to the differences in MPOD (Figure 4) were smaller than the ones that were observed following exposure of the subjects to bright light (Figure 6).

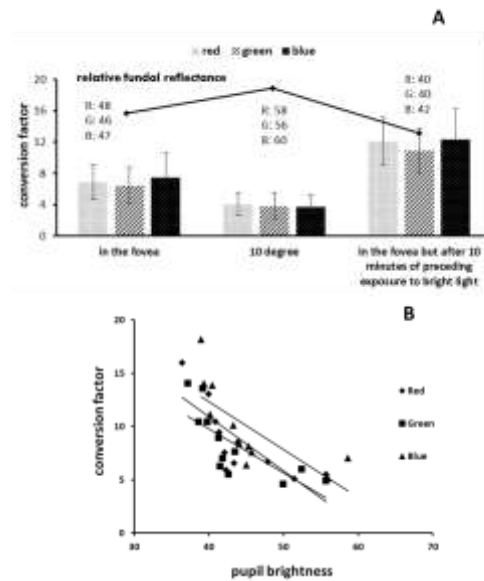


Figure 6. (A) Conversion factors before exposure to bright light in the fovea and at 10 deg from the fixation axis, and in the fovea after 10 minute exposure to bright outdoor illuminance. The thick black line indicates relative fundal reflectance (expressed as the average pixel values in the pupil). Numbers represent average pixel grey levels in the pupil. Note that pupil brightness decreased in the fovea after exposure to bright light and that the conversion factors were inversely correlated to fundal reflectance. (B) Relationship between pupil brightness and conversion factors.

3.5 Which are the most important variables to determine conversion factors? Multiple regression with the SPSS Model

It was found that conversion factors in blue channel were correlated to MPOD and axial length. To determine the relative importance of these variables, a multiple regression analysis was performed using SPSS. An enter model with one dependent variable, the conversion factor for the blue channel, and three independent variables, MPOD, and axial length, was built. The highest impact variable was axial length (beta = -0.560). The finding was significant (ANOVA: $F = 8.6$, $df = 11$; $p < 0.01$) and axial length accounted for 67.5% of the variance of conversion factor (adjusted $R = 0.874$). MPOD (beta = 0.425) had less impact than axial length. Similar results were found for the red channel (beta = 0.569, $p < 0.01$; ANOVA: $F = 9.7$, $df = 11$; $p < 0.01$; $R = 0.826$) and the green channel (beta = 0.699, $p < 0.01$; ANOVA: $F = 9.3$, $df = 11$; $p < 0.01$; $R = 0.882$). Obviously, axial length had the highest impact on conversion factors in all three channels. We found no significant correlations of the conversion factors to any of the higher order aberrations, as measured with the WASCA wavefront Analyzer.

4. Discussion

We found that the conversion factors are correlated with eye length, macular pigment optical density (MPOD), and previous history of light exposure. All these factors affect the amount of light reflected back from the fundus during photorefraction. Apparently, the brightness of the pupil during photorefraction is an important variable to determine the conversion factor, after

it was verified that the response of the RGB camera was linear in the luminance range used during calibration. The individual factors affecting the conversion factor are discussed in detail below.

4.1 Axial length, refractive error and conversion factor

A new finding was that the conversion factor increased with myopic refractive error and with axial length. It is clear that myopia and axial length are related in axial myopia [18-20]. In a longer eye with the same pupil size [21], the same amount of light entering the pupil is distributed over a larger retinal area. Therefore, the retinal image is darker and the $f/\#$ of the eye is higher. For the same reason, the brightness of photoretinoscopic reflexes in the pupil is reduced. Darker pupils generate a larger conversion factor as was found in the experiments described above. It follows that calibrations in subjects with axial anisometropia result in different conversion factors of both eyes, in line with personal observations (unpublished).

4.2 Macular pigment and conversion factor

Macular pigment is a yellowish screening pigment in the central human retina, protecting the underlying photoreceptors from photo-oxidative damage by short wavelength light [22-24]. The peak absorption of macular pigment is around 460 nm [25]. Therefore, we would have expected that absorption of short wavelength light in the foveal center would have increased the conversion factor in particular in the B channel. Surprisingly, the conversion factor became similarly larger in the fovea in all three R, G and B channel, even though the absorption of the macular pigment is known to be low in the red. The absorption coefficient in the mid wavelengths range (500 - 550 nm) is around 0.5 [25]. In the long wavelength range (i.e. 620 nm), it is less than 0.1. Therefore, this question remains puzzling at present.

4.3 Why does pupil brightness affect the conversion factor?

The answer to this question seems surprisingly simple. In photorefraction, the brightness of the pupil is proportional to its area since the brightness of the image of the LEDs of the photorefractor on the retina which gives rise to the light seen in the pupil, is proportional to pupil area. For instance, if the pupil increases in diameter by only square root of 2, its area is doubled and appears twice as bright. Accordingly, the pixel grey levels are proportionally higher and, according to the linear response function of the camera, they are multiplied by a factor, the slope of the camera response function. As a result the measured brightness slope (based on pixel values) will be steeper, and the conversion factor needs to be lower to generate the same refractive error. As long as measurements occur in the linear range of the camera, the correction can simply be done by normalizing the measured refractions to pupil brightness by a linear function. An example, taken from measurements with an infrared photorefractor, is shown in Figure 7 (unpublished data from another study).

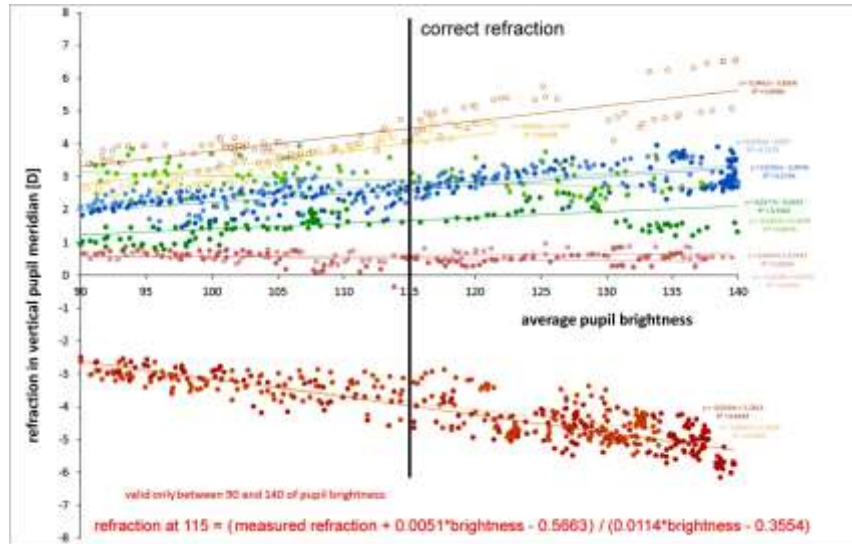


Figure 7. When pupil brightness is modified by changing the aperture stop of the video camera, the measured refractive errors decline when the pupil becomes darker and become larger when pupil brightness increases. In the linear range of the camera, the measured refractions can be corrected for pixel brightness in the pupil so that the spectacle refraction of the subject is reproduced, independently from pupil size and brightness (note the equation in red for a linear correction that was valid for the infrared photorefractor used in that study). Data are from both eyes of seven subjects. Note that there was little change in the measured refractions with pupil brightness when the refractive error of the subject was low.

4.3 Summary and Conclusions

The current study shows that, the brighter the pupil, the lower the conversion factor during eccentric photorefraction. This results has a number of important implications:

- (1) when accommodation is measured and a pupillary near response is elicited, pupil brightness drops and the conversion factor needs to be adjusted to a higher value. If this is not done, the accommodation response will be underestimated and an apparently larger lag of accommodation is measured. Young subjects lacking pupillary near responses may still be measured correctly.
- (2) when different ethnic groups are refracted who vary in fundal reflectance, the measured refractive errors may be incorrect. It is necessary to normalize refractions to the pupil brightness to keep the conversion factor valid.
- (3) higher myopia may be underestimated because a longer axial length increases the f/number (aperture stop) which results in a darker pupil. As a result, calibration in subjects with axial anisometropia results in different conversion factors for both eyes.
- (4) An important question is how previous work dealt with the problem. A commercial infrared photorefractor (i.e. A12R by Plusoptix (www.plusoptix.de), and its predecessors) bypasses the problem elegantly by adjusting the brightness of the infrared LEDs to maintain pupil brightness constant. Therefore, their conversion factors remain valid also when pupil size change or when different ethnic groups are refracted. The first commercially successful infrared photorefractor, the PowerRefractor in 1998 [3], employed an empirically determined correction factor that adjusted the conversion factor continuously depending on pupil brightness. An advantage of the latter procedure may be that it can be done online for each single video frame, while the continuous adjustment of LED brightness during measurements of accommodation may have limitations at high temporal sampling rates. It is clear however that photorefraction without adjustment of the conversion factor for pupil brightness provides

incorrect refraction data in different ethnic groups - i.e. underestimation of refractive errors when fundal reflectance is low [8].

Acknowledgements - This study was supported by OpAL (Optical and Adaptational Limits of Vision). OpAL is an Initial Training Network funded by the European Commission under the Seventh Framework Program (PITN-GA-2010-264605). We thank Dr. Arne Ohlendorf and Dr. Siegfried Wahl for helpful comments on the manuscript.